Design of a Sublimation-Based Solid-State Propellant Storage for a Low-Pressure Micro-Resistojet

Christian Ștefan

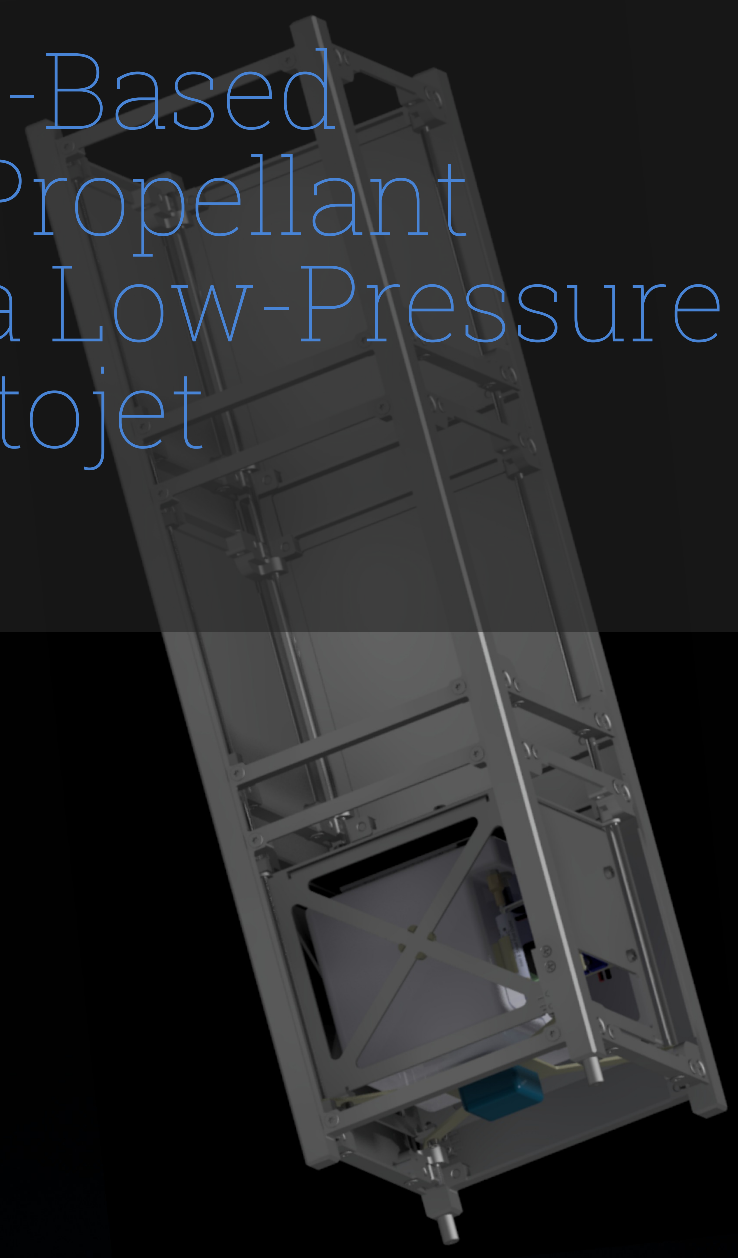

Delft University of Technology

Design of a Sublimation-Based Solid-State Propellant Storage for a Low-Pressure Micro-Resistojet

by

Christian Ștefan

Student number:	5529867
Thesis supervisor:	Dr. Angelo Cervone
Project Duration:	October 2024 - July 2025
Faculty:	Faculty of Aerospace Engineering, Delft

TU Delft

Preface

This thesis marks the end of my life as a student, it has been a very interesting, engaging and fun time. After 9 months of hard work, I am proud to present my final assignment for the Technical University of Delft. It was a challenging process through which I have learned a great deal of things. At the start of this thesis, I was faced with a choice: either test an existing low-pressure micro-resistojet thruster or venture into uncharted territory by developing an entirely new system. In order to engage in innovative thinking, test my knowledge, and challenge my abilities, I chose to pursue something I had little experience with: designing a completely new system from scratch. Even with all the challenges along the way, I am certain that choosing to pursue something new was the right decision for me. Besides learning a lot, I also improved upon, or pickup up on a new set of skills like CAD modeling, Python coding and 3D printing.

If you read this thesis it is assumed that you possess basic knowledge of small satellite propulsion systems and basic modeling interpretation. For the reader interested in the conceptual design process, refer to chapter 4. If you are more interested in the validation and modeling, go to chapter 5. And if you are curious what the final design looks like, have a look at chapter 6.

I would like to thank my supervisor, Dr. Angelo Cervone, for his expert guidance, constructive feedback, and consistent support during the course of this thesis. Every question was met with an elaborate and clear answer, always providing me with new insights that proved to be invaluable for the final result of this thesis. I would also like to thank my brother, David Stefan, for general guidance throughout this process.

Christian Stefan
Delft, June 2025

Executive summary

There is an increasing demand for compact and efficient propulsion systems for small satellites, like CubeSats. One of these types of systems specifically comes to the forefront due to its inherent simplicity, the micro-resistojet thruster. Traditionally, these thrusters rely on either liquid or gaseous propellants, both presenting distinct challenges. While liquid propellants offer desirable performance characteristics, like good specific impulse and high storage density, they often require complex and heavy feed systems, which increase power demands and the overall weight of the system. Conversely, gaseous propellants require no additional feed system, but have lower density, and thus require significantly larger storage volumes that limit propellant capacity and reduce overall thruster effectiveness.

This thesis addresses these limitations by exploring the potential of a sublimation-based solid-state propellant storage system, that utilizes water ice as the propellant. The core innovation lies in leveraging the sublimation process itself to generate sufficient pressure to feed the propellant to the thruster, thereby eliminating the need for complex mechanical feed systems without imposing significantly larger storage requirements. Although prior studies have conceptually validated this approach, a comprehensive and verified design was still lacking.

Following a careful concept development and selection process, a simplified 3D design was established. This design was used to conduct calculations and construct a model. During the modeling phase it became apparent that a detachable heat sink is crucial for the design to limit the energy usage of the system. In addition, it also provided insights in the overall behavior of the system, such as the inverse exponential relationship between freezing time and cooling power, the variable heat input required to maintain constant sublimation during operation, and the confirmed structural robustness of the design under expected launch conditions.

The final design is composed of 26 individual components, out of which 13 are commercial of the shelf items and 13 are custom made. The custom components are made from either aluminum 6061 or polypropylene, reflecting an optimized material selection where each material's properties align with the requirements of its specific component. The design utilizes a thermoelectric cooler for thermal control, as it can both heat and cool, it is supported by passive thermal regulation through an attachable heat sink with the rest of the spacecraft to avoid overheating. This way, the propellant tank itself can be thermally isolated when the thruster is not in use, significantly reducing the amount of heat flow during this phase, thereby limiting the system's overall energy requirements. Other electrical components include; pressure and temperature sensors to monitor the state of the propellant, a solenoid valve to regulate the propellant flow to the thruster, and a micro-servo engine to control the heat sink connection. These components have a combined estimated peak power usage of $20\,W$.

Finally, a physical 3D-printed prototype provided crucial practical insights into assembly, spatial relationships, and maneuverability that were not apparent in the digital CAD environment, leading to important design refinements and enhancing the overall feasibility of the system.

Overall, the project lays a strong foundation for more reliable and streamlined micropropulsion systems. It demonstrates the practical feasibility of a sublimation-based approach for future microsatellite missions. Moving forward, experimental validation of the thermal management system, and the development of an integrated control system, are essential for advancing this design.

Nomenclature

Roman symbols

Symbol	Definition	Unit
A	Area	$[m^2]$
A_s	Expansion slot cross-sectional area	$[m^2]$
F	Thrust	$[N]$
g_0	Gravitational acceleration at sea level	$[m/s^2]$
H	Height	$[m]$
I_{sp}	Specific impulse	$[s]$
k	Boltzmann's constant / Thermal conductivity	$[J/K]/[W/m{\cdot}K]$
L	Length	$[m]$
M	Mass	$[kg]$
M_w	Molar mass	$[g/mol]$
m	Mass flow	$[kg/s]$
m_a	propellant molecule mass	$[kg]$
N_A	Avogadro number	$[mol^{-1}]$
N_s	Number of expansion slots	$[-]$
P	Power	$[W]$
p	Pressure	$[Pa]$
Q	Heat source term per unit volume	$[W/m^3]$
R	Mass ratio, specific gas constant, or Radius	$[J/kg{\cdot}K], [m]$
R_A	Absolute gas constant	$[J/mol{\cdot}K]$
R_{th}	Thermal resistance	$[K/W]$
T	Temperature	$[K], [^\circ C]$
U	Flow velocity	$[m/s]$
V	Volume	$[m^3]$
W	Width	$[m]$
x, y, z	Cartesian coordinates	$[m]$
c	Specific heat	$[J/kg{\cdot}K]$
C	Thermal capacitance	$[J/K]$
$f(v)$	Maxwellian distribution function	$[-]$
G	Conduction conductance	$[W/K]$
n	Number of molecules per volume	$[m^{-3}]$
r	Capacitance to conductance ratio	$[s]$
t	Time	$[s]$
u_e	Exhaust velocity	$[m/s]$
v'_x, v'_y, v'_z	Propellant molecule speed in x, y, z-direction	$[m/s]$
$\underline{\varphi}$	Heater chip input power	$[W]$

Greek symbols

Symbol	Definition	Unit
α	Transmission coefficient	$[-]$
Δ	Increment or change	$[-]$
ΔH_{sub}	Enthalpy of sublimation	$[J/kg]$
ϵ	Emissivity	$[-]$
γ	Specific heat ratio	$[-]$
Γ	Vandenkerckhove constant	$[-]$
μ	Dynamic viscosity	$[Pa{\cdot}s]$
η	Efficiency of propulsion system	$[-]$
ϕ	Aspect ratio of the channel	$[-]$
ρ	Mass density	$[kg/m^3]$
σ	Stefan-Boltzmann constant	$[W/m^2K^4]$
Ψ	Flux per unit area	$[-]$
$\overline{v}$	Average thermal speed	$[m/s]$

Subscripts

Subscript	Definition
0	Initial conditions
a	Atmospheric conditions
c	Combustion chamber / Cooling
e	Nozzle exit conditions
env	Environment
h	Hot side (TEC)
id	Ideal rocket theory
ice	Ice
initial	Initial state or value
input	Input (e.g., power)
max	Maximum
p	Propellant
real	Real values
t	A given time
thruster	Thruster
tr	Translational

Contents

List of Figures

List of Tables

1 Introduction

The growing market for small satellites like CubeSats has significantly increased the demand for compact, efficient propulsion systems. In this context, micropropulsion thrusters play a key role, as they are essential for a wide range of orbital maneuvers, including attitude control, orbit raising, and de-orbiting. This increasing demand has, in turn, driven research into new innovative methods of propellant storage and delivery.

Micro-resistojet thrusters, a type of electric micropropulsion thrusters, are widely used due to their simplicity. Traditionally, these thrusters rely on either liquid or gaseous propellants, both presenting distinct challenges. While liquid propellants offer desirable performance characteristics, such as good specific impulse and high storage density, they often require complex and heavy feed systems, which then increase power demands and the overall weight of the system. Conversely, gaseous propellants require no additional feed system, but have lower density, and thus require significantly larger storage volumes that limit propellant capacity and reduce overall thruster effectiveness.

These challenges imposed by managing liquid and gaseous propellants have led to the exploration of solid-state propellant storage methods. The core innovation of this approach lies in leveraging the sublimation process itself to generate pressure to feed the propellant to the thruster, thereby eliminating the need for complex feed systems without resulting in significantly larger storage requirements. Earlier studies have shown that this conceptually works, but a fully functional design has yet to be developed.

This thesis aims to change that by developing a new design for a sublimation-based solid-state propellant storage system for a low-pressure micro-resistojet. In order to do so, the current state of propellant storage for micro-resistojets will be analyzed (chapter 2). Followed by a concept development and selection process, that results in a basic design concept (chapter 4). This basic design concept will be modeled and tested (chapter 5), eventually leading to a fully worked out detailed design (chapter 6).

2
Literature study

This chapter provides a review of the current state of propellant storage in micropropulsion thrusters, specifically for micro-resistojet thrusters. First, an overview of current storage solutions will be presented, followed by an analysis of their limitations and potential improvements. After which important characteristics to be tested and how to test them will be explored. Lastly, key findings will be presented.

2.1. General description

This thesis project focuses on the development and validation of a solid-state propellant storage system based on a sublimating propellant, designed for a Low-Pressure Micro-resistojet (LPM). It considers the possibility to store the propellant for the thruster in a solid-state. This would simplify the thruster by eliminating the propellant feed system as the proposed system uses the pressure provided by the sublimation of the propellant as a means of the propellant feed.

The main objective of this literature study is to conduct a comprehensive review of current storage systems, and concepts for sublimation-based solid-state propellant storage systems like the one provided by Cervone A, (2015) [1] and Ye X, (2001) [2]. In addition to that the goal is to find potential improvements, and means to validate, model and experimentally demonstrate a proposed design. The experimental demonstration would be tested using test setups available at TU Delft, focusing on key performance metrics like specific impulse and thrust-to-power ratio, while also demonstrating the viability of the sublimating propellant storage concept.

The rapid advancement within the field of micropropulsion is driven by the growing demand for small satellite missions, specifically those involving Cubesats. These small satellites require very efficient and compact propulsion systems to be able to perform a diverse amount of maneuvers in space. This research further elaborates on this growing field by answering research questions provided in the next paragraph.

2.2. Research questions

The literature study aimed to answer the following research questions:

1. What are current solutions used to store propellant on microsatellites?
2. How can current solutions be improved?
3. How can a sublimation-based solid-state propellant storage concept be modeled?
4. How can the performance of a sublimation-based solid-state propellant storage concept be experimentally tested and validated?
    (a) Which different test setups can be used to test a sublimation-based solid-state propellant storage concept and how?
    (b) Which characteristics will be tested and how?
        - Characteristics to be tested?
        - Test methodology?
        - Test objectives?

To answer the research questions, a solid theoretical foundation has been established through a detailed literature study. This focuses on the principles of propellant storage in micropropulsion systems, specifically those of LPM's. Interesting studies related to solid-state storage have been examined, and valuable resources such as Thermal Rocket Propulsion [3] and Micropropulsion Reader [4] gave insights to provide essential background. Relevant papers on propulsion storage like: Propulsion for CubeSats [5], LPM Design [6], and Feed and Pressurization Systems [7], have informed the research. Additionally, Garrett S.'s work on Ideal Gas Laws [8] has been referenced for understanding the propulsion mechanics. This literature study forms the basis for the research documented in further chapters and provides background information and a foundation for the list of requirements (see table 3.1 and decisions made during the design process).

2.3. Current storage solutions

Micropropulsion thrusters can be divided into two main categories: Electric and non-electric. Electric propulsion systems like micro-resistojets, electrospray, ion, and Hall thrusters actively require on-board power for their operation. Although chemical propulsion systems such as cold gas, liquid, and solid rocket systems require power only to regulate the propulsion process [9]. The amount of power required for electrical propulsion systems depends on the type of electric thruster but also the amount and type of components it contains. To increase thruster efficiency, it is important to minimize the number of electrical components, thereby reducing the power required for effective operation.

A type of electric propulsion system is a micro-resistojet. Two types of micro-resistojets are a Vaporizing Liquid Micro-Resistojet (VLM) and a Low-Pressure Micro-Resistojet (LPM). The main difference between them is the working pressure level, the VLM works under a pressure in the order of 10^5 Pa while the LPM works under a pressure in the order of 10^2 Pa.

The VLM (see figure 2.1 [4]) typically has 3 main components: Propulsion storage, Heating element, and Nozzle. It accelerates the vaporized gas by means of adiabatic expansion in a convergent-divergent nozzle.

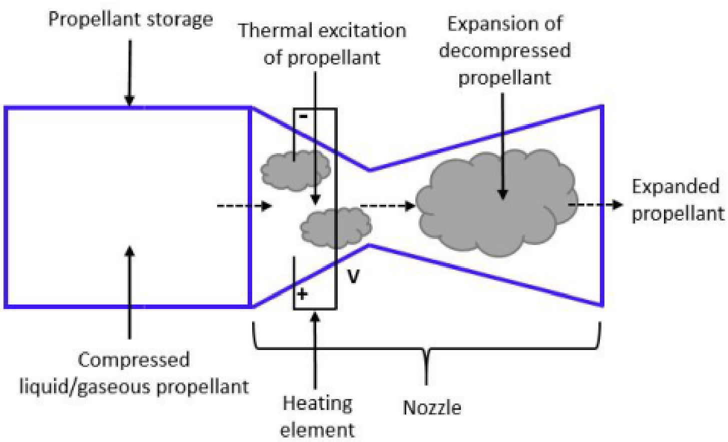

Figure 2.1: Schematic of a Vaporizing Liquid Micro-Resistojet thruster [4].

For this project the main focus was on a LPM, the LPM (see figure 2.2 [10]) also has 3 main components: Propulsion storage, Feed system and the Thruster. The propellant is stored as a solid or liquid, a heater is then used to sublimate or evaporate the propellant. After which a feed system regulates the flow towards the thruster. The thruster itself is composed of a plenum and a heater chip with slots or microchannels through which the propellant gas is expelled to outer space creating thrust [11].

Liquid monopropellant systems feature an improved specific impulse and storage density over pressurized gas systems [9]. Liquid water specifically is excellent to use as a propellant as it is a green safe to use propellant, it provides for a relatively high volumetric specific impulse due to water's high storage density and low molecular mass [9]. This also makes it relatively easy to store as it requires a smaller tank volume when compared to other propellants. In addition to this, water as a propellant has more benefits. Take for example the specific impulse, it is inversely proportional to the square root of the propellant molecular mass, however, an excessively low molecular mass is not preferred as it is typically associated to very low density and extremely large required propellant storage volumes. And

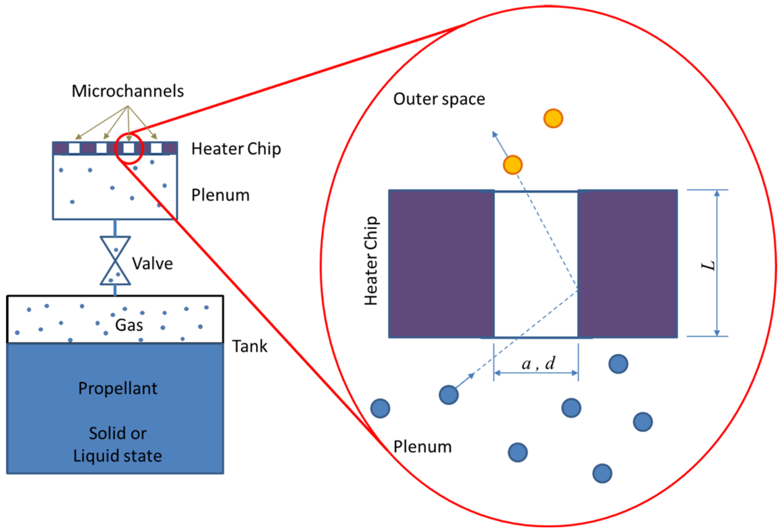

Figure 2.2: Schematic of a Low-Pressure Micro-Resistojet thruster [10].

water with a molecular mass of 18 g/mol is a good example of a propellant which is not on either end of this spectrum [12]. A downside of storing the propellant in the liquid state is that this storage technique requires for more sophisticated propellant feed system components [13]. In addition to that liquids can also provide for sloshing issues as the propellant can move inside the tank, potentially causing stability issues.

It becomes clear that liquid water is a good propellant with a few upsides and downsides. The propellant needs to be slightly pressurized for optimal performance. And in order to do so, as mentioned earlier, there should be some kind of feed system. Like a pump or a pressurized gas, which then makes the whole system more complicated and energy demanding. An example of a micropropulsion system that requires this added complexity is a system developed by Aerojet Rocketdyne, the MPS-135 [14], it is a monopropellant system that uses AF-M315E as its propellant. Which illustrates complexity of handling liquids in space, as this system requires a Pump feed propellant Management Device (PMD) [15]. The University of Tokyo has also developed a micro-resistojet using liquid water as a propellant, again proving that having water as a propellant has great benefits as its safety and availability led to shorter-period and lower-price development. But in order to operate this thruster, the water needs to be kept at room temperature at all times to prevent freezing. And the design requires a vaporization chamber, where the water needs to be vaporized before it can be used as a propellant, making the system more complicated [16].

As previously mentioned, the propellant can also be stored as a gas. For micro-resistojets this has more drawbacks than benefits however. As mentioned, gaseous propellants are less dense, meaning more storage space is required to house sufficient amounts of fuel [17]. This results in limited delta-V capabilities, often restricted to less than 10 m/s [18]. So while the system benefits from relative simplicity and reliability, its efficiency and performance are significantly lower, making it more suitable for attitude control rather than large orbital maneuvers. And if stored, potential containment breaches in the system have to be avoided by making a more sturdy and intricate design. However, storing the propellant as a gas could mean that it provides for its own feed pressure and would therefore not require an additional feed system, which simplifies the system [7].

Storing water in a solid-state could be a solution for propellant storage in LPM's as the sublimating water ice can automatically feed the propulsion system. This is something TU Delft has been working on after Andrew D Ketsdever [11] has developed and tested a similar solution, but this was never implemented in that particular concept [12]. The concept was also proposed by X.Y. Ye [2], where its viability was confirmed. However, it has been proposed that using propellants like acetone (C_6H_6O) and ammonia (NH_3) could significantly improve the system's performance. These alternative propellants offer potential for higher efficiency, thrust output and specific impulse which will be explored further in chapter 2.4.

Propellants can be stored in different ways, each offering different advantages and limitations. For a micro-resistojet, storing the propellant in its solid state proves to be the most beneficial approach for LPM's, as suggested by Cervone A, (2015) [1]. As liquid and gaseous storage methods have notable drawbacks, including the need for feed systems, stability issues, and storage inefficiencies, as highlighted by Legge (2017) [13] and Martinez (2023) [17].

2.4. Possible improvements

Chapter 2.3 already mentioned the design of a sublimation-based solid-state propellant storage provided by Cervone A, (2015) [1]. The main beneficial characteristic of this type of propellant storage is the dispensation of an additional feed system as the sublimating water can provide pressures up to around 600 Pa [19]. Which results in 0.2 to 1.2 mN/W of thrust, for an expansion slot aspect ratio of 2.5 (the ratio of expansion slot Length/Depth), while still adhering to the size, mass and power limitations associated with CubeSat requirements and constraints. [1]. However, this design is not yet optimized. There are still many things that can be changed or improved before a physical experimental concept should be designed and created for testing.

Potential points of improvements can be placed in the following 3 categories: Boosting specific impulse, Improving efficiency and Concept simplification.

Specific Impulse

Specific impulse is a measurement that represents how efficiently a reaction mass engine like a rocket motor generates thrust. and can be represented by equation (2.1) [3]:

$$I_{sp} = \frac{\int_0^{t_a} F\,dt}{g_0 \int_0^{t_a} m\,dt} = \frac{m \cdot v_e \cdot t_a}{m \cdot t_a \cdot g_0} = \frac{v_e}{g_0} \tag{2.1}$$

Where,

$v_e =$ exhaust velocity

$g_0 =$ gravitational constant

In order to increase the specific impulse one can increase the exhaust velocity as the gravitational constant is constant, even if the satellite would fly in mars' orbit, earths gravitational constant would still be used. This is because it provides a standardized way of comparing propulsion systems across different environments [20].

The general equation in terms of thermodynamic and nozzle properties for exhaust velocity is not applicable to LPM's as Ideal Rocket Theory does not apply for these types of micropropulsion thrusters. In addition to that, for LPM's, exhaust velocity is the average gas velocity at micro channel exit and depends on the translational kinetic temperature. Non-ideal effects such as viscous losses and heat dissipation at small scales can further reduce the applicability of this equation, which assumes ideal expansion through a nozzle. Therefore the following exhaust velocity equation, equation (2.2) is more applicable [21]:

$$v_e = \sqrt{\frac{\pi k T_{tr}}{2 m_a}} \tag{2.2}$$

Where,

$k =$ Boltzmann's constant

$T_{tr} =$ translational kinetic temperature

$m_a =$ propellant molecule mass

Looking at this equation, in order to increase the exhaust velocity one could either increase the translational kinetic temperature or decrease the initial mass flow rate. Translational kinetic temperature is directly influenced by the heater chip expansion slot wall temperature, so increasing that will increase the translational kinetic temperature [21]. An analytical model developed by Ketsdever (2005) [11], that can be used to estimate the performance of the a Free Molecular Micro-Resistojet (FMMR, which is a type of LPM [4]) [22]. The general formulation for the flux per unit area Ψ of any physical quantity Ψ in the direction of the flow can be described as [11]:

$$\Psi = \int_{-\infty}^{\infty}\int_{-\infty}^{\infty}\int_{0}^{\infty} \Psi v'_x f(v'_x) dv'_x dv'_y dv'_z \tag{2.3}$$

Where,

$v'_x =$ propellant molecule speed in x direction

$f(v'_x) =$ maxwellian distribution function

Using this, an expression for the axial mass flow can be derived by setting $\Psi = \alpha m n$, where α is the transmission probability, which is the probability a molecule that enters the expansion slot will actually exit and produce thrust, and n is the number of molecules per unit volume. In order to calculate the transmission coefficient as a function of the channel's aspect ratio the following relations have been derived by Lafferty (1998) [23]:

$$\alpha = 0.5\left(1 + \sqrt{1+\phi^2 - \phi}\right) - \frac{1.5[\phi - \ln(\phi + \sqrt{1+\phi^2})]^2}{\phi^3 + 3\phi^2 + 4 - (\phi^2+4)\sqrt{1+\phi^2}} \tag{2.4}$$

$$\alpha = 1 + \phi^2 - \phi\sqrt{\phi^2+1} - \frac{[(2-\phi^2)\sqrt{\phi^2+1+\phi^3-2}]^2}{4.5\phi\sqrt{\phi^2+1-4.5\ln(\phi+\sqrt{\phi^2+1})}} \tag{2.5}$$

Equation (2.4) gives the transmission coefficient of molecules through short uniform rectangular cross sections (slots), where the aspect ratio ϕ is defined as the ratio between the length of the slot in the direction of the flow and the smallest cross-sectional dimension. Equation (2.5) does the same for cylindrical cross sections. In this case, ϕ is defined as the ratio between the channel's length and its diameter.

The mass flow exiting the LPM is therefore given by Equation (2.6), $\bar{v}$ is the average thermal speed of the propellant molecules, given by Equation (2.7).

$$\dot{m} = \alpha m_a n \frac{\bar{v}}{4} A_e \tag{2.6}$$

$$\bar{v} = \sqrt{\frac{8kT_0}{\pi m_a}} \tag{2.7}$$

By combining the two equations above with the ideal gas law $(P = nkT)$ [8], the following expression for the mass flow, where P_0 is the plenum pressure, can be derived [11]:

$$\dot{m} = \alpha P_0 \sqrt{\frac{m_a}{2\pi k T_0}} A_e \tag{2.8}$$

where,

$\alpha =$ transmission coefficient

$P_0 =$ plenum fluid pressure

$m_a =$ molar mass

$k =$ Boltzmann's constant

$T_0 =$ plenum fluid temperature

$A_e =$ expansion slot cross-sectional area

Note that both equation (2.2) and (2.8) only provide a very approximate description of the thruster performance as they are based on a number of assumptions, collision-less flow for example. A more accurate model of the thruster is therefore necessary.

The sublimation pressure of water vapor provided by ice sublimation at the vapor–liquid–solid triple point at 273.16 K is 611.657 Pa with an uncertainty of $\pm\ 0.01$ Pa [24, 25]. Which means this is the maximal achievable pressure if the thruster uses sublimating water ice as a propellant, and does not utilize an additional pressurization or feed system.

While water ice provides safe, sustainable propulsion with a relatively good balance of specific impulse and pressure, other propellant options may offer enhanced performance. Different propellants have been proposed in earlier designs to boost specific impulse and thrust efficiency [2]. Ammonia (NH_3), for instance, is an alternative with higher energy density compared to water but also requires careful control of decomposition and stability within the micro-resistojet. Ammonia at levels above approximately 100 ppm are irritating to the eyes, respiratory tract and skin [26]. Nevertheless, an ammonia micro-resistojet was produced by the NASA Goddard Space Flight Center, this thruster has a nominal $25\,W$ power level with a specific impulse level of between 150 and 210 s and thrust of 5 to 12 mN[27]. This specific impulse is higher when comparing them to water-based micro-resistojets [1, 2, 18], it is important to note however, that other factors such as size, power consumption, and system efficiency also play a significant role in this regard. The trade-off between safety, performance and system complexity plays a significant role in the choice of propellant for micropropulsion systems.

Efficiency

The efficiency of the system depends on a number of factors, important factors are the thrust efficiency and the power efficiency. First looking at the thrust equation, the thrust (F_T) of a propulsion system is composed of the sum of pressure thrust and momentum thrust. Pressure thrust results from the pressure differential between the exit and ambient pressure (P_e and P_a). The moment thrust is related to the linear momentum transported through the exit of expansion slots [11]. As the pressure thrust can be assumed negligible [11], the thrust equation, equation (2.9), becomes:

$$F_T = \dot{m}v_e + (P_e - P_a)A_e \approx \dot{m}v_e \tag{2.9}$$

Where $\dot{m}$ is given by (2.8) and v_e is given by (2.2). Combining these equations gives the following analytical expression for the theoretical thrust of the LPM:

$$F_T = \frac{\alpha P_o A_e}{2}\sqrt{\frac{T_{ie}}{T_0}} \tag{2.10}$$

The efficiency of the propulsion system η is given by equation (2.11), where φ is the heater chip input power [11].

$$\eta = \frac{F_T I_{sp} g_0}{2\underline{\varphi}} = \frac{F_T^2}{2\dot{m}\varphi} \tag{2.11}$$

The power efficiency of this system can be improved by increasing the heating/cooling efficiency or by optimizing the sublimation process. The heaters of micro-resistojets produced at TU Delft were manufactured using silicon-based Micro Electro Mechanical Systems (MEMS) technology including a heater made of molybdenum for better operations at high temperature [6]. But this component is not influenced by or influencing the propellant storage directly. Improving the power efficiency in the propellant storage component can be done by optimizing sublimation process and optimizing storage isolation.

The design provided by Cervone A, (2015) [1], uses a Peltier device attached to two heat transfer elements to cool or heat the propellant in the propellant tank (note: this is not the same component as the earlier mentioned heater chip in the thruster). Although Peltier devices are useful for precise temperature control, their main disadvantage is that the thermoelectric module has got less efficiency compared to other cooling methods [28]. The design also utilizes a thermal connection to the spacecraft actuated by a linear electric motor, which allows thermal conduction during operation and keeps the system insulated during the rest of the mission. This transition between active and inactive phases in space can can lead to issues like inefficient sublimation or re-solidification as this thermal system can induce thermal transients. Thermal transients in phase changing materials used in space can result in long dissipation times which can prevent the system from maintaining a uniform thermal state, which is critical for consistent propulsion. These factors can lead to inefficiencies in the sublimation process. The fast thermal shifts could prevent the desired phase transition from happening which would affect the overall system reliability [29].

Concept Simplification

Looking at concept simplification, it is very general and can therefore refer to many things. Decreasing the amount of moving components for example or valve-less or passive propellant management. The current design provided by Cervone A, (2015) [1] uses 3 valves and 2 different motors of which some could potentially become obsolete in a different design configuration. The concept design process will naturally come across opportunities for simplification as it progresses.

Although current designs, such as the one proposed by Cervone A, (2015) [1], have a good foundation, they remain incomplete and present opportunities for further development. Improving specific impulse could be achievable through a detailed analysis of propulsion equations and by exploring potential improvements in important characteristics. Power efficiency could be optimized by investigating alternative heating and cooling mechanisms, as well as by evaluating different materials or techniques for thermal insulation. And finally, current designs still offer significant scope for simplification, as the current iterations can still be relatively underdeveloped, leaving room for refinements and improvements.

2.5. Concept modeling

Before commencing physical testing, a model must be developed, so that the concept can be simulated and analyzed to ensure its viability. First it is important to understand the fundamentals of spacecraft thermal control. All satellite components have a certain range of allowable temperatures that cannot be exceeded to meet operational requirements during all mission phases. The net heat of the spacecraft is determined by absorbed, stored, generated, and dissipated heat. Figure 2.3 shows a simplified overview of the heat exchange of a satellite orbiting the Earth.

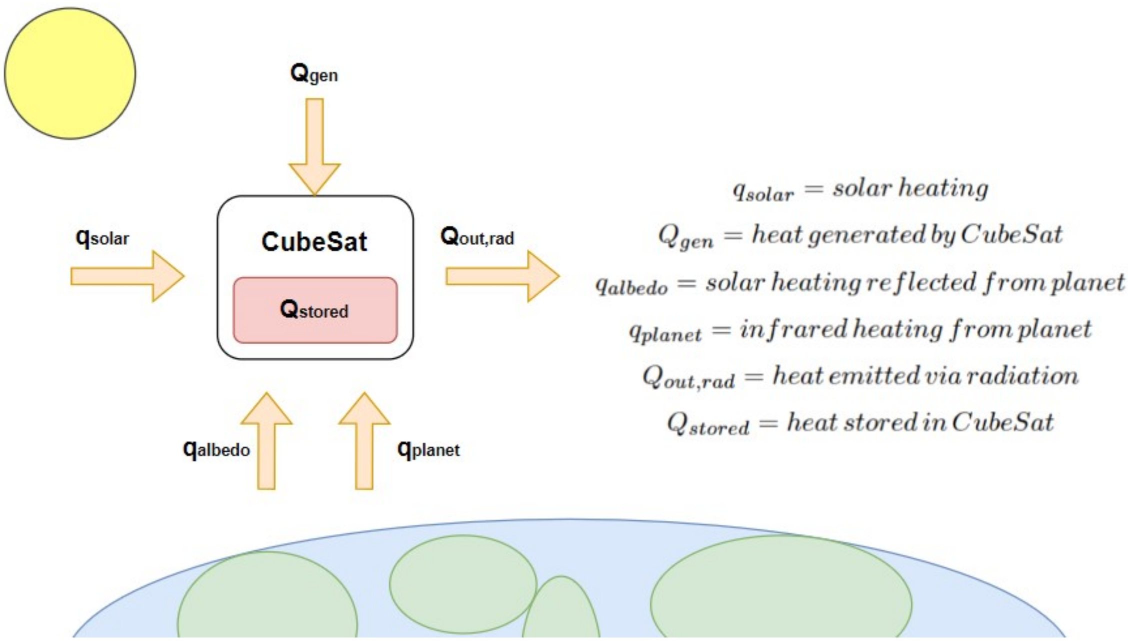

Figure 2.3: Net heat exchange of a CubeSat in Earth orbit, illustrating absorbed, generated, stored, and dissipated heat.

The heat exchange depends on several factors, the thermal control of the satellite is achieved by balancing them according to the following energy equation:

$$q_{solar} + q_{albedo} + q_{planet} + Q_{gen} = Q_{stored} + Q_{out,rad} \tag{2.12}$$

- q_{solar} depends on the solar flux, determined by the distance to the sun, the surface area viewing the sun and the solar absorptivity of that particular surface.
- q_{albedo} depends on the planetary albedo, the fraction of solar radiation reflected by the planet, the surface of the CubeSat facing the planet, and the absorptivity of that surface.
- q_{planet} depends on the IR emissivity of the planet, the surface of the CubeSat that faces the planet and the IR absorptivity of that surface.
- Q_{gen} depends on the power dissipation of the components on board the CubeSat.
- Q_{stored} is quantified by the CubeSat's thermal capacitance, which is a measure of its capacity to store thermal energy for a given change in temperature.
- $Q_{out,rad}$ includes the potential radiator surface, the IR emissivity of the surface, and the difference in temperature between the CubeSat radiator and the heat sink to which it dissipates. It also includes heat loss from other surfaces not specifically intended to function as radiator.

This heat balance will help form a basis for the model of the storage system. The model should be a close approximation to the real system and incorporate most of its salient features. However, it should not be so complex that it is impossible to understand and experiment with it. A good model is a judicious trade-off between realism and simplicity [30]. For a study provided by Rossi, C [31], a model of a solid-state propellant microrocket-application was made, with a number of fundamental equations using the SIMULINK package from Matlab. This proved that modeling can result in promising advantages, namely:

- Enabling optimization by having a flexible and adaptable thruster model that can be easily adjusted to accommodate different types of thrusters and materials by modifying the database.
- Having low calculation time of only a few minutes.
- Being correct and usable for both the subsonic and supersonic regime.

A paper presented at the 36th International Electric Propulsion Conference at the University of Vienna, titled 'Thrusters Modelling, Propellant Choice and Plume Expansion', demonstrated that Python is a highly useful tool for modeling electric micropropulsion systems [32]. They created a model called 'openPlumeEP', which was developed with Python to analyze electric propulsion plumes. Python was the chosen language due to its high adaptability and flexibility when it comes to modifications. No compilation is necessary and the python scripts allow quick modification of the code. Although this model was created for a different application and has a distinct structure from the one required for modeling a propulsion storage system, the presented benefits of using Python are still relevant.

For the solid-state propulsion storage, thermal control of the system is crucial as much of the power required for the operation of the system is directly linked to thermal control (as mentioned in chapter 2.4). And thermal mathematical models form the basis of thermal analysis to solve satellite thermal control problems. To develop a thermal mathematical model for the propulsion storage system, a combined conduction and radiation heat transfer equation with environmental heating and cooling defined as boundary conditions can be used [33]. The general partial differential equation of combined heat conduction and radiation:

$$\rho c \frac{\partial T}{\partial t} = \nabla \cdot (k \nabla T) + \nabla \cdot (q') + Q \tag{2.13}$$

In this equation Q consists of the internal heat sources from the power dissipation of components and heaters and the external heat sources from the absorbed orbital heating on the boundary surfaces. This equation should be converted into a system of finite differential equations by constructing finite difference nodes with the help of a Taylor series approximation. But there is a simpler thermal analytical model that can be derived. This way the general energy equation 2.13 is reduced to a simplified case of pure radiation heating or cooling for the isothermal body to the environment such as deep space or a thermal vacuum oven wall (where heat conduction is neglected). This simplified model, represented by equation 2.14 [33], is applicable under specific assumptions and with certain limitations. The primary assumption is that the entire body is isothermal, which means that it has uniform temperature throughout the system at any given time. This eliminates the internal temperature gradients. In addition to this, this model assumes that heat transfer to and from the body occurs only via radiation, which neglects the conductive and convective heat transfers. The environment (space) is assumed to have a uniform and constant temperature. And finally, the thermal properties of the body are assumed to remain constant over the temperature range. These simplifications would imply some limitations. If the satellite does experience significant temperature gradients, the model would provide inaccurate results. Besides that, it is feasible that the atmosphere would allow for convective heat transfer, this simplified model would not capture those thermal behaviors. While the equation is a differential equation and can model transient behavior, its simplicity means it may not accurately capture rapid or complex thermal transients, especially those involving phase changes or non-linear material properties.

$$C\frac{dT}{dt} = \varepsilon A\sigma\left(T_{env}^4 - T^4\right) \tag{2.14}$$

Here $\varepsilon A\sigma T_{env}^4$ can be obtained from the sum of the body-absorbed radiation energy from the environment Q_a and the internal power dissipation Q_i in steady state, that is,

$$\varepsilon A\sigma T_{env}^4 = Q_a + Q_i \tag{2.15}$$

So equation 2.14 can be solved with theoretical analysis, and the result expressed in a compact mathematical formulation. While equation 2.13 can only be solved by numerical computation. Both the simpler and the more complicated models are equally important to the thermal control problem as the complicated model can lead to complete and quite accurate solutions, while the simpler can be a powerful tool to get quick estimates for the overall system.

A full thermal model of the propulsion storage system's thermal control will inevitably involve a larger set of equations. Nevertheless, the equations presented here form a critical foundation for further development of a thermal model.

2.6. Experimental testing and validation

Experimental testing and validation are critical components in the development and optimization of a sublimation-based solid-state propellant storage concept. The proposed concept can be tested for performance, efficiency and reliability under representative space conditions. Leveraging the available test setups at TU Delft will help to identify the strengths and limitations of the system, so that it can be redefined to ensure it meets space level mission requirements for small-scale satellites. The following subsection will present the different test setups available at TU Delft and how these setups can be used to measure and validate important system performance characteristics. Whether all the tests outlined in this section will be conducted depends on the feasibility of completing them effectively within the given time constraints.

Available test setups

TU Delft has access to a number of test facilities. At the Aerospace Engineering faculty there is a cleanroom with various instruments for measuring thruster characteristics. Whether or not all of these test setups will actually prove to be usefull for testing the sublimating propellant storage has yet to be seen. It is still good to know the test possibilities however. First of all there are a range of devices capable of conducting mundane tests like measuring voltage, current and noise. In addition to these, there are more specific test setups. Thrust can be measured using the AE-TB-5m thrust pendulum [34] [35], see figure 2.4. The pendulum consists of a hanging element that rotates around smooth hinges, with a thruster attached. Thrust produces a displacement and a small rotary spring and mass on top of the pendulum cause the thruster to return to its original position. The distance between two points on the pendulum is then measured. The thruster pendulum is able to measure up to a maximum thrust of 5 mN.

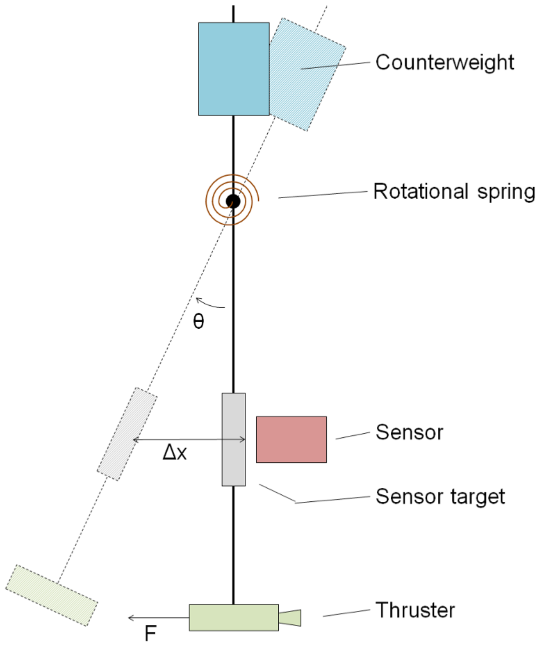

Figure 2.4: Schematic representation of the AE-TB-5m basic functioning (exaggerated rotation) [36].

The determination of the current-force characteristics of the AE-TB-5m calibration actuator is done using the Variable Turn-Density Coil (VTDC). The VTDC, as the name suggests, is a coil wound with a variable turn-density. This coil was designed by R. Bijster [35] to allow for the calibration of the AE-TB-5m in both atmospheric as vacuum conditions. With the variable turn-density configuration of the VTDC, the creation of a parallel homogeneous magnetic field within the coil is created. If a magnet is suspended in this field, a constant force is exerted on the magnet. The magnet is attached via a beam to the sensor target. The supplied current trough the coil will thus result in a force acting on the sensor target. The goal of the magnetic VTDC calibration is to obtain an accurate relation between the current supplied to the coil, and the resulting force exerted on the sensor target. This information can then be used to calibrate the AE-TB-5m by applying the known magnetic force on the sensor target and measuring the resulting displacement, and in that way finding the relation between displacement and force [36].

The vacuum chamber used for conducting measurements in space like conditions is the Heraeus Vacutherm vacuum oven [37] located in the Space Engineering cleanroom (see figure 2.5). The vacuum oven uses an external vacuum pump to depressurize the chamber to a low vacuum of 1.5 mbar. The time required for depressurization from atmospheric conditions to 1.5 mbar is approximately 2 hours. The pressure inside the vacuum chamber is determined from the analog pressure gauge on the front of the oven. The pressure gauge indicator dial is divided in 100 mbar increments. The vacuum chamber contains eight color coded female banana connectors for the connection of electrical equipment inside the enclosure. Furthermore, four RS-232 (9 pins) female connectors are also available for the connection of sensor systems. Propellant is supplied through the feedline with a 1/4 inch male quick connector manufactured by Swagelok. Furthermore three generic throughputs are available to connect custom wiring/piping to the vacuum chamber using vacuum rated adaptors [36].

Figure 2.5: Heraeus Vacutherm vacuum oven containing the AE-TB-5m [36].

Besides that, tests like a leakage test or measuring propellant flow can easily be conducted using the General Purpose Feed system (GPF, see figure 2.6). This system allows for controlling clean airflow to the thruster. This can become usefull for testing the thruster's capability when operating under conditions representable to those if it were to be supplied with the feed pressure provided by the sublimating propellant.

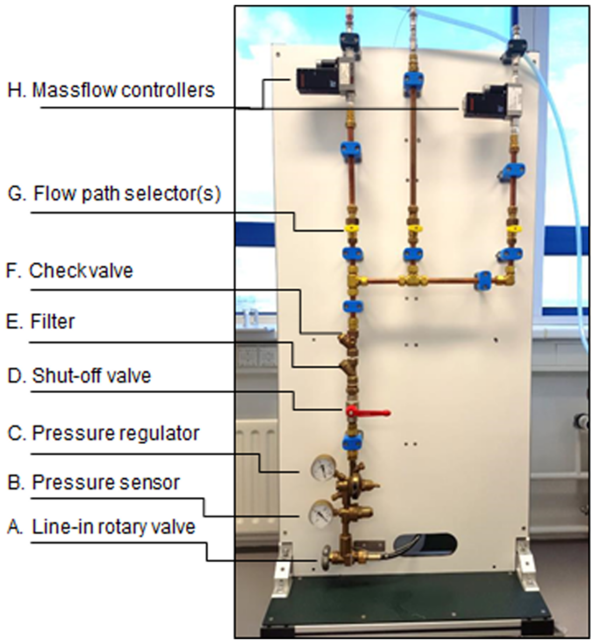

Figure 2.6: General Purpose Feed System [36].

How the setups can be used

Most test setups in the clean room at TU Delft mainly focus on measuring thrust characteristics. While these are valuable for finding out propulsion performance, the primary goal of this thesis project is to evaluate the feasibility of the sublimation-based solid-state propellant storage concept itself. Testing should therefore concentrate on understanding the stability, efficiency and phase transition behavior of the propellant storage, under conditions that simulate space environments. This will help to determine the practicality and reliability of the concept as a viable option for micropropulsion systems. So how can the setups be used for testing these specific types of characteristics?

1. The thrust pendulum can be used to measure the thrust generated by the thruster under conditions where the propellant's pressure and temperature match those expected when supplied by sublimating water ice. This way the viability of the feed pressure provided by the sublimating propellant can be validated.
2. The vacuum chamber can be used to test thermal characteristics of the concept under space like conditions.

What will be tested and how

In order to validate and test the viability of the design for the sublimation-based solid-state propellant storage concept a comprehensive test procedure is critical. The concept must undergo various types of tests that simulate conditions the design will be exposed to in operation in space in order to ensure that the design meets the performance requirements to be used on microsatellites. The following section will outline the key characteristics to be tested, the methodology for conducting these tests, and the objectives behind them. By testing aspects like thermal stability, pressure and efficiency, the feasibility and reliability of the design can be demonstrated. Table 2.1 summarizes the following section.

Characteristics to be tested:

- **Thermal stability:** It is essential for the thermal conditions to be stable to ensure that the concept operates within the designed thermal range without excessive unexpected phase transitions. This category will focus on how the propellant storage reacts to temperature changes and whether sublimation occurs consistently at the expected rates. An interesting paper regarding Thermal stability is [38].
- **Thermal control:** This is crucial to ensure the concept functions properly in a space environment with extreme temperature variations. It involves managing the heat input to the storage concept to maintain the propellant within the desired phase state, and ensuring consistent sublimation. Effective thermal control can prevent these unwanted phase transitions that can disrupt the propellant feed and reduce efficiency. An interesting papers regarding thermal control is [39].
- **Pressure retention:** In order for the sublimation to provide for a stable feed to the propulsion concept, maintaining the appropriate pressure is critical. This category assesses how well the concept can hold the internal pressure generated by the sublimating propellant to ensure it is suitable for feeding the thruster. Interesting papers regarding sublimation pressure are [40], [41].
- **Sublimation performance:** This characteristic is about how efficiently the sublimating propellant converts into usable gas to feed the thruster. It indicates whether or not the design enables controlled and sustained sublimation, providing the right amount of propellant at the required pressure.
- **Endurance:** This will determine the long-term reliability of the storage concept under operational conditions in space. This can include repeated cycles of heating and cooling, vacuum exposure, and other mechanical stresses. The goal is to ensure the design can withstand the demands of long-term space missions without failure or significant performance degradation. Interesting papers on reliability of satellites are [42], [43].
- **Thrust:** It is important to verify the storage system can actually be integrated with the thruster and so that it provides consistent thrust levels. Using setups like the AE-TB-5m thrust pendulum to measure thrust output when supplied with propellant with a pressure of around 611 Pa [24].

Test methodology:

- **Thermal stability:** In order to test the thermal stability of the system, thermocouples will be placed in and around the storage unit to measure how effectively it maintains the required temperature range under simulated space conditions. The Heraeus Vacutherm vacuum oven at the Aerospace Engineering faculty of TU Delft will simulate these extreme temperature changes in a repetitive cycling manner. This way potential unwanted phase transitions in the system can be monitored. Besides that the sublimation rate can be measured across different thermal conditions to verify the thermal stability of the system.
- **Thermal control:** Thermal control involves both passive insulation and active heating/cooling mechanisms. In order to asses these characteristics testing will include controlled heat input

to simulate solar heating, evaluating how well the thermal control system prevents undesired phase transitions of the propellant. Measuring temperature and manual inputs over time will help to evaluate the system's response and control accuracy. This can be done using the Heraeus Vacutherm vacuum oven at the Aerospace Engineering faculty of TU Delft.

- **Pressure retention:** Testing the pressure retention involves sealing the propulsion storage and monitoring pressure levels over time under different temperature conditions. A range of temperatures will be applied to simulate changes, while pressure sensors will monitor stability and retention within the desired operational limits. This can be done using pressure sensors, under controlled conditions in the cleanroom at the Aerospace Engineering faculty of TU Delft.
- **Sublimation performance:** The sublimation rate can be measured by monitoring the rate at which the propellant transitions to a gas under set thermal conditions. A mass flow meter can measure the exact gas output from an enclosed system to verify this sublimation rate. The test setup will include controlled heating to induce sublimation while monitoring to ensure the consistency and adequacy of the propellant feed. This can be done using a flow meter, under controlled conditions in the cleanroom at the Aerospace Engineering faculty of TU Delft.
- **Endurance:** Endurance can be tested by subjecting the system to repeated thermal and pressure cycles to simulate long-term exposure to space conditions. Continuous monitoring over many cycles will help to identify potential weak points in materials or the design, identifying these weak points will allow for improvements at critical points to ensure reliability for extended missions. This can be done using the Heraeus Vacutherm vacuum oven at the Aerospace Engineering faculty of TU Delft.
- **Thrust:** The thrust measurement setup AE-TB-5m at the Aerospace Engineering faculty of TU Delft can be used to assess thrust levels achieved with the sublimating propellant. This test will verify whether or not the system provides consistent pressure and mass flow rate to meet the thrust requirements. The results will show if the storage system effectively supplies the propulsion system with stable propellant pressure.

Test objectives:

- **Thermal stability:** To ensure the overall system maintains consistent thermal behavior and does not experience any unexpected phase transitions or degradation in sublimation performance.
- **Thermal control:** To verify that the system's thermal management can keep the propellant in a stable stage, even when subjected to external temperature variations. Effective thermal control should prevent overheating or excessive cooling, ensuring the propellant sublimates at a controlled and predictable rate.
- **Pressure retention:** To confirm that the system can consistently retain the pressure generated by the sublimating propellant and maintain it within the specified operational range.
- **Sublimation performance:** To demonstrate that the propellant sublimates efficiently and consistently, providing the necessary mass flow to feed the thruster.
- **Endurance:** To evaluate the long-term durability of the storage system, ensuring that it can withstand the stresses of repeated thermal and pressure cycles without significant performance degradation.
- **Thrust:** To measure the actual thrust produced by the propulsion system when fed with propellant from the solid-state storage.

Table 2.1: Summary of characteristics to be tested, test methodologies, and test objectives

#	Category	Characteristics to be Tested	Test Methodology	Test Objectives
1	Thermal Stability	Consistency of thermal performance, no unexpected phase changes	Temperature cycling tests, thermal chamber experiments in the Heraeus Vacutherm vacuum oven at TU Delft	Ensuring stable behavior in the operational thermal range
2	Thermal Control	Efficient thermal management	Heat input control, temperature gradient testing in the Heraeus Vacutherm vacuum oven at TU Delft	Preventing overheating or excessive cooling and phase shifts
3	Pressure Retention	Ability to maintain pressure generated by sublimation	Pressure tests, leak rate measurements in the cleanroom at TU Delft	Ensuring consistent pressure to feed the thruster
4	Sublimation Performance	Sublimation rate, mass flow control, efficient gas production	Controlled sublimation tests, mass flow measurement in the cleanroom at TU Delft	Verifying consistent sublimation and gas feed for propulsion
5	Endurance	Long-term reliability under cyclic thermal and pressure stresses	Long-duration testing, multiple thermal/pressure cycles in the Heraeus Vacutherm vacuum oven at TU Delft	Confirming durability over extended mission durations
6	Thrust	Actual thrust performance with integrated propellant storage system	Thrust pendulum measurements, performance benchmarking using the AE-TB-5m at TU Delft	Confirming the system provides reliable and consistent thrust

2.7. Core insights

This section shows the most important insights derived from the literature study, highlighting the most significant findings and the implications they impose for the design and development of a sublimation-based solid-state propellant storage concept. While looking into the different types of storage solutions used in micropropulsion systems today, it became clear water is an excellent choice of propellant [9, 12]. Besides this, earlier studies have also indicated that storing the propellant in the solid-state is a promising solution as it could lead to a simplified design by eliminating the need for an additional feed system [1, 2].

Possible improvements were analyzed and categorized in 3 main sections: Boosting specific impulse, Improving power efficiency and Concept simplification. The literature study showed that specific impulse can be boosted in a number of different ways, but for a LPM based on a sublimating solid propellant it mostly comes down to propellant type, temperature and pressure [3, 8]. It is important to note for a sublimating water ice propellant the initial temperature and pressure will be 273.16 K and around 611 Pa respectively, which are characteristics of the vapor-liquid-solid triple point of water [24]. Power efficiency can be improved by having an optimal thermal control system. It is important the propellant has a constant temperature, so good insulation is crucial, as well as having an efficient heating and cooling mechanism. While concept simplification can refer to various approaches, focusing on reducing the number of moving parts and implementing passive propellant management techniques could be particularly beneficial.

Earlier research on micropropulsion systems showed that modeling the design before making an experimental test version was very beneficial [31, 32]. This can be done using a program like SIMULINK in Matlab or Python. For the concept, the thermal control system is crucial, so modeling that will give important insights into the performance of the design.

Finally, for the literature study various test setups were analyzed as well as their possible application. And in addition to that, which characteristics should be tested, the test methodology for each characteristic and the objectives. Table 2.1 gives a clear overview of the possible tests that can be conducted to research the viability of the propellant storage concept.

Overall, the literature study provided a strong foundation for further exploration of the sublimation-based solid-state propellant storage concept. It highlighted the benefits of solid-state propellant storage over liquid and gaseous alternatives, while also identifying areas for improvement in current proposals that require further investigation.

2.8. Answering the research questions

Looking back at the research questions from the beginning of the literature study, the following can be concluded:

1. *What are current solutions used to store propellant on microsatellites?* For each of the three types of propellant storage: gaseous, liquid, and solid, there are examples of micro-resistojets that utilize them. However, research does show that storing the propellant in the solid state is the most beneficial for micro-resistojets.
2. *How can current solutions be improved?* Specific impulse can be boosted in a number of different ways, but for a micro-resistojet based on a sublimating solid propellant it mostly comes down to propellant type, temperature and pressure [3, 8]. It is important to note for a sublimating water ice propellant the initial temperature and pressure will be 273.16 K and around 611 Pa respectively, which are characteristics of the vapor-liquid-solid triple point of water [24]. Efficiency can be improved by having an optimal thermal control system. It is important the propellant has a constant temperature, so good insulation is crucial, as well as having an efficient heating and cooling mechanism. While concept simplification can refer to various things, focusing on reducing the number of moving parts and implementing passive propellant management techniques could be particularly beneficial.
3. *How can a sublimation-based solid-state propellant storage concept be modeled?* A model can be made using a program like SIMULINK in Matlab or Python. For the concept, the thermal control system is crucial, so modeling that will give important insights into the performance of the design.
4. *How can the performance of a sublimation-based solid-state propellant storage concept be experimentally tested and validated?* The concept can be tested using various methods and equipment available at the TU Delft cleanroom of the Aerospace Engineering faculty. Like the thrust pendulum and vacuum chamber. Besides these larger equipment, the tests would also require temperature and pressure sensors, and a flow meter.

3
Research plan

This chapter defines the plan of the study, it includes the problem statement, research objectives and scope, research questions, a work breakdown structure and finally a list of requirements for the design. Together, these elements provide a structured framework for investigating the use of a sublimation-based solid-state propellant storage for LPM thrusters.

3.1. Problem Statement

The increasing demand for highly efficient, compact propulsion systems for microsatellites has driven research into new methods of propellant storage and delivery. Micro-resistojet thrusters, which are widely used due to their simplicity, often make use of liquid or gaseous propellant storage. Storage of the propellant as a liquid provides better specific impulse and storage density than gaseous storage, but requires a complex feed system. Which results in increased system complexity, adding weight and increasing power consumption. While gaseous storage might provide for a simpler overall system, it is less efficient as it requires more storage space.

These challenges imposed by managing liquid and gaseous propellants have led to the exploration of solid-state propellant storage methods, which could simplify the propulsion system by eliminating the need for complex feed mechanisms. However, the solid-state propellant storage concept remains underdeveloped, with few experimental validations and several areas for improvement, particularly in optimizing the thermal system, system efficiency, and long-term storage stability.

The lack of a well-established, computationally modeled, and experimentally demonstrated sublimation-based solid-state propellant storage solution for micro-resistojet thrusters presents a critical gap in micropropulsion technology. Addressing this gap could lead to more efficient and simpler propulsion systems for microsatellite missions, enhancing performance while reducing the complexity, cost, and energy demands of current systems.

3.2. Research Objectives and Scope

The main objective of this research was to evaluate existing solutions for sublimation-based solid-state propellant storage in micropropulsion thrusters and develop an optimized design specifically for a low-pressure micro-resistojet thruster. This concept has been computationally modeled and 3D printed. To achieve this objective, the research has been structured around the following topics:

- **Concept Design:** Designing an optimized storage solution for a micro-resistojet micropropulsion thruster by identifying improvements that simplify the system while maintaining or enhancing performance metrics such as sublimation stability and power efficiency. It was an iterative circular process involving concept designs, comparison, improvement, and evaluation.
- **Model and Simulation:** Modeling and Simulating the solution to predict how the optimized system performs under realistic conditions. Initially, the model focuses on the thermal system of the propellant storage, in addition to this strength analyses have given insight into the ability to survive launch conditions.
- **Experimental Validation:** Testing an experimental demonstration made using prototyping techniques like 3D printing. This way the solid-state propellant storage can be tested in combination with a micro-resistojet thruster, so that its performance can be analyzed and compared with both the simulation, as with gaseous or liquid stored propellant storage based micro-resistojet thrusters. Due to time constraints it was not possible to conduct performance tests as specified in the literature study. However, a 3D printed design has been established to give insight in the the practical

feasibility of the design.

3.3. Research questions

The next section of the report focuses on the design of the sublimation-based solid-state propellant storage for micro-resistojet thrusters. It is structured around the research objectives and aims to answer the following main question with a set of sub questions:

Main research question:

What is the optimal design for a sublimation-based solid-state propellant storage system for a low-pressure micro-resistojet thruster?

Sub research questions:

1. What are the key functions the propellant storage must fulfill to ensure successful operation for a low-pressure micro-resistojet thruster?
2. Which components, materials, and design characteristics are most suitable for fulfilling the key functions required by the propellant storage system?
3. What is the optimal propellant storage design configuration for improved efficiency and reliability?
4. What is the most effective method for modeling the behavior and performance of the propellant storage?
5. What is the most effective method for testing the behavior and performance of the propellant storage?

3.4. Work Breakdown Structure

In order to successfully complete the thesis project within the given timeline the project has been divided into the 3 main topics as listed in chapter 3.2: Concept Design, Model and Simulation and Experimental Validation. In addition to that the literature study and project finalizing have also been added. Each topic has been given a time frame and a number of tasks that need to be completed. The Modeling and Experimental validation phases have been planned to partially overlap as experiments can be risky and unpredictable. This way, in case some experiments had to be postponed, the time could be used to improve the model and simulation. This is not visualized in the Work Breakdown Structure (WBS, see the following figure).

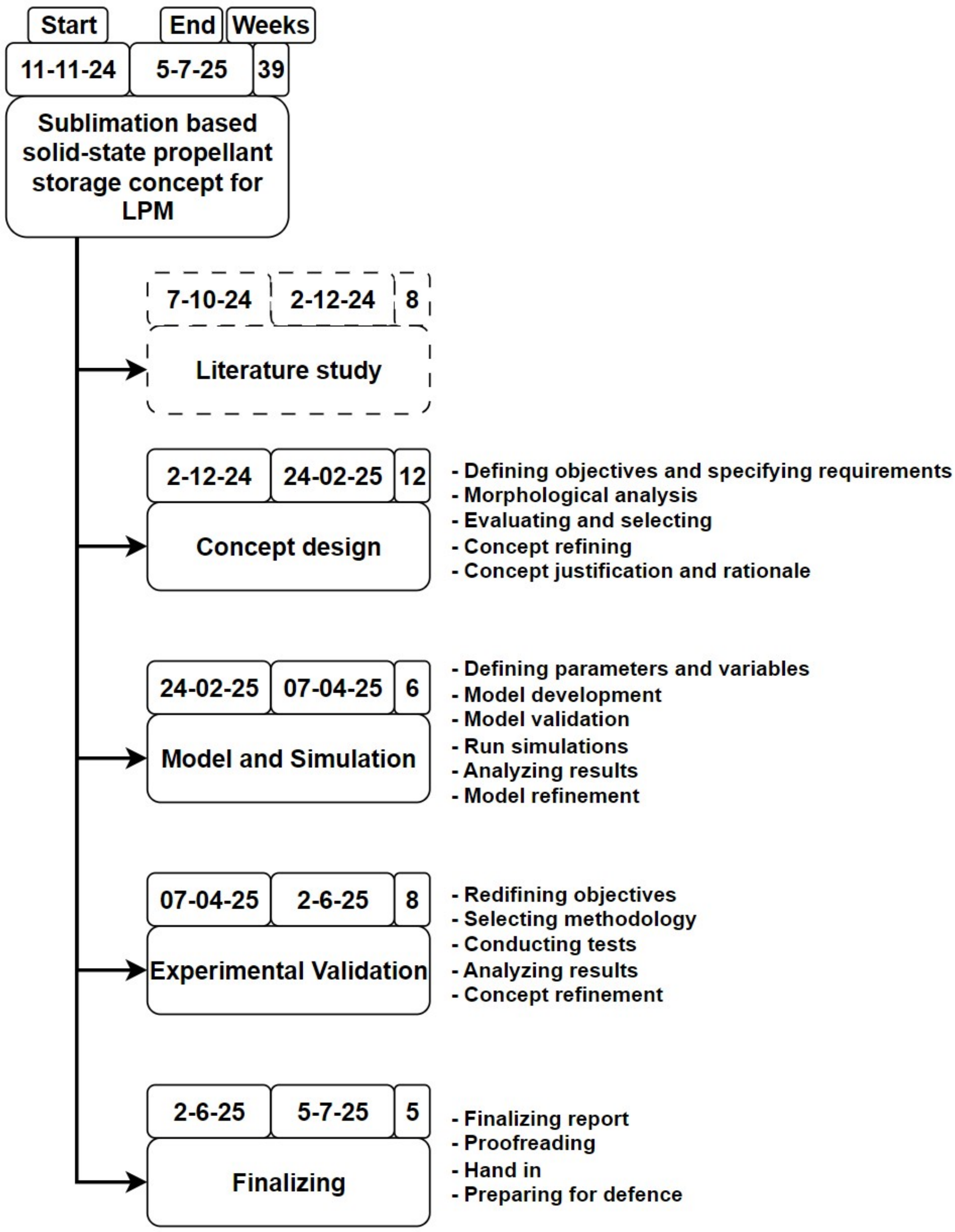

Figure 3.1: Thesis project Work Breakdown Structure

3.5. List of Requirements

The design concept will have to adhere to a number of requirements. Table 3.1 outlines these requirements each with a rationale and a means of verification.

Table 3.1: List of design requirements for the propellant storage system.

ID	Requirement	Description	Rationale	Verification	Source
1. Thermal					
1.1	Propellant temperature above 270.16 K	The storage heating/cooling element must ensure the system maintains a temperature above 270.16 K.	Ensures the propellant remains close triple point of water, resulting in the highest amount of pressure the sublimating water ice can provide.	Thermal testing in a vacuum chamber or verifying with thermal model.	[24] [41]
1.2	Propellant temperature below 273.16 K	The storage heating/cooling element must ensure the system maintains a temperature below 273.16 K.	Ensures the water ice temperature stays below the triple point of water.	Thermal testing in a vacuum chamber or verifying with thermal model.	[24] [41]
1.3	Thermal Insulation	The storage system must be insulated so that the heating/cooling element has enough capacity to comply to requirements 1.1 and 1.2.	Minimizes energy consumption.	Insulation testing in vacuum oven or verifying with thermal model.	N.A.
1.4	Operational between $0\,^{\circ}$C and $40\,^{\circ}$C	The storage system must be able to operate between $0\ ^{\circ}$C and $40\,^{\circ}$C	The system must be able to operate within the minimal and maximal internal spacecraft temperature fluctuations common.	Temperature testing in vacuum oven.	[44] [33]
2. Pressure					
2.1	Pressure tolerance of 733 Pa	The system must be able to operate under a pressure of above 611 Pa without leaking (so 733 Pa when taking into account Requirement 5.3).	This is the maximum pressure the Water ice sublimation will result in.	Pressure testing in a controlled environment.	[24]
2.2	Pressure fluctuations below $2-3$ Pa	The system must maintain stable pressure levels during operation, with fluctuations below $2-3$ Pa.	This will ensure a stable sublimation pressure which is required for stable thrust output.	Pressure testing in a controlled environment.	[45]
3. Performance characteristics					
3.1	Maximum peak power of 20 W	The storage system should require no more than 20 W to operate.	This will minimize overall power required by the thruster and improve efficiency.	Calculate power requirement of the design.	[46]

Table 3.1: Continuation of the list of design requirements for the propellant storage system.

ID	Requirement	Description	Rationale	Verification	Source
3.2	Mass flow rate of 1 mg/s	The sublimation rate should be adjusted so that it results in a mass flow rate of 1 mg/s with an accuracy of 50%.	This is required for the LPM to operate.	Mass flow rate measurement.	
4. Physcial characteristics					
4.1	Wet weight below 380 g	The storage system wet weight cannot be over 380 g.	Should weigh no more than earlier sublimation based solid-state thruster provided by Cervone A, (2015).	Weight measurement of the design.	[1]
4.2	Dimensions below 1 U	The dimensions of the whole thruster (including the propellant storage system) should not exceed 1 U.	This will leave enough space on the CubeSat for the payload.	Measurement.	N.A.
5. General					
5.1	Environmental Compatibility	The storage system must be able to operate under the vacuum of space.	Ensures the system operates reliably in space.	Environmental testing in vacuum oven.	N.A.
5.2	Structural durability for $4.9\,G$	The storage system must be able to withstand $4.1\,G$ (so $4.9\,G$ when taking into account Requirement 5.3) .	Must be able to withstand the maximal amount of G forces experienced during launch of a falcon 9 rocket as it is likely it will be launched with this rocket.	Structural analysis.	[47]
5.3	Safety margin of 20%	The storage system must incorporate a safety margin of 20% to account for uncertainties.	Ensures the system can deal with unexpected events.	N.A.	[48]

4
Concept design

This chapter details the design process for the sublimation-based solid-state propellant storage concept. It begins with the conceptualization of various 2D design solutions, followed by a systematic selection process for individual components. And finally, the selected elements are synthesized into a refined and simplified 3D block design, laying the foundation for the modeling and simulation of the design.

4.1. Conceptualization in 2D

The design of the system posed a number of unique challenges, particularly concerning the thermal management, propellant expansion, and the overall integration of the components and the whole system inside the CubeSat. Before diving into the different specific design choices, it is crucial to have a general understanding of the system's overall architecture and the functions of the primary elements.

A sublimation-based solid-state propellant storage system for LPM's, such as the one conceptually explored by Cervone A. [1], typically have a propellant storage, a thermal regulation system, and a mechanism to regulate the propellant flow to the thruster. The core innovation of the new system lies in leveraging the sublimation of the solid propellant to generate the necessary pressure for feeding and operating the thruster. Which would significantly simplify the feed system compared to traditional liquid or gaseous propellant systems. The most important elements of the system include:

- **Propellant storage:** Contains the solid propellant. The design needs to accommodate for the volume change which is a result of the liquid water freezing in space. It also needs to ensure no propellant is able to escape, so it has to be completely sealed.
- **Thermal control system:** Manages the temperature of the propellant throughout all phases of the mission, this includes cooling the propellant to solidify it, maintain its solid state, and heating the propellant to induce sublimation.
- **Structural integrity:** Ensures the physical robustness of the system having an optimal material selection, allowing it to withstand expected launch loads and maintain its mechanical integration within the CubeSat to ensure reliable operation.

This next section develops an optimized design for such a system. The conceptualization process began by identifying the following general functions, which the propellant storage system has to fulfill, each requiring specific design solutions.

1. **Heating element placement:** Where in the system should the heating element be placed for optimal functionality and efficiency.
2. **Propellant expansion accommodation:** The system must ensure that the propellant is allowed to expand when frozen in space without damaging storage or components.
3. **Thermal insulation:** The system should ensure that the heat exchange with the surrounding components of the satellite is controlled.
4. **Material selection:** The selected materials should withstand the operating conditions while ensuring compatibility with the propellant. Also be structurally robust enough to survive the launch as this is the moment of peak stresses.
5. **Leak prevention:** The system must ensure leak prevention for both liquid propellant during the initial phase and sublimated gases during operational phases to prevent damage and ensure controlled delivery.
6. **System integration:** The system needs to be well integrated with the rest of the spacecraft.

Each of these functions has been fulfilled with 4 solutions. Out of all considered possible solutions, the 4 most reasonable have been presented. A useful tool to present these potential solutions is a morphological chart. This overview allows for combinations of solutions which will eventually form basic design concepts.

Table 4.1: Morphological chart of potential design solutions for functions of the propellant storage system.

ID	Function	Solution 1	Solution 2	Solution 3	Solution 4
1	**Heating element placement**	Within the propellant	Opposite of the mass flow exit	Towards the mass flow exit	Surrounding the propellant
2	**Propellant expansion acc.**	Flexible membrane	Spring loaded plate	Extra internal volume	Elastic bladder
3	**Thermal insulation**	Multi-layer insulation	Aerogel	Vacuum insulation	Reflective coating
4	**Material selection**	Aluminum alloy	Carbon fiber composite	Stainless steel	Polymer composite
5	**Leak prevention**	One piece container	Elastic sealing material	Glue/kit	Double-walled containment
6	**System integration**	Modular mounting	Direct structural attachment	Quick-disconnect interfaces	Bracket-mounted design

Some solutions can already be ruled out when looking at the list of requirements (table 3.1) presented in chapter 3.5, or simply because of impracticality, these are:

- **1.1. Within the propellant:** Would result in pockets of sublimated or melted water inside the ice near the heater which could result in uneven heating, making it harder to maintain the temperature between 270.16 K and 273.16 K (Requirements 1.1 and 1.2). Thermal gradients within the propellant could also lead to pressure instability (Requirement 2.2).
- **6.3. Quick-disconnect interfaces:** Can be excluded based on the need for a permanent fix, a quick-disconnect interface is simply not required for the design.

These different solutions have been combined to form 3 basic 2D concepts (see appendix A.1, A.2 and A.3). They have been established by selecting the most logical combinations. In order to select the best concept for further development, they have been evaluated based on a set of important characteristics:

1. **Practicality:** Defines whether or not the concept is practically viable. And if it could work and be able to meet the requirements realistically.
2. **Reliability:** Defines whether or not the concept would be reliable. And if the solutions it uses could function under the conditions specified in the list of requirements.
3. **Mass:** The overall mass of the solution.
4. **Efficiency:** To what extend do the materials/concepts used, benefit the efficiency of the system.
5. **Cost:** The cost of the solution.

These characteristics have been assigned weights to reflect their relative importance as some characteristics are more critical than others. This has been done with a pairwise comparison provided in a table provided in figure 4.1. Each characteristic has been argued in terms of its impact on the overall concept. In addition to that relative importance has been substantiated by benchmarks from similar systems which for example prove that performance metrics are prioritized over power consumption, as small satellites are often more constrained by weight and size than by energy. To calculate the weights, first the numbers have been normalized by dividing all entries by the sum of the respective column. After which the average of each row gives the weight of the respective characteristic. Table 4.2 gives the weights for each characteristic.

Table 4.2: Weights of characteristics used for selecting a concept.

Characteristic	Practicality	Reliability	Mass	Efficiency	Cost
Normalized Weight	0.370	0.274	0.188	0.115	0.052

The concepts have all been graded with a number from 1 to 5 which correspond to:

- **Very Poor (1):** Significantly below minimum requirements; unacceptable performance.
- **Poor (2):** Below minimum requirements; barely functional.
- **Average (3):** Meets minimum requirements; adequate but not exceptional.
- **Good (4):** Exceeds minimum requirements; demonstrates good effectiveness.
- **Excellent (5):** Significantly exceeds requirements; outstanding performance.

Figure 4.1 shows the scores of the concept characteristics multiplied by their respective weight.

Characteristic	Practicality	Reliability	Mass	Efficiency	Cost
Practicality	1,00	3,00	2,00	3,00	4,00
Reliability	0,33	1,00	3,00	3,00	5,00
Mass	0,50	0,33	1,00	3,00	4,00
Efficiency	0,33	0,33	0,33	1,00	4,00
Cost	0,25	0,20	0,25	0,25	1,00
Sum	2,42	4,87	6,58	10,25	18,00

Characteristic	Practicality	Reliability	Mass	Efficiency	Cost
Normalized Weight	0,370	0,274	0,188	0,115	0,052

Concept	Practicality	Reliability	Mass	Efficiency	Cost	Weighed total
1	2,00	3,00	2,00	3,00	3,00	2,441774467
2	3,00	4,00	3,00	4,00	2,00	3,336788608
3	1,00	2,00	4,00	3,00	3,00	2,174951608

Figure 4.1: Pairwise comparison and weighted decision matrix concept selection.

This means concept 2 is the chosen concept (see appendix A.2). In order to validate this selection process, a sensitivity analysis has been conducted by adding/subtracting 10% to each of the normalized weights. This way the outcome remained the same.

4.2. Component selection

The process demonstrated in chapter 4.1 was repeated for the selection of the individual components required for the concept. The following general functions for components have been identified:

1. **Propellant heating:** Regulate the temperature by heating the propellant to control the sublimation process.
2. **Propellant cooling:** Regulate the temperature by cooling the propellant to control the sublimation process and dissipate excess heat to prevent the propellant from becoming liquid.
3. **Monitoring pressure:** Ensure consistent real-time measurement of internal pressure to maintain stable sublimation and propellant flow within operational limits.
4. **Monitoring temperature:** Ensure consistent real-time measurement of internal temperature to maintain stable sublimation and propellant flow within operational limits.
5. **Mass flow control:** Regulation of sublimated gas to plenum of the thruster.

Solutions for each function have been presented with a short description and some pros and cons in Appendix B.1, the morphological chart with these solutions is given in table 4.3.

Table 4.3: Morphological chart of potential design solutions for functions of the propellant storage system.

ID	Function	Solution 1	Solution 2	Solution 3	Solution 4
1	**Propellant heating**	Resistive heater	Cartridge heater	Radiative heater	Thermoelectric heater
2	**Propellant cooling**	Radiative cooling	Heat pipes	Conduction to radiators	Thermoelectric cooler
3	**Monitoring pressure**	Pressure transducer	Piezoelectric sensor	Capacitive pressure sensor	
4	**Monitoring temperature**	Thermocouples	Resistance Temperature Detector (RTD)	Infrared Sensor	Thermistors
5	**Mass flow control**	Solenoid valve	Butterfly valve	Piezoelectric valve	

Some solutions could already be ruled out when looking at the list of requirements presented in chapter 3.5, table 3.1, these are:

- **2.1. Radiative cooling:** This passive cooling solution will most likely not be able to provide sufficient cooling capacity to maintain requirement 1.2. [49].
- **4.3. Infrared sensor:** Only capable of measuring surface temperature which does not accurately reflect the temperature of the propellant which makes it difficult to meet temperature requirements 1.1 and 1.2.
- **5.4. Orifice plate:** Does not provide active control, can therefore not stop thruster from being activated. Could also result in significant pressure fluctuations and affect thrust stability, requirement 2.2.

The solutions have been compared using the following characteristics assigned with weights:

Table 4.4: Weights of characteristics used for selecting the components.

Characteristic	Performance	Reliability	Efficiency	Mass	Cost
Weight	0.377	0.253	0.200	0.117	0.054

The solutions provided in the morphological analysis have again been graded with a number from 1 to 5 corresponding to the list provided earlier in chapter 4.1. Figure 4.2 shows the scores of the solution characteristics multiplied by their respective weight.

This means the following solutions come out on top per function:

- Propellant heating: **Resistive heater**
- Propellant cooling: **Thermoelectric cooler (TEC)** [1]
- Monitoring pressure: **Pressure transducer** [2]
- Monitoring temperature: **RTD** [3]
- Mass flow control: **Solenoid valve** [4]

Although resistive heater is the best means of heating the propellant, a TEC can both heat and cool, it would therefore be unnecessary to have both a resistive heater and a thermoelectric cooler. Only

[1] https://uk.rs-online.com/web/p/peltier-modules/2172401
[2] https://nl.mouser.com/ProductDetail/TE-Connectivity-First-Sensor/HCLA12X5DU?qs=RtU67MWp17BR9wF4eKH3FA
[3] https://nl.rs-online.com/web/p/rtd-sensors/8919139
[4] https://www.theleeco.com/product/hypodermic-port-outlet-vhs-series-solenoid-valve/

a thermoelectric cooler would suffice. This also decreases the total amount of components, and thus weight and energy requirements.

Characteristic	Performance	Reliability	Mass	Efficiency	Cost
Performance	1,00	3,00	2,00	3,00	4,00
Reliability	0,33	1,00	2,00	3,00	5,00
Mass	0,50	0,50	1,00	3,00	4,00
Efficiency	0,33	0,33	0,33	1,00	4,00
Cost	0,25	0,20	0,25	0,25	1,00
Sum	2,42	5,03	5,58	10,25	18,00

Characteristic	Performance	Reliability	Mass	Efficiency	Cost
Weight	0,377	0,253	0,200	0,117	0,054

ID	Solution	Performance	Reliability	Mass	Efficiency	Cost	Weighed total
1.1	Resistive heater	5	3	3	3	4	3,806754538
1.2	Cartridge heater	4	2	3	4	3	3,240259679
1.3	Radiative heater	5	4	1	2	1	3,382240851
1.4	Thermoelectric heater	3	2	4	4	2	3,010140666
2.1	Radiative cooling	2	5	4	2	1	3,105682226
2.2	Heat pipes	3	4	2	3	2	2,999425394
2.3	Conduction to radiators	3	4	4	3	3	3,453104024
2.4	Thermoelectric cooler	5	2	4	4	2	3,763314146
3.1	Pressure transducer	5	3	4	2	2	3,782913028
3.2	Piezoelectric sensor	1	2	3	4	3	2,110499461
3.3	Capacitive pressure sensor	1	2	4	4	3	2,310548246
4.1	Thermocouples	2	4	5	2	1	3,052675774
4.2	RTD	3	3	4	3	2	3,146467727
4.3	Infrared sensor	3	3	3	2	2	2,829690763
4.4	Thermistors	3	3	4	2	2	3,029739548
5.1	Solenoid valve	5	5	3	3	3	4,259283956
5.2	Butterfly valve	3	3	3	3	4	3,053581059
5.3	Piezoelectric valve	4	3	4	3	2	3,523054466

Figure 4.2: Pairwise comparison and weighted decision matrix component selection.

4.3. Concept synthesis

This section further develops the very basic concept established in section 4, concept 2. It shows the development of a three-dimensional representation, initially a simplified 'block' design. This simplification allows for efficient calculations by representing key components (propellant storage, TEC, insulation, thruster interface) as basic geometry shapes. This initial model allows for the assessment of overall thermal performance and identification of critical design parameters, which serves as a foundation for subsequent refinement.

4.3.1. Design assumptions

Geometry and material

- **Homogeneous materials**: Every component is made of a single uniform material with constant material properties.
- **Perfect contact**: No thermal contact resistance between components.
- **Simplified shapes**: Components are represented as simple geometric shapes (cubes, cylinders, etc.).

Thermal and sublimation process

- **Homogeneous temperature distribution**: Each component has a single, uniform temperature.
- Constant sublimation rate: Constant sublimation rate equal to the required mass flow rate of the thruster.
- **Ideal gas behavior**: Water vapor behaves as an ideal gas.
- **No vapor pressure buildup**: Sublimated water is immediately expelled by the thruster, so there will be no significant pressure buildup that will affect the sublimation rate.

External boundary condition

- **Perfect vacuum**: The system will be in perfect vacuum so no convective heat transfer.
- Minimal and maximal spacecraft internal temperature of 0 and $40°C$ respectively (as stated in the list of requirements, table 3.1).

4.3.2. Conceptual block design

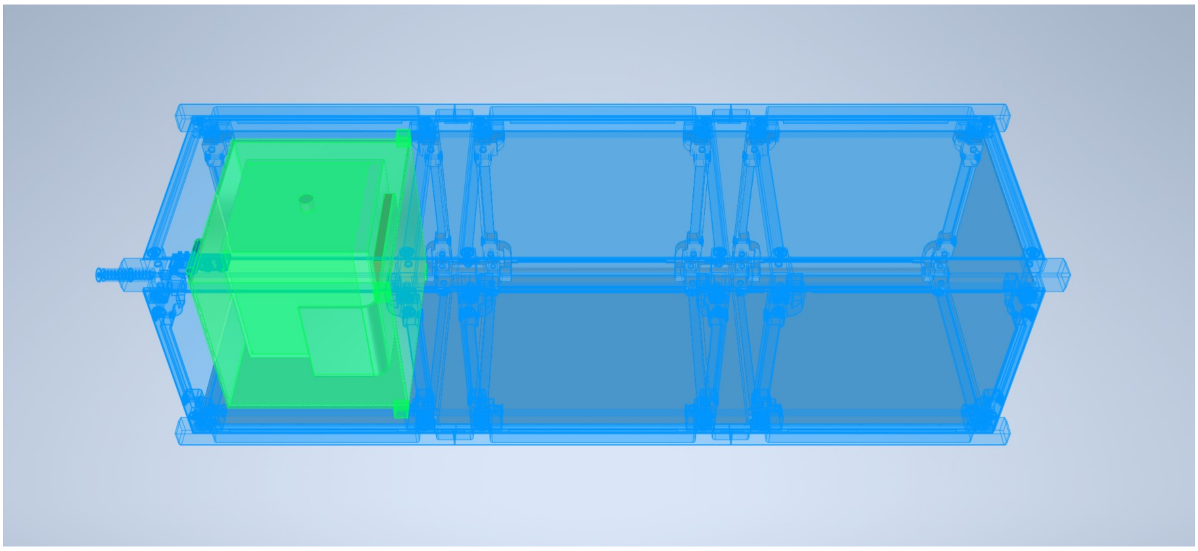

(a) Simplified block design integrated within a CubeSat structure.

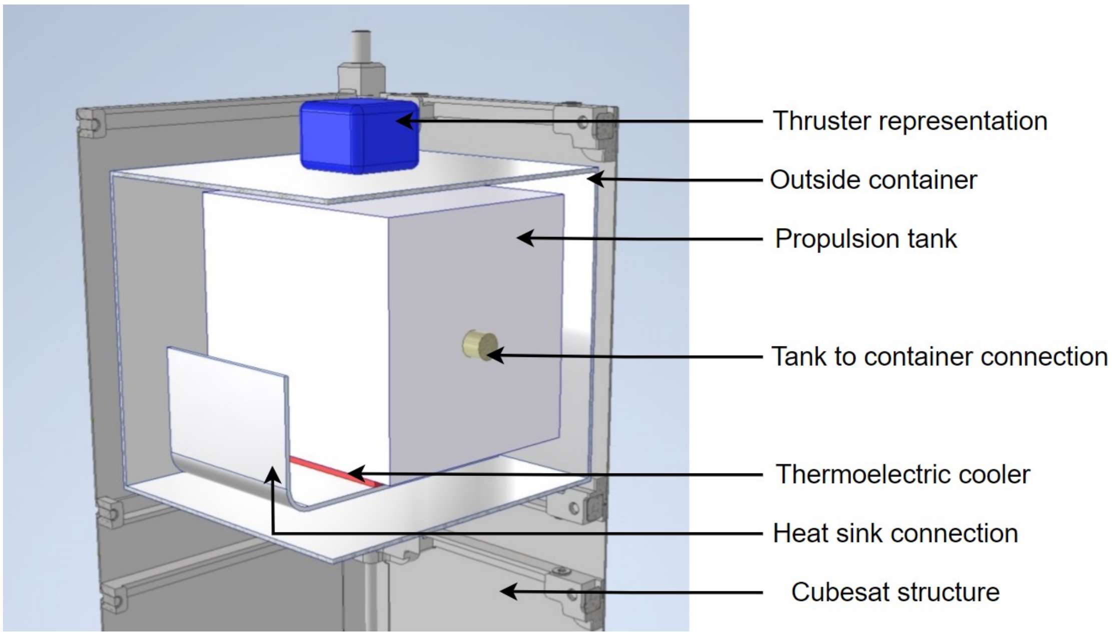

(b) Annotated view of the block design, highlighting key components: the thruster representation, outside container, propulsion tank, tank to container connection, thermoelectric cooler, heat sink connection, and CubeSat structure.

Figure 4.3: Conceptual block design for the propellant storage system.

The outside container dimensions have to fit within the structure of the CubeSat, and are therefore $83.2\,x\,73.7\,x\,74$ mm, which complies with requirement 4.2 from table 3.1, this includes the components except for the thruster which is located on top. The thruster has been represented with a box with dimensions $20x20x10$ mm [22], this is because the thruster and its interfaces are outside the scope of this thesis project. The tank, with internal dimensions $59.7\,x\,53\,x\,55$ mm, and other components will fit in the outside container which is attached to the CubeSat structure.

In order to minimize heat transfer between the tank and the spacecraft, the outer surface of the tank will consist of polished aluminum, providing low infrared emissivity and high reflectivity. Polished aluminum is commonly used in spacecraft thermal control systems to reduce radiative heat absorption from nearby warm components by reflecting incoming infrared radiation. At thermal wavelengths, low emissivity corresponds directly to low absorptivity and high reflectance, making such surfaces highly effective for radiative isolation.

The tank will be held in place via 3 tank to container connections made of Polycarbonate. The TEC will be located on the bottom of the tank to limit the influence it will have on other components. The heat sink connection is an aluminum plate connected to the TEC with thermal glue. It will transfer the heat from the hot side of the TEC to the outside container which is then connected to the entire CubeSat structure for passive thermal management, this ensures that the heater does not overheat. Since the heater is directly attached to a thermally conductive propulsion storage tank, the heat will be gradually dispersed to the whole propulsion tank. This ensures that the surface area to heat or cool the propellant is optimal.

4.3.3. Power usage

This section provides an analysis of the power consumption of the propellant storage system. The analysis considers the power requirements of individual electrical components across identified operational phases: pre-operational, standby, and operational. Values presented are derived from component data sheets or calculated. A breakdown of the power consumption of each consumption is presented in Table 4.5.

Table 4.5: Estimated power consumption per component across operational phases

Component	Pre-operational (W)	Standby (W)	Operational (W)
TEC	20	0	2.84 [5]
Pressure Sensor	0.025	0.025	0.025
Temperature Sensor	$\sim$	$\sim$	$\sim$
Solenoid Valve	0	0	0.05
Micro Servo [6]	$\sim$	$\sim$	$\sim$
Total Power usage	20.025	0.025	2.865

The main influence on the power consumption throughout all 3 phases is the TEC, as this component has a significantly higher power consumption than the other components. The power consumption of the temperature sensor is negligible, and hence represented by a $\sim$. The power consumption of the micro servo is also considered to be negligible as it is only used occasionally to switch between operational phases, and is therefore not a continuous power consumer throughout the different phases.

4.3.4. Operating principles

Pressure retention

When the sublimated water vapor is expelled through the nozzle, the internal pressure is lowered to below the vapor pressure which then induces more water to sublimate. As the propellant is depleted, the ”left over” volume will have to be substituted either physically/mechanically or with extra propellant substituting this added volume in the storage unit. A physical or mechanical solution would increase complexity of the system, but substituting the extra volume with extra propellant means some propellant will not be able to be expelled by the thruster. To calculate the maximum amount of propellant that would have to remain as a pressurant in the storage unit, the following conditions have been assumed:

$$\text{Pressure, } P = 600\,\text{Pa}$$
$$\text{Volume, } V = 1.74 * 10^{-4}\,\text{m}^3$$
$$\text{Ideal Gas Constant, } R = 8.314\,\text{J/(mol·K)}$$
$$\text{Temperature, } T = 273.15\,\text{K}$$

Using Ideal Gas Law [8], the number of moles of water vapor n can be calculated:

[5] This value has been determined by taking the value that corresponds with 1 mg/s when looking at the values for the range of power required for specific mass flow rates in chapter 4.3.4 (0.77 W for 0.27 mg/s and 5.57 W for 1.96 mg/s).

[6] This component will be used to control the heat sink connection, by attaching/detaching the hot side of the TEC to the heat sink.

$$n = \frac{P \cdot V}{R \cdot T} = \frac{600 * 1.74 * 10^{-4}}{8.314 * 273.15} = 4.5978 * 10^{-5} \tag{4.1}$$

With the molar mass of water $M_{H2O} = 18.015$ g/mol, the amount of water vapor can be calculated:

$$m = n \times M_{H2O} = 4.5978 * 10^{-5}\, mol \times 18.015\, g/mol = 8.283 * 10^{-4}\,\text{g} = 0.8283\, mg \tag{4.2}$$

This means the maximal amount of unusable propellant on board under the assumed conditions, if the increasing left over volume would not be filled physically/mechanically, would only be 0.83 mg. Which is less than 1% of the total mass of the propellant (calculated in chapter 5.1.1). Considering this, it seems irrational to use a physical or mechanical way to maintain the left over volume constant as the propellant depletes.

Energy input

As the ice molecules sublimate they lose heat, this is because sublimation is an endothermic process, which means it requires energy. When ice sublimates, it absorbs heat from its surroundings, causing a cooling effect. To quantify this, the heat absorbed is calculated as the product of the rate of sublimation and the enthalpy of sublimation of water, which is around 2.84 MJ/kg at the given vapor pressure. In order to maintain a constant mass flow into the plenum at the preferred pressure, temperature equilibrium must be maintained. For this to be the case, a heating element should pump the same amount of heat into the ice as is lost due to sublimation. The amount of heat can be calculated by multiplying the sublimation rate $\frac{dm_{ice}}{dt}$ with the enthalpy of sublimation ΔH_{sub}.

$$Q_{in} = \left(\frac{dm_{ice}}{dt}\right) \cdot \Delta H_{sub} \tag{4.3}$$

The system will be in dynamic equilibrium where the sublimation rate $\frac{dm_{ice}}{dt}$ is in equilibrium with the mass flow rate of the thruster $\dot{m}_{thruster}$. Earlier studies have shown that the LPM with a Grid of Small Slots (GSS) chip has a measured mass flow rate of $0.27 - 1.96$ mg/s when tested at plenum pressures of 300 Pa. As enthalpy of sublimation is primarily a function of temperature rather than pressure [50], the earlier assumed enthalpy of 2.84 MJ/kg at $0°$C and a vapor pressure of 600 Pa can still be used. This approximation will induce minimal errors in the calculation for the required heat input to sustain sublimation at lower pressures. The amount of heat required under these conditions would range from 0.77 W to 5.57 W. A study provided by Maxence, D [51] showed that for that specific setup, once exceeding an ideal heater power of 2.8 W, the sublimation process is no longer facilitated by the heat added but counteracts the very process. This is assuming that no heat loss occurs in the system. Given the required mass flow rate of 1 mg/s as stated in the list of requirements (Table 3.1), the required energy input would be 2.84 W which corresponds perfectly with the ideal heater power determined by Maxence, D.

Heat sink connection requirements

It is crucial that the heat on the hot side of the TEC is effectively dissipated, particularly during the initial phase when the TEC actively cools the propellant to induce freezing. In addition to this the TEC also generates its own heat due to internal electrical resistance. This heat needs to be adequately dissipated, if not the hot side temperature (T_h) will rise excessively. Which results in a reduced cooling capacity (Q_c) and thus overall efficiency of the cooling process, as the performance of a TEC degrades significantly with increasing temperature difference ($\Delta T = T_h - T_c$). Also, an excessively high T_h can exceed the TEC's maximum operating temperature, potentially resulting in permanent damage or device failure. For these reasons, proper thermal management of the TEC's hot side is paramount for successful and reliable operation. The TEC has a maximal allowable temperature of $80\,°C$ taking into account a safety margin of 20% as provided by the list of requirements, this means the maximum allowable temperature is $64\,°C$. Heat dissipation required to keep the hot side below $64\,°C$ can simply be calculated by considering all significant heat sources within the system.

Given that the maximum allowable power input for the entire system is $20\,W$, and the TEC is the main power consumer, this value will be used for further calculations. The TEC's Coefficient of Performance (COP) is 0.5, so the cooling load during the freezing process (Q_c) can be calculated using equation 4.4:

$$Q_c = P_{input} * COP = 20 * 0.5 = 10\,W \tag{4.4}$$

This gives a total heat load on the hot side of the TEC Q_h of $10\,W$. To ensure that the hot side of the TEC remains below $64\,°C$, the thermal resistance (R_{th}) of the heat sink connection must be sufficiently low. Equation 4.5 can be used to calculate the maximum allowed thermal resistance:

$$R_{th} = \frac{T_{h,max} - T_{env}}{Q_h} \tag{4.5}$$

where,

$R_{th} =$ Maximum allowable thermal resistance of the heat sink connection (K/W)

$T_{h,max} =$ Maximum allowable temperature of the hot side($°$C)

$T_{env} =$ Temperature of the surrounding environment ($°$C)

For this initial calculation, an environmental temperature T_{env} of $40\,°$C is assumed, which approximates the temperature of nearby surfaces as well as the surface the heat sink connection will be linked too. Substituting the known values:

$$R_{\text{th}} = \frac{64°C - 40°C}{10\,W} = 2.4\,K/W \tag{4.6}$$

Therefore, the heat sink connection should have a thermal resistance of 2.4 K/W or lower. This value represents the upper limit for the entire thermal path, starting with the thermal glue, the aluminum plate itself and the connection area to the heat sink. One of the simplifying assumptions in chapter 4.3.1 assumed perfect contact so the thermal contact resistance between components will be neglected. The thermal resistance for each connection can be calculated using equation 4.7:

$$R_{th} = \frac{L}{kA} \tag{4.7}$$

Where L is the thickness of the material in meters, k is the thermal conductivity of the material in w/(mK), and A is the cross-sectional area through which heat flows in m^2. The thermal resistance values for the thermal glue and the heat sink connection are presented in Table 4.6. The dimensions and geometry parameters are derived from the simplified block design presented in Figure 4.3b, while material properties have been obtained from Felba, J. [52] for the thermal glue and Spira, Natalie [53] for the heat sink connection.

Table 4.6: Thermal resistance calculation for thermal glue and heat sink connection

Component	L (m)	A (m^2)	k (W/(mK))	R$_{th}$ (K/W)
Thermal glue	0.0002	0.0016	2.5	0.05
Heat sink connection	0.001	0.00004	167	0.1497

These calculations show a thermal resistance of 0.05 K/W for the thermal glue and 0.1497 K/W for the aluminum plate. Meaning the connection to the heat sink must have a thermal resistance of 2.2 K/W or less to maintain the TEC's hot side temperature below $64\,°$C during operation in the worst conditions. The required contact surface area of the heat sink connection can then be calculated by rewriting equation 4.7, resulting in a minimal required contact area of $A = 2.722$ mm^2.

4.4. Concept design conclusion

This chapter detailed the systematic design process for the sublimation-based solid-state propellant storage concept. It started with the conceptualization of 3 different 2D designs, using a morphological chart, after which concept 2 was carefully selected for further development using a pairwise comparison method with weighted characteristics. After this, the same selection process was used again to select the components to be used on the design. The outcomes of these processes were used to synthesize these selected elements into a simplified 3D block design. This block design, along with a number of key assumptions, power usage estimations, and operating principles, serves as the basis for the modeling and simulation process presented in the subsequent chapter.

5
Modeling and Simulation

This chapter outlines the model and simulation of the behavior of the system. It looks into the detailed definitions of the geometrical model, material properties and boundary conditions. It identifies 3 different operational phases considered for the simulation, and uses these 3 phases to find out key information about the performance characteristics of the design.

5.1. Methodology

This section outlines the methodology used to model and simulate the behavior of the system. While the preliminary calculations in chapter 4.3 provided reasonable estimations for power usage and input, they relied on simplified assumptions and did not fully capture the dynamic thermal behavior or intricate heat transfer mechanisms of the actual proposed design. For these reasons this section details the definitions of the geometrical model, material properties and boundary conditions to enable a more accurate simulation. It identifies 3 different operational phases considered for the simulation. And utilizes these phases to derive important insights into the performance characteristics of the system.

5.1.1. Geometry

Tank geometry

The storage tank is modeled as a rectangular prism with initial dimensions of $59.7\,x\,53\,x\,55\,mm$. Which gives a volume of the storage tank of $V = L \cdot W \cdot H \quad = 1.74 * 10^{-4}\,m^3$.

Listing 5.1: Section of code of the init method for the TankGeometry class, initializing tank dimensions.

```
def __init__(self, length, width, height):
    self.length = 0.0597  # in meters
    self.width = 0.053    # in meters
    self.height = 0.055  # in meters
```

The `__init__` method of the `TankGeometry` class initializes the dimensions of the tank: `length`, `width`, and `height` in meters.

Initial propellant volume and mass

The propellant occupies a fraction of 90% of the total tank internal volume, so the initial mass of the propellant can be calculated by; $M_{initial} = \rho_{propellant} \cdot V_{propellant} = \rho_{propellant} \cdot (V_{tank} \cdot \eta) = 0.144\,kg$

Listing 5.2: Section of code of the method for calculating volume change due to ice formation within the TankGeometry class.

```
def volume_change(self, ice_volume):
    """Calculate volume change due to ice formation."""
    return ice_volume * 0.09  # 9% expansion
```

The `volume_change` method calculates the change in volume due to the freezing of the propellant. It takes the `ice_volume` as an argument and returns a value that is 9% of the `ice_volume`, representing the expansion.

Time-dependent volume and mass

As the propellant sublimates, its mass decreases over time. The mass at time t is given by: $M(t) = M_{initial} - \dot{m} \cdot t$. Where $\dot{m}$ is the sublimation rate in kg/s and t the time in seconds.

The following section of code calculates the total mass of the propellant that has sublimated (`mass_lost`) at a given time `t` by multiplying the constant sublimation rate (`SUBLIMATION_RATE`) with the elapsed time.

It then determines the remaining mass of the propellant (`mass_remaining`) by subtracting the `mass_lost` from the initial mass (`self.mass_initial`). So here the `SUBLIMATION_RATE` constant ($1\,mg/s$) represents the mass flow rate of the sublimating propellant.

Listing 5.3: Section of code calculating the total mass lost and remaining mass of propellant over time due to sublimation.

```
# Total mass lost at time t
mass_lost = SUBLIMATION_RATE * t  # kg

# Remaining mass at time t
mass_remaining = self.mass_initial - mass_lost
```

Time-dependent surface area

The surface area of the propellant is an important parameter as it directly influences the rate of heat transfer required for sublimation. To maintain a constant sublimation rate of 1 mg/s, enough heat needs to be supplied to the propellant's surface. The area available for this heat exchange changes as the propellant sublimates. At any given time t, the surface area $A(t)$ of the rectangular ice block is calculated as:

$$A(t) = 2 \cdot (L(t) \cdot W(t) + L(t) \cdot H(t) + W(t) \cdot H(t)) \tag{5.1}$$

The following Python code implements the calculation of these time-dependent dimensions and the resulting surface area:

Listing 5.4: Section of code showing methods within the IceBlockSublimation class for calculating time-dependent ice block dimensions and surface area.

```
def dimensions_at_time(self, t):
    """
    Calculate the dimensions of the ice block at time t.
    Assumes uniform sublimation from all sides.
    """
    # Total mass lost at time t
    mass_lost = SUBLIMATION_RATE * t  # kg

    # Remaining mass at time t
    mass_remaining = self.mass_initial - mass_lost

    # If mass_remaining <= 0, the ice block is fully sublimated
    if mass_remaining <= 0:
        return 0, 0, 0

    # Remaining volume at time t
    volume_remaining = mass_remaining / DENSITY_ICE  # m^3

    # Scale factor for dimensions (assuming uniform sublimation)
    scale_factor = (volume_remaining / self.ice_volume_initial) ** (1/3)

    # Current dimensions at time t
    length = self.length_initial * scale_factor
    width = self.width_initial * scale_factor
    height = self.height_initial * scale_factor

    return length, width, height

def surface_area_at_time(self, t):
    """
    Calculate the surface area of the ice block at time t.
    """
    length, width, height = self.dimensions_at_time(t)
    if length == 0 and width == 0 and height == 0:
        return 0  # Ice block is fully sublimated
    return self.calculate_surface_area(length, width, height)  # m^2
```

The `dimensions_at_time(self, t)` method calculates the evolving dimensions based on the constant sublimation rate (`SUBLIMATION_RATE`), initial mass (`self.mass_initial`), and density of ice (`DENSITY_ICE`), assuming uniform sublimation. The `surface_area_at_time(self, t)` method then uses these dimensions to compute the current surface area via the `calculate_surface_area` method. This time-dependent surface area is essential for determining the heat input required to sustain the desired sublimation rate.

5.1.2. Material properties

To accurately model the thermal behavior of the propellant and the storage tank, it is essential to accurately define the material properties. The following python code listings show some sections of the materials code. First the base `Material` class has been defined:

Listing 5.5: Section of code for base Material class defining common material properties for the simulation.

```
class Material:
    def __init__(self, name, density, specific_heat, thermal_conductivity):
        self.name = name
        self.density = density  # kg/m^3
        self.specific_heat = specific_heat  # J/kg*K
        self.thermal_conductivity = thermal_conductivity  # W/m*K
```

This base class, `Material`, defines the different material properties that have been used for the model. It initializes fundamental properties such as `name`, `density`, `specific_heat`, and `thermal_conductivity`.

Next, the properties of the propellant in its solid state have been defined:

Listing 5.6: Section of code of the WaterSolid class, inheriting from Material, defining properties specific to ice.

```
class WaterSolid(Material):
    def __init__(self):
        super().__init__(name="Water␣(solid)",
                         density=917,  # Approximate density of ice at 0°C (kg/m^3)
                         specific_heat=2100,  # Approximate specific heat of ice (J/kg*K)
                         thermal_conductivity=2.2)  # Thermal conductivity of ice (W/m*K)
        self.melting_point = 273.15
```

The `WaterSolid` class is derived from the `Material` class and defines the specific properties of ice, including its density, specific heat, thermal conductivity and melding point. For the sublimation process, the latent heat of sublimation is a critical property, defined as follows:

Listing 5.7: Section of the SublimationWater class, defining the latent heat of sublimation for water.

```
class SublimationWater:
    latent_heat = 2.83e6  # Latent heat of sublimation of water (J/kg)
```

The `SublimationWater` class defines the `latent_heat`, which represents the energy required to convert one kilogram of ice directly into water vapor. It should be noted that for this specific model, the latent heat of sublimation, along with other properties like density, specific heat and thermal conductivity for both solid and vaporized water, are treated as constant values. This assumption is considered sufficiently accurate as the enthalpy of sublimation is primarily a function of temperature rather than pressure [50]. Provided that the system operates within a narrow temperature range around the triple point of water (as stated in requirements 1.1 and 1.2), the variations in these properties are expected to be negligible. Even though small fluctuations may exist in the actual system, the impact they impose on the overall system behavior was considered less significant for the scope of this conceptual modeling phase in comparison with other factors, such as the changing surface area of the propellant. More complex, variable-property models could be explored in future experimental validation.

Listing 5.8: Section of the Aluminum class, inheriting from Material, defining properties for the tank material.

```
class Aluminum(Material):
    def __init__(self):
        super().__init__(name="Aluminum",
                    density=2700,  # Density of aluminum (kg/m^3)
                    specific_heat=897,  # Specific heat of aluminum (J/kg*K)
                    thermal_conductivity=237)  # Thermal conductivity of aluminum (W/m*K)
```

The Aluminum class, also inheriting from Material, defines the properties of aluminum used for the storage tank. This approach allows for a modular and organized way to manage the material properties used throughout the simulation. And finally, the material of the connection points, polypropylene, is also considered.

Listing 5.9: Section of the Polypropylene class, inheriting from Material, defining properties for connection point material.

```
class Polypropylene(Material):
    def __init__(self):
        super().__init__(name="Polypropylene",
                        density=900,  # Approximate density of polypropylene (kg/m^3)
                        specific_heat=1900,  # Approximate specific heat of polypropylene (J/kg*K
                            )
                        thermal_conductivity=0.15)  # Approximate thermal conductivity of
                            polypropylene (W/m*K)
```

The Polypropylene class, also inheriting from the base Material class, defines the material properties for polypropylene, including its density, specific heat capacity, and thermal conductivity.

5.1.3. Boundary conditions

To accurately model the thermal and mass flow behavior of the system, appropriate boundary conditions have been defined. These conditions precisely determine how heat is transferred and how mass flows within the system.

Thermal Boundary Conditions

The propellant storage system operates within the CubeSat, which is subjected to significant external temperature fluctuations in space due to direct solar heating, Earth albedo and infrared radiation, and the cold of deep space. However, due to the CubeSat's thermal control systems, the internal environment is maintained within a more constrained operational temperature range, fluctuating between $0\,°$C and $40\,°$C. The interaction of the propellant tank with this internal fluctuating temperature is crucial for modeling the system, this means the external heat exchange with the deep space environment directly from the propellant tank itself are considered to be negligible. So the thermal analysis primarily focuses on the internal heat fluctuations present in the CubeSat. Besides these fluctuations, the heat supplied to induce sublimation, the hot side of the TEC, and conductive heat transfer between the tank and the connection points to the outside container are crucial.

Mass Flow Boundary Conditions

The propellant mass loss directly results from the controlled sublimation process, controlled by the supplied heat. The following boundary conditions are applied:

- The sublimation rate is the same as the required mass flow rate. This is because all mass that is sublimated is expected to be expelled through the thruster. This makes the mass flow rate inherently equivalent to the sublimation rate, both measured in mg/s, as there is no expected significant accumulation of vapor within the storage tank (as the vapor that is required to fill up the empty space as the block sublimates is limited, as calculated in chapter 4.3.4 Pressure retention).
- Sublimation occurs at the surface of the ice where the local temperature reaches the sublimation point.
- No external mass enters the system after the initial propellant is loaded.

The mass flow rate and hence the sublimation rate is 1 mg/s as provided by requirement 3.2 from the list of requirements (table 3.1).

Structural Boundary Conditions

The tank is assumed to be structurally rigid and not affected by internal pressure variations, this means the thermal expansion effects are considered to be negligible. In addition to that all interfaces between components are assumed to be perfect so no thermal resistance at the joints.

These boundary conditions ensure for a controlled modeling approach, focusing on the most important interactions that govern the system.

5.1.4. Operational phases

To model the systems behavior across its entire mission duration, the following three operational phases have been identified. This approach allows for the distinct thermal and mass flow characteristics of each phase to be simulated and analyzed, which is crucial for understanding the system's overall performance characteristics.

- **Pre-operational (transient):** Initial phase where the propellant temperature will be lowered from a maximum of $40\,°$ to a freezing temperature of $-1\,°$.
- **Standby (steady-state):** Internal tank pressure will be kept constant at around 600 Pa throughout the orbit with a minimal and maximal internal spacecraft temperature of 0 to $40\,°$C respectively.
- **Operational (steady-state):** Water will be heated to induce sublimation to sustain a mass flow rate of 1 mg/s and a pressure of 600 Pa.

5.2. Results

Pre-operational (transient)

As mentioned earlier, during this phase the liquid water will be frozen to a temperature of $-1\,°$C or roughly 272 K. Given the maximum power requirement of 20 W from table 3.1, and a TEC COP of 0.5, the time this takes can simply be calculated. It is determined by the total heat that needs to be removed from the propellant, and the effective cooling power of the TEC. The total heat removed (Q_{total}) accounts for three distinct phases, as calculated in the `calculate freezing time` function within the Python code lines 27 to 38 (see appendix C.3).

1. Cooling liquid water to freezing point:

$$Q_{liquid} = m_{water} \cdot c_{p,liquid} \cdot (T_{initial} - T_{freezing}) \tag{5.2}$$

2. Phase change of water:

$$Q_{fusion} = m_{water} \cdot \Delta H_{fusion} \tag{5.3}$$

3. Cooling solid ice to target temperature:

$$Q_{solid} = m_{water} \cdot c_{p,solid} \cdot (T_{freezing} - T_{target}) \tag{5.4}$$

where,

m_{water} = mass of the water propellant (`water_mass`)

$c_{p,liquid}$ = specific heat capacity of liquid water (`water_liquid.specific_heat`)

$c_{p,solid}$ = specific heat capacity of ice (`water_solid.specific_heat`)

$T_{initial}$ = initial temperature of the liquid water ($40°$C or 313.15K) (`initial_temp`)

$T_{freezing}$ = freezing temperature of water ($0°$C or 273.15 K) (`water_liquid.melting_point`)

T_{target} = desired final temperature of the frozen propellant ($-1°$C or 272.15 K) (`target_temp`)

ΔH_{fusion} = latent heat of fusion for water (`fusion_water.latent_heat`)

The total heat to be removed is then:

$$Q_{total} = Q_{liquid} + Q_{fusion} + Q_{solid} \tag{5.5}$$

The effective cooling power ($P_{cooling}$) of the TEC is calculated from its input power (P_{input}) and its COP:

$$P_{cooling} = P_{input} \cdot \text{COP} \tag{5.6}$$

Finally, the freezing time (t_{freeze}) is given by:

$$t_{freeze} = \frac{Q_{total}}{P_{cooling}} \tag{5.7}$$

This calculation considers the "worst case scenario" where the ambient temperature is $40\,°$C. Figure 5.1 shows a graph of the freezing time (hours) as a function of the cooling power limit (W). Here the freezing time speaks for itself, and the cooling power limit is the maximum rate at which heat is removed from the water by the TEC. This is a controlled parameter (independent variable) in the simulation expressed in W (J/s). With a maximum allowed power of 20 W, the freezing time would be 2 hours, 11 minutes and 24 seconds. The code used to produce this graph can be found in appendix C.3.

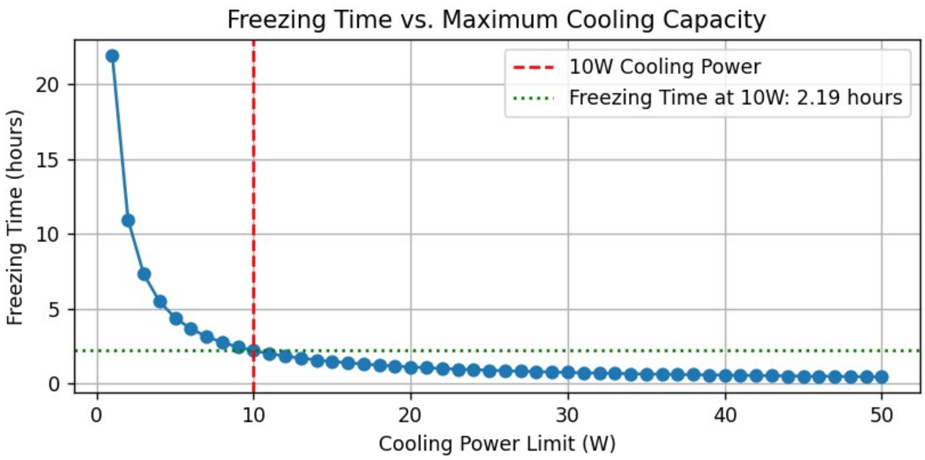

Figure 5.1: Freezing time as a function of maximum cooling capacity for the propellant storage system. The graph illustrates the inverse relationship between cooling power limit (W) and the time required to freeze the propellant (hours).

Another crucial aspect that was be considered for the pre-operational phase, is whether or not the design is strong enough to survive the launch. The list of requirements specifies that the storage must be able to withstand 4.9 G. With a propellant mass of 0.1436 kg, as calculated earlier. Now to calculate the total amount of force experienced during launch, equation 5.8 can simply be used.

$$F = m * g = 0.1436 * 9.81 * 4.9 = 6.9028\,N \tag{5.8}$$

The direction of this force depends on the orientation of the spacecraft in the launcher, since the exact orientation is hard to predict, all relevant orientations have been evaluated. Figure 5.2a shows the results of the Von Mises Stress analysis, figure 5.2b the results of the 1st Principal Stress analysis, both of one specific orientation.

An overview of maximum stresses for other spacecraft launch orientations is provided in Table 5.1.

Table 5.1: Overview of maximum stresses for different spacecraft launch orientations.

Maximum stress [MPa]	Orientation 2	Orientation 3	Orientation 4
Von Mises	1.862	1.924	2.888
1st Principal	2.482	1.962	2.992

Since the maximum yield strength of aluminum 6061, is 275 MPa, and the ultimate tensile strength is approximately 310 MPa, the stresses presented in Table 5.1 are well within safe limits for aluminum. Similarly for the 3D printed connection points made of polypropylene, with a tensile strength of 20 to 40 MPa, can also withstand these stress levels without any issue. Therefore, these stresses experienced during spacecraft launch pose no concern for both materials in all orientations in terms of structural integrity.

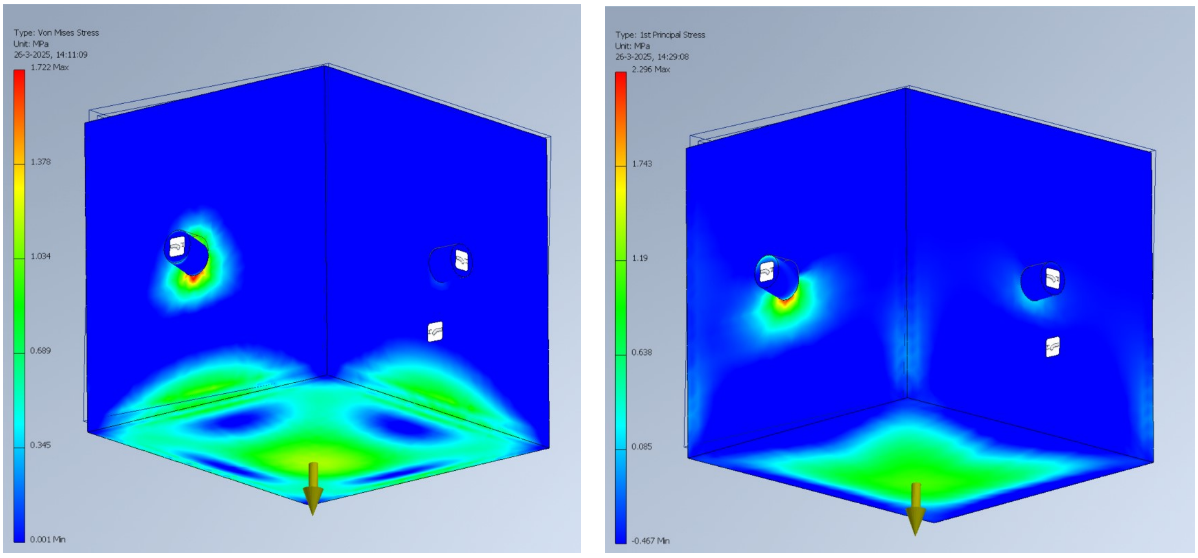

(a) Maximum Von Mises stress $1.722\ MPa$.

(b) Maximum 1st Principal stress $2.296\ MPa$.

Figure 5.2: Autodesk Inventor stress analysis for an upward-oriented launch.

Standby (steady-state)

The main purpose of this analysis was to determine the conductive heat flow towards the propellant tank for a detachable or a continuous heat sink connection. For this analysis, the internal radiative heat transfer between system components has not be considered. Only conductive heat transfer between solid components, giving insight into the conduction characteristics of the two different options.

For the pre-operational phase calculation the thermal boundary conditions were assumed to be adiabatic, this would mean the propellant temperature would stay stable at any time throughout the orbit without requiring any cooling power. In reality the tank is not perfectly insulated as it has some connection points to hold it in place. In order to calculate the heat flowing towards the tank through these connection points equation 5.9 has been used:

$$Q = \frac{k \cdot A \cdot \Delta T}{L} \tag{5.9}$$

Where,

$$Q = \text{Total heat load (W)}$$
$$k = \text{Thermal conductivity (W/mK)}$$
$$A = \text{Cross sectional area (m}^2\text{)}$$
$$\Delta T = \text{Temperature difference (K)}$$
$$L = \text{Connection thickness (m)}$$

The two standby phase scenarios that were considered were subjected to a 90-minute Low Earth Orbit (LEO), where the spacecraft's internal temperature fluctuates between $0\,°C$ and $40\,°C$, as specified in the design requirements (Table 3.1). The internal tank temperature is maintained at $-1\,°C$.

For the first case, a detachable heat sink link, during the standby phase, the storage tank will be connected with the spacecraft only with 3 cylindrical connection points with a diameter of 6 mm and a length of 5 mm, made of the printable relatively thermally isolating material polypropylene. This gives a minimal and maximal heat flow of 0.0025 and 0.1043 W respectively. For the second case where the heat sink link is considered to be continuous, it would increase the connection area with at least 2.722 mm^2 (as calculated in chapter 4.3.2), with the thermal conductivity of aluminum, resulting in a minimal and maximal heat flow of 1.7947 and 73.5634 W respectively. Although this analysis does not consider the thermal resistance of the TEC itself or radiative heat transfer, it still shows the impact of a continuous heat sink and thus why a detachable heat sink is crucial for the design. Figure 5.3 compares the heat flow for both options. The code used to produce these graphs can be found in appendix C.4.

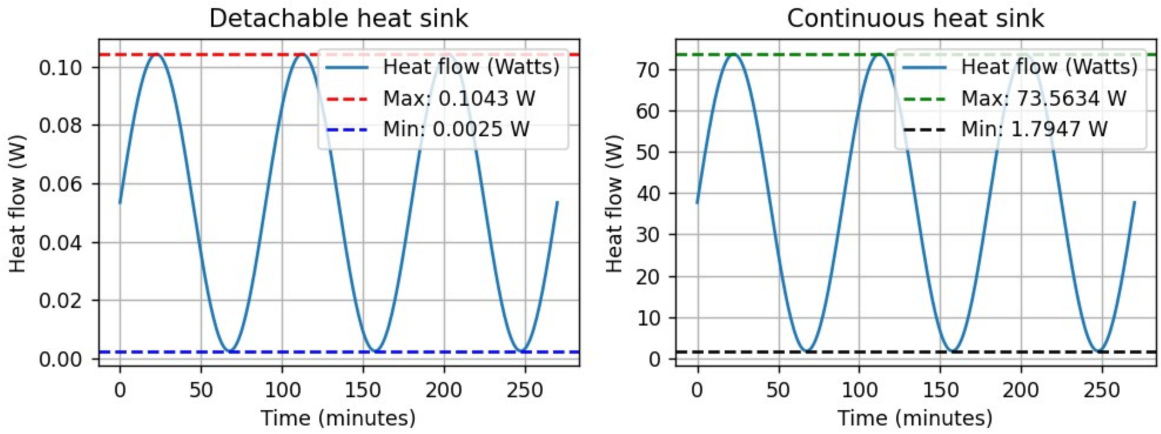

Figure 5.3: Heat flow to storage tank as a function of internal spacecraft temperature for detachable and continuous heat sinks, assuming a constant tank temperature of $-1\,°C$.

These results prove the effectivity of the detachable heat sink and why it is an important design characteristic. Lower heat flow towards the propellant during standby phase (or in general), also means lower required energy input to keep the propellant temperature stable, and thus higher system efficiency. The exemption from this analysis does however not mean that the radiative heat transfer should be completely ignored, therefore the following 'worst-case scenario' calculation for radiative heating of the propellant tank has been considered to give insight into this form of heat transfer present within the CubeSat:

The propellant tank is maintained at approximately $-1\,°C$, and a radiating internals of the CubeSat is at the maximal temperature of $40\,°C$. In order to minimize heat transfer between the tank and the spacecraft, the outer surface of the tank consists of polished aluminum, providing low infrared emissivity and high reflectivity.

Using the Stefan-Boltzmann equation:

$$Q = \epsilon \sigma A (T_{hot}^4 - T_{cold}^4) \tag{5.10}$$

where,

$\epsilon =$ Emissivity $= 0.09$ (characteristic of highly reflective surfaces in the infrared, such as polished aluminum[54])

$\sigma =$ Stefan-Boltzmann constant $= 5.67 \times 10^{-8}$ W/(m^{2}K^4)

$A =$ Area $= 2(LW+LH+WH) = 0.0201$ m^2 (based on external tank dimensions of $61.7 \times 55 \times 57$ mm)

$T_{hot} = 40\,°C$ or 313.15 K (maximal internal spacecraft temperature)

$T_{cold} = -1\,°C$ or 272.15 K (propellant tank temperature)

This gives a value of:

$$Q_{rad} = 0.09 \times 5.67 \times 10^{-8} \times 0.0201 \times (313.15^4 - 272.15^4)$$
$$Q_{rad} = 0.4236 \text{ W}$$

Operational (transient)

With the given dimensions, density and sublimation rate, the operational time could simply be calculated by dividing the total propellant mass by the sublimation rate. Giving a total operational time for the thruster of 143623.25 seconds which is 39.90 hours or 1.66 days. Using the latent heat of sublimation, the total energy required to sublimate all the propellant could be calculated by multiplying it with the propellant mass, giving a value of 406453.78 J. This combined with the operational time allowed to calculate for the total required power, giving a value of 2.83 W which corresponds with the value calculated in chapter 4.3.4. However, this simple approximation does not accurately reflect the actual behavior. The aim is to match the sublimation rate of the propellant to the mass flow rate of the thruster, which is set at 1 mg/s. As the surface area of the propellant decreases due to depletion, the required heat to maintain this sublimation rate also decreases. This relationship is shown in figure 5.4. The code used to produce these graphs can be found in appendix C.5.

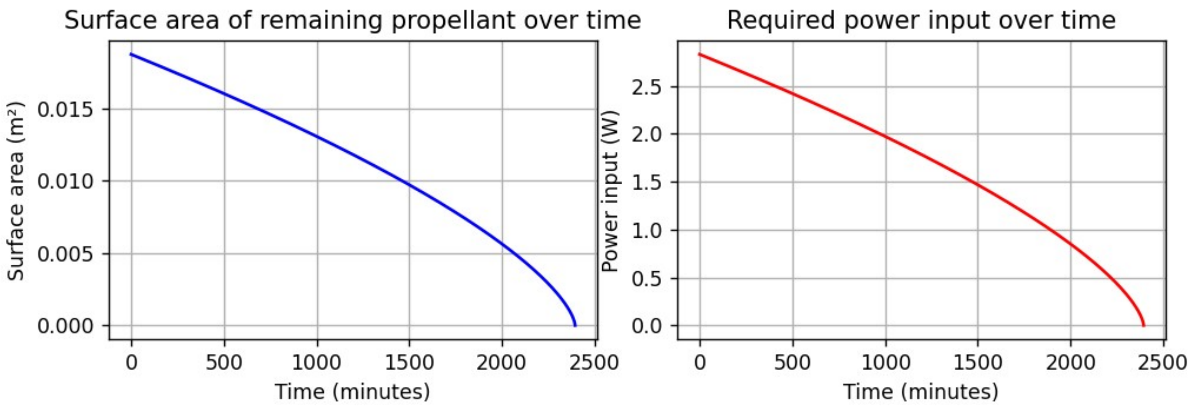

Figure 5.4: Time-dependent behavior of propellant surface area and required power. The left graph shows the surface area of remaining propellant over time, while the right graph shows the corresponding required power input over time to maintain a constant sublimation rate of 1 mg/s. Earlier hand calculations validate the model as both determine an initial power input of 2.83 W.

The graph on the left shows how the surface area of the remaining propellant decreases over time as the propellant sublimates, the graph on the right shows the corresponding reduction in the required power input to maintain a constant sublimation rate and a pressure of 600 Pa in the tank. As the propellant depletes, the surface area for sublimation decreases, which coincidentally decreases the heat input needed to sustain the same sublimation rate. So the power input supplied by the TEC decreases steadily over time.

5.3. Key insights

For the overall system it is crucial to limit the amount of power required throughout the different phases of the mission. In order to do so, it became apparent that good thermal insulation is critical. Models show that a detachable heat sink and small connection points are required to limit the amount of heat flow between the tank and the rest of the spacecraft to below the specified amount mentioned in requirement 3.1 from the list of requirements in chapter 3.5.

There is an inverse exponential relationship between freezing time and maximum cooling power. Freezing time decreases significantly as cooling power increases initially, but this benefit decreases significantly after a certain point, which proves that excessively high cooling power is not necessarily much more beneficial. During operation it is important to note that the input heat is variable throughout the lifetime of the thruster. As the surface area of the remaining propellant decreases, so should the heat input. This will ensure a stable mass flow rate of 1 mg/s.

Even though the models gave interesting insights into the behavior of the system, due to a number of assumptions and simplifications, the model may not reflect the real system completely accurately. Nevertheless these insights will help to further develop the simplified block design into a final design.

6 Detailed design

This chapter presents the detailed design for the sublimation-based solid-state propellant storage.

6.1. Design overview

Figure 6.2 shows a representation of the final design. In total there are 26 different components, out of which 13 are Commercial Off The Shelf items (COTS) and 13 are custom made. Figure 6.1a and 6.1b show numbers that correspond to the item number given to each component in table 6.1.

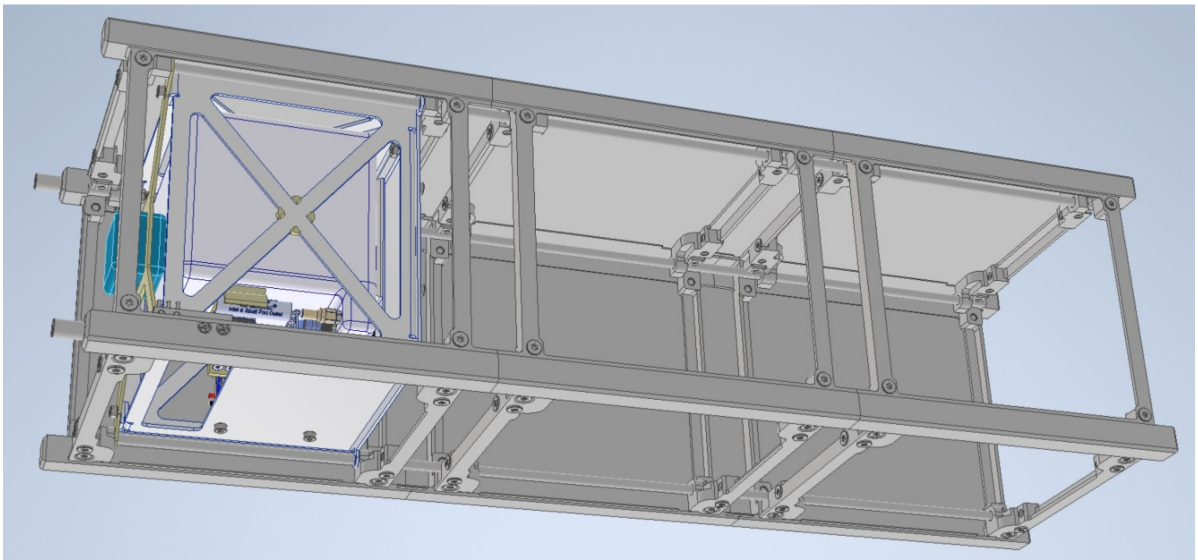

Figure 6.1: Frontside view of the fully integrated propellant storage system.

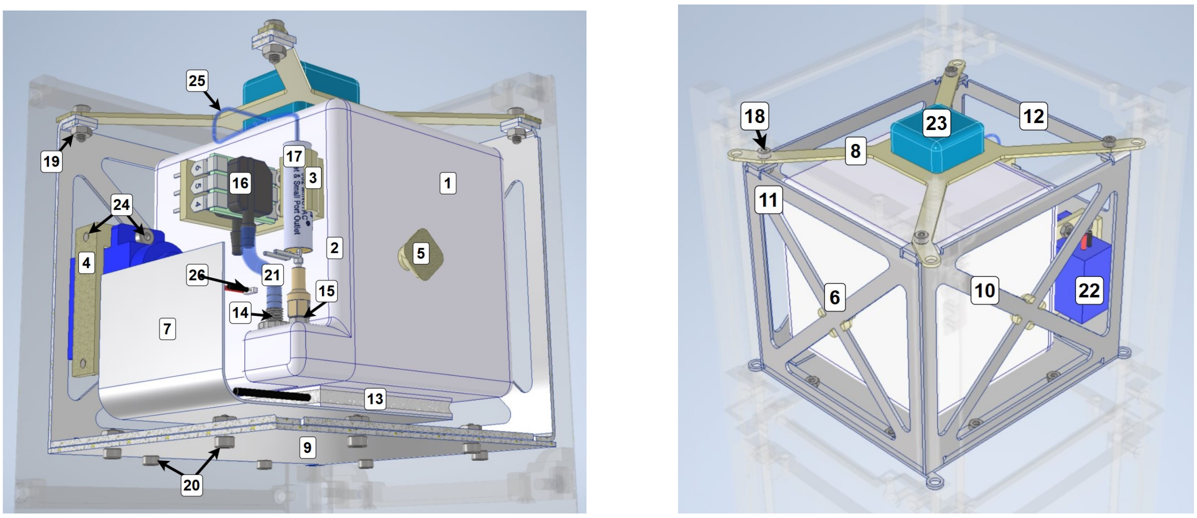

(a) Quarter section view showing internal component arrangement.

(b) Backside view detailing connections and external components.

Figure 6.2: Detailed views of the integrated propellant storage system, with components numbered according to Table 6.1

Table 6.1 provides a list of the different components, their category (custom or COTS), material, mass, and how they should be produced (if applicable). The total dry mass of the system is 137.11 g, giving a wet mass of 280.11 g, which is lower than the maximum wet mass provided in the list of requirements of 380 g.

Table 6.1: Parts list for the detailed design.

ITEM	QTY	TITLE	TYPE	MASS [g]	PRODUCTION/PRICE
1	1	Storage tank 1	Custom	40	Deep drawing, Drilling
2	1	Storage tank 2	Custom	12	Deep drawing, Drilling, Milling
3	1	Tank attachment	Custom	1	3D Printing
4	1	Servo connector	Custom	1	3D Printing
5	2	Tank connection 1	Custom	Negligible	3D Printing
6	1	Tank connection 2	Custom	Negligible	3D Printing
7	1	Heat sink connection	Custom	5	Laser cutting, Bending
8	1	Outside container top	Custom	1	3D Printing
9	1	Outside container bottom	Custom	17	Laser cutting
10	1	Outside container wall 1	Custom	8	Laser cutting, Bending
11	1	Outside container wall 2	Custom	7	Laser cutting, Bending
12	1	Outside container wall 3	Custom	12	Laser cutting, Bending
13	1	peltier_40x40	COTS	5	45 EUR
14	1	Barbed tube fitting	COTS	1	< 1 EUR
15	1	Compression fitting	COTS	1	< 1 EUR
16	1	Pressure sensor	COTS	2	N.A.
17	1	Solenoid valve	COTS	2	N.A.
18	6	M2 x 0.4mm 6mm SCREW	COTS	0.21*6 = 1.26	< 1 EUR
19	18	M2 x 0.4mm HEX NUT	COTS	0.11*18 = 1.98	< 1 EUR
20	11	M2 x 0.4mm 4mm SCREW	COTS	0.17*11 = 1.87	< 1 EUR
21	1	Pressure sensor tube	COTS	1	< 1 EUR
22	1	Micro servo	COTS	8	4.5 EUR
23	1	Thruster representation	Custom	6	3D Printing
24	4	M2 x 0.4mm 8mm SCREW	COTS	0.25*4 =1	< 1 EUR
25	1	Mass flow tube	COTS	1	< 1 EUR
26	1	Temperature sensor	COTS	1	29 EUR

6.2. Design considerations

6.2.1. Materials

To ensure stable thermal conditions, the design incorporates both practical thermal management strategies and a careful selection of materials for different components. First of all the storage tank is made of polished aluminum which reduces radiative heat absorption. Besides this when the thruster is not operational, the storage tank is physically connected to the rest of the system at only three connection points (item 5 and 6). It is crucial that these connection points are as thermally insulating as possible. And although not as crucial, this is also the case for the top of the outside container (item 8) and the pressure sensor/solenoid valve connector (items 3). As the temperature fluctuations induced by the TEC should not affect these components. For the connection points and the pressure sensor/solenoid valve connector it is also important they are not too rigid and have ”some give” to them as they will be locked by clicking onto the outside container or have to click the solenoid valve into place. These components are custom 3D printed components made of polypropylene.

Polypropylene is chosen for its excellent thermal insulation properties, low density and relatively low stiffness [55], making it ideal for minimizing conductive heat transfer and overall system mass. While it offers moderate resistance to radiation, less than high-performance polymers like PEEK or ULTEM, its compatibility with standard 3D printing processes makes it a practical and accessible choice for manufacturing the custom components at TU Delft [56].

All other custom components (item 1,2,7,9,10,11 and 12) are made of aluminum 6061, this includes most of the outside container, the heat sink connection and the storage tank itself. Aluminum 6061 is selected due to its favorable combination of thermal conductivity, mechanical strength, maneuverability and availability. Aluminum 6061 offers relatively high thermal conductivity compared to most common aluminum alloys. It supports even heat distribution and helps to mitigate localized thermal stresses, which helps to mitigate localized thermal stress which is a crucial consideration for all mentioned components. Although it is not the strongest alloy available, the strength-to-weight ratio is sufficient for the structural demands on the design as visible in the strength analysis presented in chapter 5.2, in figure 6.3. Comparing aluminum 6061 to aluminum 5052, which has better corrosion resistance but lower strength [57], aluminum 6061 provides improved mechanical performance while maintaining sufficient corrosion resistance. Another common alloy, aluminum 7075, offers superior strength, but in return has reduced weldability, higher brittleness, and significantly lower corrosion resistance, which makes it less suitable [53]. Especially for the heat sink connection, due to its elastic properties a plate of aluminum 6061 would spring back into place if it was bend a little, which is exactly what the heat sink connection (item 7) needs to do. It would only deform if the yield strength of around 276 MPa were to be exceeded.

The chosen alloy is widely available, cheap, and compatible with the preferred manufacturing techniques like laser cutting and bending. These properties make it a well suited solution for producing the custom and precise components with small fabrication complexity.

6.2.2. Structural integrity

The main structure of the system, the outside container (item 9, 10, 11, 12, excluding the top, item 8), is made of the earlier mentioned aluminum 6061. The container is designed in such a way that the less strong top, is not required for the overall structural integrity of the system. The 1 mm thickness chosen for the outside container plates is a common and available thickness suitable for laser cutting. This thickness is also sufficient to withstand the peak load of 4.9 g's, which occurs during launch, while still maintaining a low weight. This is demonstrated by the strength analysis shown in figure 6.3, it shows a maximal displacement of only 0.0532 mm at the critical points. Table 6.2 shows the details of the conducted analysis.

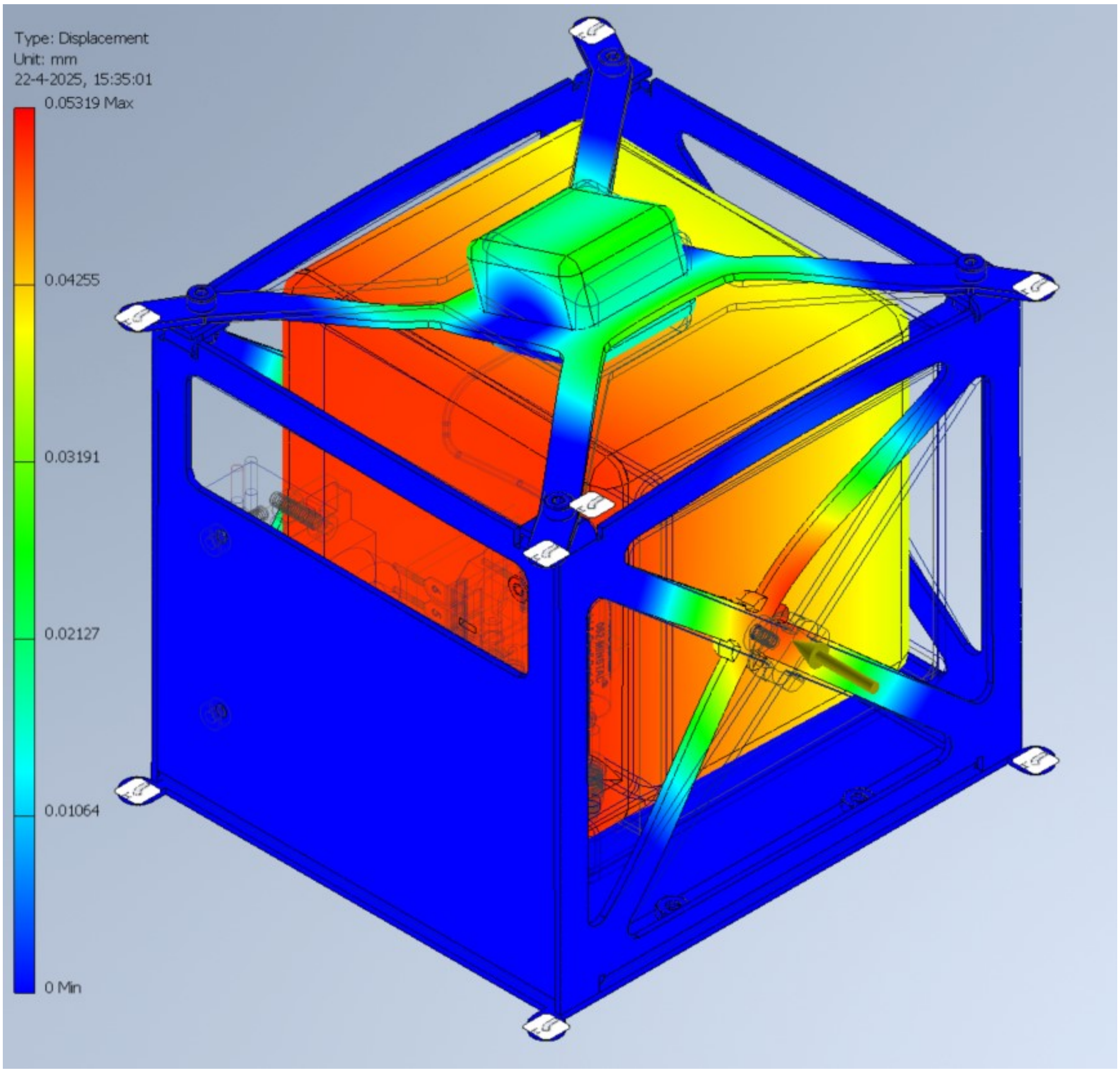

Figure 6.3: Simulated displacement of the propellant storage and thruster (modeled as a solid block of ABS plastic) under a launch with 4.9 g's.

Table 6.2: Summary of Structural Analysis Simulation Details

Category	Detail
Software	Autodesk Inventor Professional
Analysis Type	Static Stress Analysis (Finite Element Analysis - FEA)
Model Representation	The propellant storage system was modeled as an assembly of custom components crucial for structural integrity, including aluminum 6061 for the main tank and outside container, and polypropylene for connection points. The thruster was represented as a solid block of ABS plastic.
Boundary Conditions	Fixed supports were applied to the four mounting points where the system integrates with the CubeSat structure, simulating a rigid attachment to the CubeSat's internal frame.
Load Application	A uniform acceleration of 4.9 g's (where g = 9.81 m/s^2) was applied. The load was applied independently along the three principal orthogonal axes (representing different launch orientations - upward, sideways, and downward) to identify the worst-case displacement scenarios. The total force on the system was calculated as $F = m \cdot g_{\text{launch}} = 0.1436\ kg \cdot 9.81\ m/s^2 \cdot 4.9 = 6.9028\ N$.
Meshing	An automatic mesh generation was utilized by Autodesk Inventor, consisting of 556714 nodes and 328324 elements. Local refinements were applied to areas of expected high-stress concentration such as connection points and sharp corners, with an average element size of 0.100 (as a fraction of bounding box length), a minimum element size of 0.200 (as a fraction of average size), a grading factor of 1.500, and a maximum turn angle of 60.00 degrees. The element type used was typically solid tetrahedral elements, with a part-based measure utilized for the assembly mesh.
Key Outputs	A maximal displacement of 0.0532 mm at the critical points, proving the structural integrity of the design under expected loads.

6.2.3. Assembly

The system is integrated in the CubeSat via the metal bars within the structure of the CubeSat. It fits exactly within one of the 3 units available in a 3U CubeSat. It is designed in such a a way that the components can be assembled using simple tools and by clicking them into place. But some components require a more complex manufacturing process before they can be assembled into the system. The system can be divided in two main subsystems, the storage tank and the outside container.

Storage tank

Due to the hollow shape of the storage tank, it needs to be manufactured in two parts and welded together (item 1 and 2). Before the two parts are welded together, for storage tank 1; the 3 screws and tank connections (item 5 and 6) need to be inserted. And for storage tank 2; the barbed tube fitting, compression fitting and tank attachment (item 14, 15 and 3) need to be inserted and attached. After this is done the two parts can be welded together. After this the TEC has to be fixed to the heat sink link and the storage tank using a thermal adhesive. This acts as a glue, while still allowing for excellent thermal conductivity.

Outside container

The outside container can be assembled using screws and bolts. As the micro servo is attached to the outside container, and not the storage tank, this section of the outside container (item 12) has to be assembled after the storage tank has been clicked into place.

6.3. Prototyping

In order to get an idea what the design would look and feel like in real life all parts have been 3D printed. To accommodate for the expansion of the plastic, all bolt holes have been enlarged tot 2.2 mm for the 3D printed model. Due to budged limitations the COTS components have not been acquired and are therefore not present in the model. Figure 6.4 shows the 3D printed model from two angles.

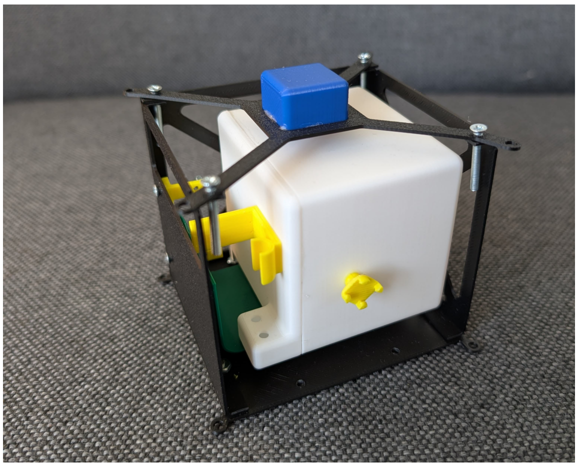

(a) Front view showing integrated components within the design structure.

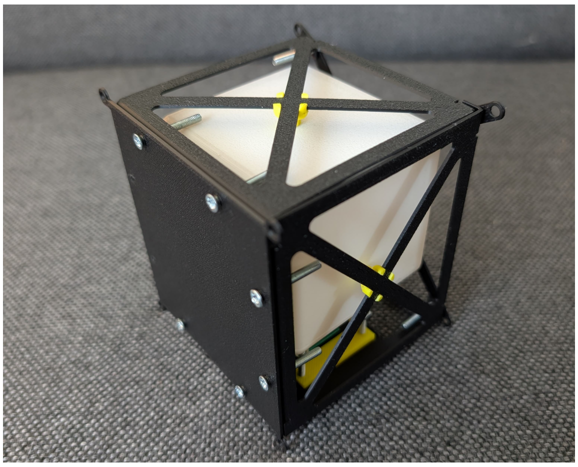

(b) Back view showing the design structure.

Figure 6.4: 3D printed prototype of the propellant storage system design.

While the digital CAD model allowed for understanding of the overall geometry and design, the construction of the physical 3D-printed model gave additional insights that did not become clear in the CAD environment. These include subtle spatial relationships and practical design considerations. A summary of these insights is provided in the following table:

Table 6.3: Observed problems which became apparent from the physical model and their respective solutions.

ITEM	TITLE	OBSERVED PROBLEM	SOLUTION
3	Tank attachment	Holes too close to the edge, easy to break when screwing tight.	Holes moved 1 mm towards center.
4	Servo connector	Holes too close to the servo, hard to screw bolts in.	Holes moved 2 mm closer to the edge.
5	Tank connection 1	Fit too tight, hard to snap on the outside container structure, had to be filed to fit.	Enlarged dimensions.
6	Tank connection 2	Fit too tight, hard to snap on the outside container structure, had to be filed to fit.	Enlarged dimensions.
12	Outside container wall 3	Holes not in line with new servo connector.	Holes location moved 2mm to accommodate new servo connector holes location.

The final design mostly aligns with the design presented in chapter 6.1. The required changes that were presented in chapter 6.3 have been applied. All drawings of the custom components with their applied changes can be found in appendix D.

7 Conclusion

This thesis successfully developed a design for a sublimation-based solid-state propellant storage system for a low-pressure micro-resistojet thruster. The work addressed the growing demand for simpler, more efficient micropropulsion solutions for small satellites like CubeSats. A solid-state propellant was found to be a promising choice due to its ability to simplify the feed system by leveraging sublimation as a pressurization mechanism.

To answer the main research question:

> ***What is the optimal design for a sublimation-based solid-state propellant storage system for a low-pressure micro-resistojet thruster?***

a careful concept development and selection process was carried out, resulting in a system design composed of 26 individual components, out of which 13 are commercial of the shelf (COTS) items and 13 are custom made. The design uses aluminum 6061 and polypropylene for their thermal and structural properties, features thermal control via a thermoelectric cooler and detachable heat sink, and incorporates pressure and temperature sensors, and a solenoid valve for propellant regulation. A 3D-printed prototype validated aspects of the assembly and spatial configuration, further reinforcing the design's feasibility.

The sub-questions were addressed as follows:

1. ***What are the key functions the propellant storage must fulfill to ensure successful operation for a low-pressure micro-resistojet thruster?***
   To ensure reliable operation, the propellant storage system must fulfill several key functions, including maintaining thermal control, allowing for propellant expansion when freezing, preventing leaks, ensuring structural robustness, and integrating effectively within the CubeSat. These were specified into six core functions: heating element placement, propellant expansion accommodation, thermal insulation, material selection, leak prevention, and system integration. Each function was explored through a morphological chart, listing four viable solutions per function. This structured approach guided the concept development process which eventually culminated in the selection of concept 2. Consisting of a propellant tank made of an aluminum alloy with extra internal volume to accommodate for the expanding propellant, where the heat input surrounds the propellant, with modular mounting that enables it to be easily assembled into the CubeSat.
2. ***Which components, materials, and design characteristics are most suitable for fulfilling the key functions required by the propellant storage system?***
   The most suitable components were selected to be a thermoelectric cooler to heat/cool the propellant, pressure transducer for pressure measurements, RTD for temperature measurements and finally a solenoid valve to control the propellant flow to the thruster. Besides these and the other COTS components, 13 custom components were designed, and made from either aluminum 6061 or polypropylene, reflecting an optimized material selection where each material's properties align with the requirements of its specific component. Aluminum 6061 was used for thermally conductive and load-bearing parts, while polypropylene was used for thermally isolating sections. Design characteristics such as surrounding heating, a detachable heat sink (using a micro servo engine actuated heat sink connection), and sensor integration support efficient and reliable operation.

3. ***What is the optimal propellant storage design configuration for improved efficiency and reliability?***
   The final design minimizes energy usage by utilizing a detachable heat sink, limiting the amount of unwanted heat flowing towards the propellant tank, thereby limiting the system's overall energy requirements. It is thermally insulated using insulating or reflective materials like polypropylene and polished aluminum. This also ensures reliability as stable thermal conditions are critical for consistent sublimation and prevents issues like re-solidification or inefficient phase transitions, which could disrupt propellant feed and affect the overall system performance. Furthermore, the material selection contributes to the system's structural integrity, allowing it to reliably withstand expected launch loads without failure. The ability to precisely control the temperature and isolate the tank when not in use significantly enhances the system's long-term operational stability and reduces the risk of thermal transients affecting performance.
4. ***What is the most effective method for modeling the behavior and performance of the propellant storage?***
   Physics-based Python models and CAD models were developed to simulate thermal behavior, sublimation dynamics, and launch conditions. The models revealed key behaviors such as the inverse exponential relationship between freezing time and cooling power. The nonlinear heating requirement for a constant sublimation rate, as the necessary heat input decreases over time due to the reduction in propellant surface area. And the modeling highlighted that a detachable heat sink is crucial to limit unwanted heat flow during all phases but specifically the standby phase. The models also confirmed the structural robustness of the design under expected launch conditions, showing that stresses and displacements remained well within safe limits for the chosen materials.
5. ***What is the most effective method for testing the behavior and performance of the propellant storage?***
   A 3D-printed prototype allowed for preliminary spatial and assembly testing. It highlighted issues not visible in the CAD environment, such as misaligned holes, insufficient space for fastening components, and overly tight fits between parts. These practical challenges were resolved by adjusting hole positions, enlarging dimensions for better fit, and refining component geometries. The prototype also offered a tangible understanding of the spatial constraints within the design structure and informed minor but critical design improvements.

Overall, the project lays a strong foundation for more reliable and efficient micropropulsion systems. It demonstrates the practical feasibility of sublimation-based approach for future microsatellite missions. Moving forward, experimental validation of the thermal management system, and the development of an integrated control system, are essential for advancing this design, these and other recommendations have been presented in the subsequent chapter.

8 Recommendations

To further advance the sublimation-based solid-state propellant storage system design, several critical areas require additional research and development, focusing on both performance optimization and practical implementation.

Thermal regulation: In order to get a better idea of the thermal regulation of the spacecraft, a comprehensive assessment of the passive thermal management of the overall satellite is paramount. Even though the design incorporates elements to carefully regulate the heat transfer, further experimental validation is needed to confirm that the passive measures of the spacecraft are sufficient to prevent certain components from overheating. Mainly during the pre-operational phase as this is the phase with the highest risk of overheating. Closely related to this is the need to determine the maximal allowable cooling time during the pre-operational phase so that the system won't overheat. This testing will ensure the TEC can efficiently freeze the propellant without leading to overheating issues within the spacecraft.

3D-printed parts characteristics: Given the use of 3D printing for several of the custom components, real life characteristics might differ from the simulated uniform material characteristics as 3D-printed parts often exhibit a matrix-like structure not accounted for in the models. This matrix structure likely means that the parts could in fact be stronger and more thermally resistant than the initial models suggest. Validating these properties through testing is essential for accurate performance prediction and might allow a next iteration of the design to have smaller connection points for example, and overall better performance.

Control system: The development of an integrated control system for the overall system, and specifically for the heat sink connection is another key recommendation. Such a system would enable precise and automated control over the cooling and heating cycles, by operating the micro servo. This integration is crucial for having consistent propellant temperature and pressure, optimizing efficiency, and ensuring reliable long-term operation of the thruster.

Outside container top improvement: The structural integrity of the outside container top requires attention in future design iterations. While the current simplified block design served its purpose for initial modeling, a finalized design should integrate the outside container top with the thruster itself. This would ensure sufficient strength for all mission phases, particularly during launch, and provide a more cohesive and durable overall propulsion module.

Potential utilization of internal spacecraft temperature: Future iterations of the design could investigate the potential to use the spacecraft's internal temperature to heat the propellant by leveraging the heat sink connection. Since the spacecraft internal temperature ranges from 0 to $40\,°C$, the heat sink connection can serve a dual purpose by selectively enabling thermal conductivity between the propellant tank and the spacecraft structure. This could completely take over the heating of the propellant, which means the relatively inefficient TEC module would no longer be required and can be replaced by a cooling element.

Dynamic stress analyses: While the static stress analysis performed on the propellant storage system demonstrated its structural integrity under 4.9 g launch load conditions, future work should also consider the dynamic launch conditions. Launch events subject the design to vibrations and shock loads that a static analysis could not fully capture. Therefore it is recommended that subsequent design iterations include an analysis to identify the natural frequencies of the system and ensure they do not coincide with the expected launch frequencies, which could lead to resonant amplification and higher stresses. This would provide a more accurate and comprehensive assessment of the system's structural integrity, enhancing its reliability under dynamic conditions.

References

[1] Angelo Cervone, Alexandru Mancas, and Barry Zandbergen. “Conceptual design of a low-pressure micro-resistojet based on a sublimating solid propellant”. In: *Acta Astronautica* 108 (Mar. 2015), pp. 30–39. ISSN: 0094-5765. DOI: 10.1016/J.ACTAASTRO.2014.12.003.

[2] X. Y. Ye et al. “Study of a vaporizing water micro-thruster”. In: *Sensors and Actuators A: Physical* 89.1-2 (Mar. 2001), pp. 159–165. ISSN: 0924-4247. DOI: 10.1016/S0924-4247(00)00540-9.

[3] Barry T.C. Zandbergen. *Thermal Rocket Propulsion*. 2.09. Delft, 2022.

[4] Dr. A. Cervone. *AE4S07-READER*. Tech. rep. Delft: TUDelft, 2022.

[5] Kristina Lemmer. “Propulsion for CubeSats”. In: *Acta Astronautica* 134 (2017), pp. 231–243. ISSN: 0094-5765. DOI: https://doi.org/10.1016/j.actaastro.2017.01.048. URL: https://www.sciencedirect.com/science/article/pii/S0094576516308840.

[6] Daduí C Guerrieri et al. “Fabrication and characterization of low pressure micro-resistojets with integrated heater and temperature measurement”. In: *Journal of Micromechanics and Microengineering* 27.12 (Oct. 2017), p. 125005. DOI: 10.1088/1361-6439/aa90fb. URL: https://dx.doi.org/10.1088/1361-6439/aa90fb.

[7] Ahmed Nosseir and Angelo Cervone. “Feed and Pressurization Systems and Architectures for Green Chemical Micro-Propulsion”. In: Oct. 2024, pp. 135–160. ISBN: 978-3-031-62573-2. DOI: 10.1007/978-3-031-62574-9{_}5.

[8] Steven L Garrett. “Ideal Gas Laws”. In: *Understanding Acoustics: An Experimentalist’s View of Sound and Vibration*. Cham: Springer International Publishing, 2020, pp. 333–356. ISBN: 978-3-030-44787-8. DOI: 10.1007/978-3-030-44787-8{_}7. URL: https://doi.org/10.1007/978-3-030-44787-8_7.

[9] Akshay Reddy Tummala and Atri Dutta. “An Overview of Cube-Satellite Propulsion Technologies and Trends”. In: *Aerospace* 4.4 (2017). ISSN: 2226-4310. DOI: 10.3390/aerospace4040058. URL: https://www.mdpi.com/2226-4310/4/4/58.

[10] Marsil A.C. Silva et al. “A review of MEMS micropropulsion technologies for CubeSats and PocketQubes”. In: *Acta Astronautica* 143 (Feb. 2018), pp. 234–243. ISSN: 0094-5765. DOI: 10.1016/J.ACTAASTRO.2017.11.049. URL: https://www.sciencedirect.com/science/article/pii/S0094576517304290.

[11] Andrew D Ketsdever, Riki H Lee, and Taylor C Lilly. “Performance testing of a microfabricated propulsion system for nanosatellite applications”. In: *Journal of Micromechanics and Microengineering* 15.12 (Oct. 2005), p. 2254. DOI: 10.1088/0960-1317/15/12/007. URL: https://dx.doi.org/10.1088/0960-1317/15/12/007.

[12] A Cervone et al. “Green micro-resistojet research at Delft University of Technology: new options for Cubesat propulsion”. In: *CEAS Space Journal* 9.1 (2017), pp. 111–125. ISSN: 1868-2510. DOI: 10.1007/s12567-016-0135-3. URL: https://doi.org/10.1007/s12567-016-0135-3.

[13] Robert S Legge, Emily B Clements, and Adam Shabshelowitz. “Enabling microsatellite maneuverability: A survey of microsatellite propulsion technologies”. In: *2017 IEEE MTT-S International Microwave Symposium (IMS)*. 2017, pp. 229–232. DOI: 10.1109/MWSYM.2017.8059082.

[14] Aerojet Rocketdyne. *Modular Propulsion Systems Innovative Propulsion solutions for CubeSats and SmallSats*.

[15] Ahmed E S Nosseir, Angelo Cervone, and Angelo Pasini. “Modular Impulsive Green Monopropellant Propulsion System (MIMPS-G): For CubeSats in LEO and to the Moon”. In: *Aerospace* 8.6 (2021). ISSN: 2226-4310. DOI: 10.3390/aerospace8060169. URL: https://www.mdpi.com/2226-4310/8/6/169.

[16] Aoma Fujimori et al. “AQUARIUS: The World’s First Water-based Thruster Enabled 6U CubeSat to Complete Lunar Flyby”. In: (2023).

[17] Javier Martínez Martínez and Trevor Lafleur. “On the selection of propellants for cold/warm gas propulsion systems”. In: *Acta Astronautica* 212 (Nov. 2023), pp. 54–69. ISSN: 0094-5765. DOI: 10.1016/J.ACTAASTRO.2023.07.031.

[18] Hiroyuki Koizumi et al. “Assessment of Micropropulsion System Unifying Water Ion Thrusters and Water Resistojet Thrusters”. In: *Journal of Spacecraft and Rockets* 56.5 (Apr. 2019), pp. 1400–1408. ISSN: 0022-4650. DOI: 10.2514/1.A34407. URL: https://doi.org/10.2514/1.A34407.

[19] V Fernicola, L Rosso, and M Giovannini. “Investigation of the Ice–Water Vapor Equilibrium Along the Sublimation Line”. In: *International Journal of Thermophysics* 33.8 (2012), pp. 1363–1373. ISSN: 1572-9567. DOI: 10.1007/s10765-011-1128-2. URL: https://doi.org/10.1007/s10765-011-1128-2.

[20] George P. Sutton and Oscar Biblarz. *Rocket Propulsion Elements*. 9th ed. Wiley, 2017.

[21] Daduí C Guerrieri et al. “An analytical model for characterizing the thrust performance of a Low-Pressure Micro-Resistojet”. In: *Acta Astronautica* 152 (2018), pp. 719–726. ISSN: 0094-5765. DOI: https://doi.org/10.1016/j.actaastro.2018.09.008. URL: https://www.sciencedirect.com/science/article/pii/S0094576518300882.

[22] Gabriel Alves Teixeira. “Performance Evaluation of a MEMS-based Low-Pressure Micro-Resistojet (LPM)”. In: *Performance Evaluation of a MEMS-based Low-Pressure Micro-Resistojet (LPM)* (2024).

[23] James M Lafferty and Lawrence G Rubin. “Foundations of Vacuum Science and Technology”. In: *Physics Today* 52.3 (Mar. 1999), pp. 86–88. ISSN: 0031-9228. DOI: 10.1063/1.882616. URL: https://doi.org/10.1063/1.882616.

[24] Wolfgang Wagner et al. “New Equations for the Sublimation Pressure and Melting Pressure of H2O Ice Ih”. In: *Journal of Physical and Chemical Reference Data* 40.4 (Dec. 2011), p. 043103. ISSN: 0047-2689. DOI: 10.1063/1.3657937. URL: https://doi.org/10.1063/1.3657937.

[25] Wolfgang Wagner, A Saul, and A Pruss. “International Equations for the Pressure Along the Melting and Along the Sublimation Curve of Ordinary Water Substance”. In: *Journal of Physical and Chemical Reference Data* 23.3 (May 1994), pp. 515–527. ISSN: 0047-2689. DOI: 10.1063/1.555947. URL: https://doi.org/10.1063/1.555947.

[26] Jill E. Reyer. “Health Effects of Ammonia”. In: *Extreme overexposure to ammonia can cause irreversible pulmonary damage. There, however, is no credible evidence that inhaling a small amount of ammonia leads to chronic lung impairment.* ().

[27] Michael Robin, Thomas Brogan, and Eric Cardiff. “An Ammonia Microresistojet (MRJ) for Micro satellites”. In: *44th AIAA/ASME/SAE/ASEE Joint Propulsion Conference & Exhibit*. DOI: 10.2514/6.2008-5288. URL: https://arc.aiaa.org/doi/abs/10.2514/6.2008-5288.

[28] M K Shilpa et al. “A systematic review of thermoelectric peltier devices: Applications and limitations”. In: *FDMP-Fluid Dynamics & Materials Processing* 19.1 (2023), pp. 187–206.

[29] Shanbin Shi et al. “Phase Change Processes for Thermal Management Systems and Science Investigations”. In: *Biological and Physical Sciences Research in Space 2023-2032* (2021).

[30] Anu Maria. *Introduction to Modeling and Simulation*. Tech. rep. StateUniversityofNewYorkatBinghamton.

[31] C. Rossi et al. “Design, fabrication and modeling of solid propellant microrocket-application to micropropulsion”. In: *Sensors and Actuators A: Physical* 99.1-2 (Apr. 2002), pp. 125–133. ISSN: 0924-4247. DOI: 10.1016/S0924-4247(01)00900-1.

[32] B Zitouni et al. “Thrusters modelling, propellant choice and plume expansion: openPlumeEP capabilities”. In: *the 36th International Electric Propulsion Conference, Vienna, Austria, IEPC-2019*. Vol. 211. 2019.

[33] Jih-Run Tsai. “Overview of satellite thermal analytical model”. In: *Journal of spacecraft and rockets* 41.1 (2004), pp. 120–125.

[34] D. Perez-Grande. *Design and Development of a nano-propulsion thrust bench*. Tech. rep. Delft: DelftUniversityofTechnology, 2010.

[35] R. J. F. Bijster. *Design, Verification and Validation of a Micropropulsion Thrust Stand.* Tech. rep. Deflt: DelftUniversityofTechnology, 2014.

[36] E.H.W. Jansen. “Improvement and validation of test stand performance for novel micropropulsion systems”. PhD thesis. Delft: DelftUniversityofTechnology, 2016.

[37] Thermo Scientific. *Heraeus Vacutherm datasheet*.

[38] Gwendoline Petroffe et al. “Thermal regulation of satellites using adaptive polymeric materials”. In: *Solar Energy Materials and Solar Cells* 200 (Sept. 2019), p. 110035. ISSN: 0927-0248. DOI: 10.1016/J.SOLMAT.2019.110035.

[39] R Osiander et al. “Microelectromechanical devices for satellite thermal control”. In: *IEEE Sensors Journal* 4.4 (2004), pp. 525–531. DOI: 10.1109/JSEN.2004.830297.

[40] Kaifeng Chang, Yu Ying Wang, and Yun Ze Li. “A review of water sublimation cooling and water evaporation cooling in complex space environments”. In: *Progress in Aerospace Sciences* 140 (July 2023), p. 100930. ISSN: 0376-0421. DOI: 10.1016/J.PAEROSCI.2023.100930.

[41] Rainer Feistel and Wolfgang Wagner. “Sublimation pressure and sublimation enthalpy of H2O ice Ih between 0 and 273.16 K”. In: *Geochimica et Cosmochimica Acta* 71.1 (Jan. 2007), pp. 36–45. ISSN: 0016-7037. DOI: 10.1016/J.GCA.2006.08.034.

[42] Jean Francois Castet and Joseph H. Saleh. “Satellite and satellite subsystems reliability: Statistical data analysis and modeling”. In: *Reliability Engineering & System Safety* 94.11 (Nov. 2009), pp. 1718–1728. ISSN: 0951-8320. DOI: 10.1016/J.RESS.2009.05.004.

[43] Jian Guo, Liora Monas, and Eberhard Gill. “Statistical analysis and modelling of small satellite reliability”. In: *Acta Astronautica* 98.1 (May 2014), pp. 97–110. ISSN: 0094-5765. DOI: 10.1016/J.ACTAASTRO.2014.01.018.

[44] Forough Nasihati Gourabi, Maryam Kiani, and Seid H. Pourtakdoust. “Autonomous temperature-based orbit estimation”. In: *Aerospace Science and Technology* 86 (Mar. 2019), pp. 671–682. ISSN: 1270-9638. DOI: 10.1016/J.AST.2019.01.056.

[45] Jeongmoo Huh and Sejin Kwon. “Design, fabrication and thrust measurement of a micro liquid monopropellant thruster”. In: *Journal of Micromechanics and Microengineering* 24.10 (Oct. 2014), p. 104001. ISSN: 0960-1317. DOI: 10.1088/0960-1317/24/10/104001. URL: https://iopscience.iop.org/article/10.1088/0960-1317/24/10/104001.

[46] W. P. Wright and P. Ferrer. “Electric micropropulsion systems”. In: *Progress in Aerospace Sciences* 74 (Apr. 2015), pp. 48–61. ISSN: 0376-0421. DOI: 10.1016/J.PAEROSCI.2014.10.003.

[47] sjamthe. *SpaceX-Launch-analysis*.

[48] SRE-PA & D-TEC staff. “Margin philosophy for science assessment studies”. In: *Margin philosophy for science assessment studies* (June 2012).

[49] J A S de Lima and J Santos. “Generalized Stefan-Boltzmann law”. In: *International Journal of Theoretical Physics* 34.1 (1995), pp. 127–134. ISSN: 1572-9575. DOI: 10.1007/BF00670992. URL: https://doi.org/10.1007/BF00670992.

[50] Demetris Koutsoyiannis. “Clausius–Clapeyron equation and saturation vapour pressure: simple theory reconciled with practice”. In: *European Journal of Physics* 33.2 (Jan. 2012), p. 295. DOI: 10.1088/0143-0807/33/2/295. URL: https://dx.doi.org/10.1088/0143-0807/33/2/295.

[51] D. Maxence, D.C. Guerrieri, and A. Cervone. “Preliminary results of a sublimating propellant tank for dedicated micropropulsion system”. In: ().

[52] J. Felba. “Thermally conductive adhesives in electronics”. In: *Advanced Adhesives in Electronics: Materials, Properties and Applications* (Jan. 2011), pp. 15–52. DOI: 10.1533/9780857092892.1.15.

[53] Natalie Spira. *COMPARING 7075 ALUMINUM VS 6061*. Apr. 2021.

[54] *The radiation heat transfer emissivity coefficients for some common materials like aluminum, brass, glass and many more.* URL: https://www.engineeringtoolbox.com/emissivity-coefficients-d_447.html?utm.

[55] Md. Tanvir Hossain et al. "Research and application of polypropylene: a review". In: *Discover Nano* 19.1 (2024), p. 2. ISSN: 2731-9229. DOI: 10.1186/s11671-023-03952-z. URL: https://doi.org/10.1186/s11671-023-03952-z.

[56] Xin Wang et al. "3D printing of polymer matrix composites: A review and prospective". In: *Composites Part B: Engineering* 110 (2017), pp. 442–458. ISSN: 1359-8368. DOI: https://doi.org/10.1016/j.compositesb.2016.11.034. URL: https://www.sciencedirect.com/science/article/pii/S1359836816321230.

[57] Unionfab. *5052 Aluminum vs 6061: A Comprehensive Comparison*. Sept. 2024.

[58] Ross Montgomery and Robert McDowall. "Basics of Electricity". In: *Fundamentals of HVAC Control Systems* (2008), pp. 30–60. DOI: 10.1016/B978-0-08-055233-0.00002-9.

[59] *What is a Cartridge Heater and how does it work?* URL: https://www.omega.com/en-us/resources/cartridge-heaters#:~:text=A%20cartridge%20heater%20is%20a,in%20the%20heating%20process%20industry..

[60] Faraz Afshari. "Experimental Study for Comparing Heating and Cooling Performance of Thermoelectric Peltier". In: *Politeknik Dergisi* 23.3 (2020), pp. 889–894. DOI: 10.2339/politeknik.713600.

[61] Bin Zhao et al. "Radiative cooling: A review of fundamentals, materials, applications, and prospects". In: *Applied Energy* 236 (Feb. 2019), pp. 489–513. ISSN: 0306-2619. DOI: 10.1016/J.APENERGY.2018.12.018.

[62] Thomas E. Piemme. "Pressure measurement: Electrical pressure transducers". In: *Progress in Cardiovascular Diseases* 5.6 (May 1963), pp. 574–594. ISSN: 0033-0620. DOI: 10.1016/S0033-0620(63)80017-1.

[63] Gustav Gautschi. "Piezoelectric Sensors". In: *Piezoelectric Sensorics: Force Strain Pressure Acceleration and Acoustic Emission Sensors Materials and Amplifiers*. Ed. by Gustav Gautschi. Berlin, Heidelberg: Springer Berlin Heidelberg, 2002, pp. 73–91. ISBN: 978-3-662-04732-3. DOI: 10.1007/978-3-662-04732-3{_}5. URL: https://doi.org/10.1007/978-3-662-04732-3_5.

[64] Yaser Javed, Mohtashim Mansoor, and Irtiza Ali Shah. "A review of principles of MEMS pressure sensing with its aerospace applications". In: *Sensor Review* 39.5 (Jan. 2019), pp. 652–664. ISSN: 0260-2288. DOI: 10.1108/SR-06-2018-0135. URL: https://doi.org/10.1108/SR-06-2018-0135.

[65] T J Bajzek. "Thermocouples: a sensor for measuring temperature". In: *IEEE Instrumentation & Measurement Magazine* 8.1 (2005), pp. 35–40. DOI: 10.1109/MIM.2005.1405922.

[66] *What Is RTD Sensor And How Does It Work?*

[67] Dehui Xu et al. "MEMS-based thermoelectric infrared sensors: A review". In: *Frontiers of Mechanical Engineering* 12.4 (2017), pp. 557–566. ISSN: 2095-0241. DOI: 10.1007/s11465-017-0441-2. URL: https://doi.org/10.1007/s11465-017-0441-2.

[68] wavelength electronics. *What is a thermistor*.

A
2D design concepts

A.1. Concept 1

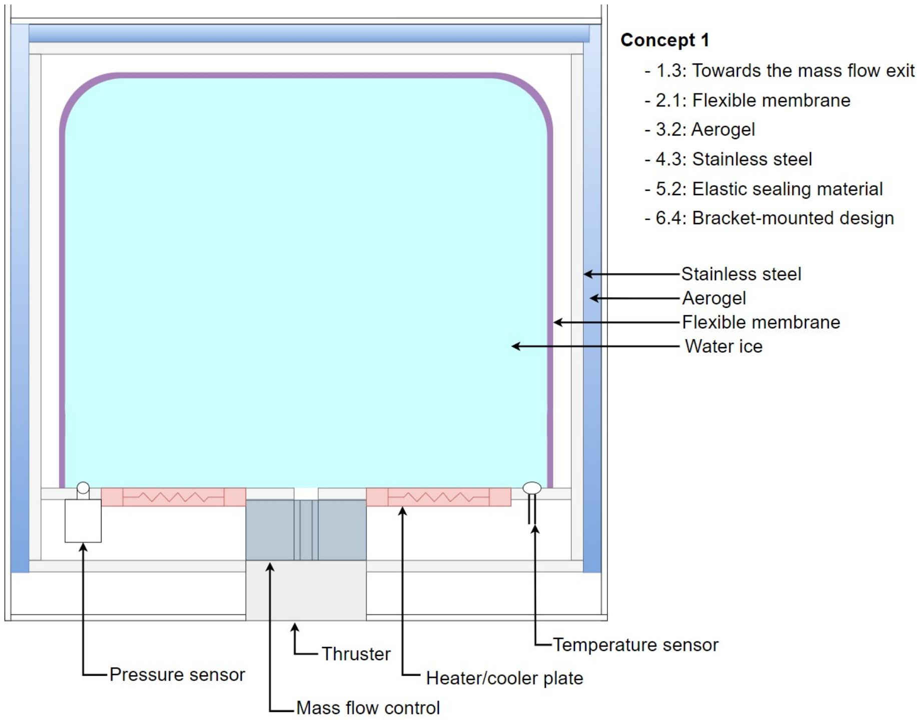

Figure A.1: Annotated 2D schematic representation of concept 1.

A.2. Concept 2

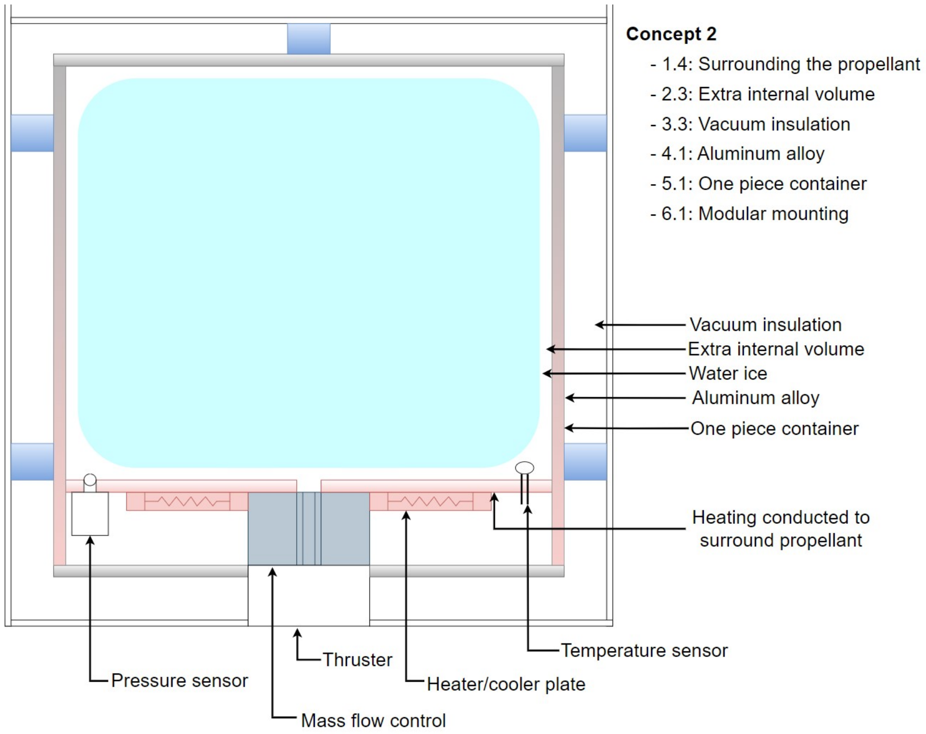

Figure A.2: Annotated 2D schematic representation of concept 2.

A.3. Concept 3

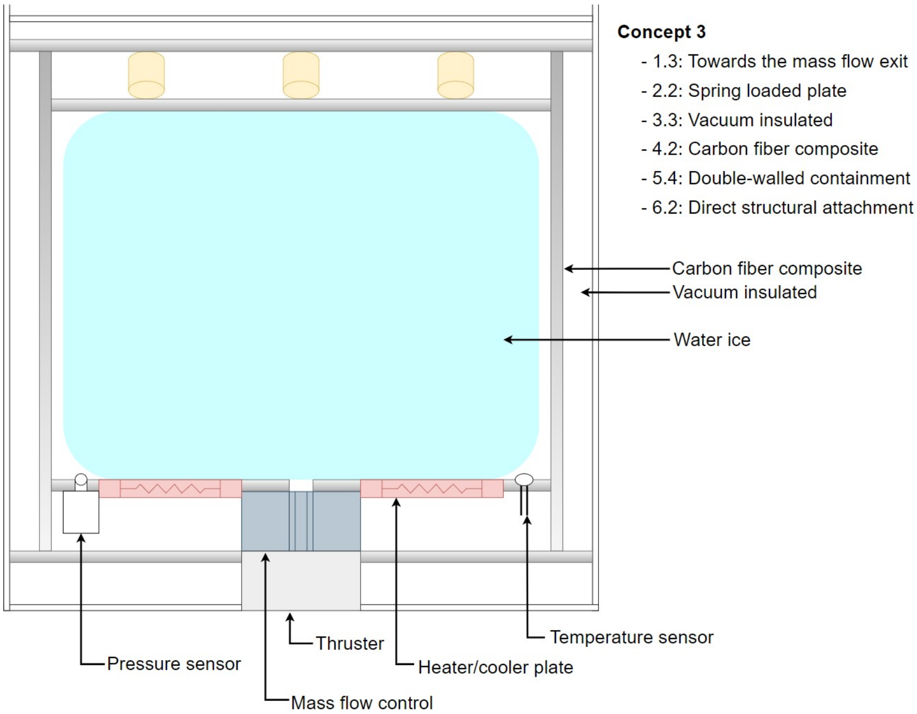

Figure A.3: Annotated 2D schematic representation of concept 3.

B
Component selection process

B.1. Components pros and cons

Propellant heating

Table B.1: Comparison of different propellant heating solutions.

#	Propellant heating solution	Description	Pros	Cons
1	**Resistive heater** [58]	Generates heat through electrical resistance.	Simple design, compact, easy to control and integrate into the power system.	Limited efficiency, potential for hot spots.
2	**Cartridge heater** [59]	Cylindrical heater inserted in hole, generating heat via internal resistive elements.	Delivers concentrated heat, durable, reliable.	Does not provide uniform heat distribution, localized heating only.
3	**Radiative heater**	Uses infrared energy to heat the surface without direct contact.	Efficient in vacuum conditions.	Hard to localize and control heat, slow response time.
4	**Thermoelectric heater (Peltier)** [60]	Uses electrical current to create heat flux, transferring heat from one side to the other heating the propellant.	Precise temperature control, compact and lightweight.	Power-intensive compared to other heating methods, especially at high temperatures.

Propellant cooling

Table B.2: Comparison of different propellant cooling solutions.

#	Propellant cooling solution	Description	Pros	Cons
1	**Radiative cooling** [61]	Passively removes excess heat by emitting thermal radiation into space.	Efficient in vacuum, no moving parts, low maintenance.	Passive cooling process, requires large surface area.
2	**Heat pipes**	Passively transfers heat from hot areas to colder areas using phase-change and capillary action.	Efficient heat transfer, lightweight, no external power required.	Dependent on system orientation and temperature gradient, limited cooling capacity.
3	**Conduction to radiators**	Transfers heat from the propellant to external radiators using conduction.	Simple and reliable design, effective for localized cooling.	Requires large surface area for radiators.
4	**Thermoelectric cooler (Peltier)** [60]	Uses electrical current to create a heat flux and cool the propellant.	Precise temperature control, can be used in small areas.	Power-intensive, low efficiency.

Monitoring pressure

Table B.3: Comparison of different pressure monitoring solutions.

#	Monitoring pressure solution	Description	Pros	Cons
1	**Pressure transducer** [62]	Converts mechanical pressure into electrical signal.	High accuracy	Sensitive to temperature fluctuations. Not fit to measure extremely low pressures
2	**Piezoelectric sensor** [63]	Measures the voltage across a piezoelectric element generated by the applied pressure.	Fast response time, high sensitivity.	Only for dynamic pressure measurements.
3	**Capacitive pressure sensors** [64]	Measures changes in pressure by converting them into changes in capacitance.	High accuracy for low-pressure environments, well suited to harsh environments.	Sensitive to temperature, requires calibration. Not fit to measure extremely low pressures.

Monitoring temperature

Table B.4: Comparison of different temperature monitoring solutions.

#	Temperature Measurement Method	Description	Pros	Cons
1	**Thermocouples** [65]	Measures temperature based on a voltage difference between two metals.	Fast response time and robust under harsh conditions.	Requires calibration, sensitive to electromagnetic interference.
2	**Resistance Temperature Detector (RTD)** [66]	Measures temperature by measuring the change in resistance of a wire as it heats up	High accuracy and repeatability	Relatively slow response time, require excitation current.
3	**Infrared Sensor** [67]	Measures temperature by detecting infrared radiation emitted by objects.	Fast contactless measurements, works under vacuum conditions.	Can only measure surface temperature, less accurate than contact methods.
4	**Thermistors** [68]	Measure temperature through a temperature-dependent resistance change.	High sensitivity, compact, and inexpensive.	Limited accuracy, limited long term stability, susceptible to environmental factors (humidity, pressure and vibrations).

Mass flow control

Table B.5: Comparison of different Propellant management solutions.

#	Management Method	Description	Pros	Cons
1	**Solenoid valve**	Electromechanical valve that opens or closes in response to an electrical signal.	Fast response time, accurate on/off control, commonly used micropropulsion.	Has potential for mechanical failure over time.
2	**Butterfly valve**	Rotating disk valve used to control flow by varying the open area electrically.	Simple lightweight mechanism, low pressure drop when open.	Not very precise at low flow rates, may leak slightly in closed position.
3	**Piezoelectric valve**	Uses piezoelectric materials that deform under voltage to actuate valve movement.	Very fast response time, precise flow control, compact and low power.	Limited displacement and force, may require amplification mechanism.

C

Codes

C.1. Geometry code

Listing C.1: Tank geometry Python code

```python
class TankGeometry:
    def __init__(self, length, width, height):
        self.length = 0.0597  # in meters
        self.width = 0.053    # in meters
        self.height = 0.055  # in meters

    def volume(self):
        """Calculate the volume of the tank."""
        return self.length * self.width * self.height  # m^3

    def surface_area(self):
        """Calculate the surface area of the tank."""
        return 2 * (self.length * self.width + self.length * self.height + self.width * self.height)  # m^2

    def info(self):
        """Print basic info about the tank."""
        print(f"Tank dimensions: {self.length*1e3} mm x {self.width*1e3} mm x {self.height*1e3} mm")
        print(f"Volume: {self.volume():.6f} m^3")
        print(f"Surface Area: {self.surface_area():.6f} m^2")

    def volume_change(self, ice_volume):
        """Calculate volume change due to ice formation."""
        return ice_volume * 0.09  # 9% expansion

    def pressure_increase(self, volume_change, bulk_modulus=8.8e9):
        """Calculate pressure increase based on volume change."""
        return bulk_modulus * (volume_change / self.volume())

    def air_pressure_increase(self, initial_pressure=1e5, initial_air_volume_ratio=0.15):
        """Calculate pressure increase due to air compression."""
        final_air_volume_ratio = initial_air_volume_ratio - 0.09  # 9% expansion reduces air volume
        if final_air_volume_ratio <= 0:
            raise ValueError("Air volume ratio cannot be zero or negative.")
        return initial_pressure * (initial_air_volume_ratio / final_air_volume_ratio)
```

C.2. Materials code

Listing C.2: Material properties Python code

```python
# materials.py
class Material:
    def __init__(self, name, density, specific_heat, thermal_conductivity):
        self.name = name
        self.density = density
        self.specific_heat = specific_heat
        self.thermal_conductivity = thermal_conductivity

# Water Solid definition
class WaterSolid(Material):
    def __init__(self):
        super().__init__(name="Water(solid)",
                         density=917,
```

```
                          specific_heat=2100,
                          thermal_conductivity=2.2)
        self.melting_point = 273.15

# Water Liquid definition
class WaterLiquid(Material):
    def __init__(self):
        super().__init__(name="Water (liquid)",
                          density=1000,
                          specific_heat=4186,
                          thermal_conductivity=0.6)
        self.melting_point = 273.15

# Latent heat of *fusion*
class FusionWater:
    latent_heat = 3.34e5

# Sublimation properties (latent heat for sublimation)
class SublimationWater:
    latent_heat = 2.83e6

# Aluminum definition
class Aluminum(Material):
    def __init__(self):
        super().__init__(name="Aluminum",
                          density=2700,
                          specific_heat=897,
                          thermal_conductivity=237)

# Polypropylene definition
class Polypropylene(Material):
    def __init__(self):
        super().__init__(name="Polypropylene",
                          density=900,
                          specific_heat=1900,
                          thermal_conductivity=0.15)
```

C.3. Freezing time vs. maximum cooling capacity code

Listing C.3: Python code for calculating freezing time.

```
import matplotlib.pyplot as plt
from geometry_final import TankGeometry
from materials_final import WaterLiquid, WaterSolid, FusionWater

def calculate_freezing_time(power):
    """Calculates the freezing time of water in the tank.

    Args:
        power: The power level in Watts.

    Returns:
        The freezing time in seconds.
    """
    # Instantiate the tank geometry here.
    tank = TankGeometry(length=0.0597, width=0.053, height=0.055)

    # Material properties
    water_liquid = WaterLiquid()
    water_solid = WaterSolid()
    fusion_water = FusionWater()

    # Initial and target temperatures
    initial_temp = 40  # °C
    target_temp = -1  # °C

    # Calculate heat to remove
    water_mass = tank.volume() * water_liquid.density * 0.9  # kg, accounting for extra space in the tank to allow ice expansion

```

```python
    # Cooling liquid water
    heat_cooling_liquid = water_mass * water_liquid.specific_heat * (initial_temp - water_liquid.melting_point + 273.15)

    # Freezing water
    heat_freezing = water_mass * fusion_water.latent_heat

    # Cooling solid water
    heat_cooling_solid = water_mass * water_solid.specific_heat * (water_solid.melting_point - target_temp - 273.15)

    total_heat_to_remove = heat_cooling_liquid + heat_freezing + heat_cooling_solid

    # Calculate freezing time
    if power > 0:
        freezing_time = total_heat_to_remove / power
        return freezing_time
    else:
        return float('inf')

# Calculate freezing times for different power levels
power_levels = list(range(1, 51))
freezing_times_seconds = [calculate_freezing_time(power) for power in power_levels]
freezing_times_hours = [time / 3600 for time in freezing_times_seconds]  # Convert seconds to hours

# Get the freezing time at 10W
freezing_time_at_10W = freezing_times_hours[9]  # index 19 corresponds to 10W, as index starts at 0

# Conditional block to only show plot when file is run directly
if __name__ == "__main__":
    # Create the plot
    plt.figure(figsize=(10, 6))
    plt.plot(power_levels, freezing_times_hours, marker='o')
    plt.title('Freezing Time vs. Maximum Cooling Capacity')
    plt.xlabel('Cooling Power Limit (W)')
    plt.ylabel('Freezing Time (hours)')
    plt.grid(True)

    # Add a vertical line at 10W:
    plt.axvline(x=10, color='r', linestyle='--', label='10W Cooling Power')

    # Add a horizontal line at the corresponding freezing time:
    if freezing_time_at_10W < 1e8:  # Check if it was originally NaN
        plt.axhline(y=freezing_time_at_10W, color='g', linestyle=':', label=f'Freezing Time at 10W: {freezing_time_at_10W:.2f} hours')

    plt.legend()
    plt.show()
```

C.4. Heat flow to storage code

Listing C.4: Python Code for heat transfer calculation.

```python
import numpy as np
import matplotlib.pyplot as plt
from materials_final import Aluminum, Polypropylene
# from geometry import TankGeometry # Import if needed later

# Orbital period in minutes
orbital_period = 90

# Time in minutes for three orbits
total_time = 3 * orbital_period
time = np.linspace(0, total_time, 300)  # 300 points for smooth curve

# Temperature calculation (sinusoidal) - Still needed for heat transfer calculation
amplitude = 20  # (max - min) / 2 = (40 - 0) / 2
offset = 20     # (max + min) / 2 = (40 + 0) / 2
```

```
temperature = amplitude * np.sin(2 * np.pi * time / orbital_period) + offset

# Material properties from materials.py
aluminum = Aluminum()
polypropylene = Polypropylene()

# Constants for heat transfer calculation
connector_length_poly = 0.005  # 5 mm in meters
connector_length_alu = 0.001
polypropylene_area = np.pi * (0.003 ** 2) * 3 # Area of three 6mm diameter connectors
aluminum_area = 2.722e-6 # Area of the heat sink connection
num_connectors = 3

# Calculate heat transfer (cooling power) for polypropylene only
temperature_difference = temperature - (-1)  # Temperature difference between connector and tank
heat_transfer_polypropylene_single = (polypropylene.thermal_conductivity * polypropylene_area * temperature_difference) / connector_length_poly
total_heat_transfer_polypropylene = heat_transfer_polypropylene_single

# Calculate heat transfer (cooling power) for polypropylene and aluminium
heat_transfer_aluminum_single = (aluminum.thermal_conductivity * aluminum_area * temperature_difference) / connector_length_alu
total_heat_transfer_combined = (total_heat_transfer_polypropylene + heat_transfer_aluminum_single)

# Calculate max and min cooling power for both cases
max_cooling_power_polypropylene = np.max(total_heat_transfer_polypropylene)
min_cooling_power_polypropylene = np.min(total_heat_transfer_polypropylene)
max_cooling_power_combined = np.max(total_heat_transfer_combined)
min_cooling_power_combined = np.min(total_heat_transfer_combined)

# Plotting - two subplots side by side
fig, (ax1, ax2) = plt.subplots(1, 2, figsize=(16, 6))

# Plot heat transfer for polypropylene only
ax1.plot(time, total_heat_transfer_polypropylene, label='Heat flow (Watts)')
ax1.axhline(y=max_cooling_power_polypropylene, color='red', linestyle='--', label=f'Max: {max_cooling_power_polypropylene:.4f} W')
ax1.axhline(y=min_cooling_power_polypropylene, color='blue', linestyle='--', label=f'Min: {min_cooling_power_polypropylene:.4f} W')
ax1.set_title('Detachable heat sink')
ax1.set_xlabel('Time (minutes)')
ax1.set_ylabel('Heat flow (W)')
ax1.grid(True)
ax1.legend(loc='upper right')

# Plot heat transfer for polypropylene and aluminium
ax2.plot(time, total_heat_transfer_combined, label='Heat flow (Watts)')
ax2.axhline(y=max_cooling_power_combined, color='green', linestyle='--', label=f'Max: {max_cooling_power_combined:.4f} W')
ax2.axhline(y=min_cooling_power_combined, color='black', linestyle='--', label=f'Min: {min_cooling_power_combined:.4f} W')
ax2.set_title('Continuous heat sink')
ax2.set_xlabel('Time (minutes)')
ax2.set_ylabel('Heat flow (W)')
ax2.grid(True)
ax2.legend(loc='upper right')

plt.show()
```

C.5. Surface area code

Listing C.5: Python code for ice block sublimation.

```
import numpy as np
import matplotlib.pyplot as plt
from geometry_final import TankGeometry
from materials_final import SublimationWater

```

```
# Constants
DENSITY_ICE = 917  # kg/m^3 (density of ice)
SUBLIMATION_RATE = 1e-6  # kg/s (1 mg/s sublimation rate)

# Material property
sublimation_water = SublimationWater()
LATENT_HEAT_SUBLIMATION = sublimation_water.latent_heat  # J/kg

# Geometry class (modified to include time-dependent surface area and power input)
class IceBlockSublimation:
    def __init__(self, tank_geometry, ice_volume_ratio=0.9):
        self.length_initial = tank_geometry.length  # Initial length (m)
        self.width_initial = tank_geometry.width    # Initial width (m)
        self.height_initial = tank_geometry.height  # Initial height (m)
        self.volume_initial = self.length_initial * self.width_initial * self.height_initial
             # Initial volume (m^3)
        self.ice_volume_initial = self.volume_initial * ice_volume_ratio  # Initial ice
            volume (90% of tank volume)
        self.mass_initial = self.ice_volume_initial * DENSITY_ICE  # Initial mass (kg)
        self.surface_area_initial = self.calculate_surface_area(self.length_initial, self.
            width_initial, self.height_initial)  # Initial surface area (m^2)

    def calculate_surface_area(self, length, width, height):
        """Calculate the surface area of a rectangular prism."""
        return 2 * (length * width + length * height + width * height)  # m^2

    def dimensions_at_time(self, t):
        """
        Calculate the dimensions of the ice block at time t.
        Assumes uniform sublimation from all sides.
        """
        # Total mass lost at time t
        mass_lost = SUBLIMATION_RATE * t  # kg

        # Remaining mass at time t
        mass_remaining = self.mass_initial - mass_lost

        # If mass_remaining <= 0, the ice block is fully sublimated
        if mass_remaining <= 0:
            return 0, 0, 0

        # Remaining volume at time t
        volume_remaining = mass_remaining / DENSITY_ICE  # m^3

        # Scale factor for dimensions (assuming uniform sublimation)
        scale_factor = (volume_remaining / self.ice_volume_initial) ** (1/3)

        # Current dimensions at time t
        length = self.length_initial * scale_factor
        width = self.width_initial * scale_factor
        height = self.height_initial * scale_factor

        return length, width, height

    def surface_area_at_time(self, t):
        """
        Calculate the surface area of the ice block at time t.
        """
        length, width, height = self.dimensions_at_time(t)
        if length == 0 and width == 0 and height == 0:
            return 0  # Ice block is fully sublimated
        return self.calculate_surface_area(length, width, height)  # m^2

    def total_sublimation_time(self):
        """
        Calculate the total time required for the ice block to fully sublimate.
        """
        return self.mass_initial / SUBLIMATION_RATE  # seconds

    def power_input_at_time(self, t):
        """
```

```python
        Calculate the power input required at time t.
        """
        surface_area = self.surface_area_at_time(t)
        if surface_area == 0:
            return 0  # No power input needed after full sublimation
        # Assuming power is proportional to the surface area for sublimation
        return (surface_area / self.surface_area_initial) * (SUBLIMATION_RATE * LATENT_HEAT_SUBLIMATION)

if __name__ == "__main__":
    # Initialize tank geometry
    tank = TankGeometry(length=0.0597, width=0.053, height=0.055)
    ice_sublimation = IceBlockSublimation(tank_geometry=tank, ice_volume_ratio=0.9)

    # Print initial information
    print("Initial Ice Block Information:")
    print(f"Initial Mass: {ice_sublimation.mass_initial:.6f} kg")
    print(f"Initial Volume: {ice_sublimation.ice_volume_initial:.6f} m³")
    print(f"Initial Surface Area: {ice_sublimation.surface_area_initial:.6f} m²")
    print(f"Total Sublimation Time: {ice_sublimation.total_sublimation_time():.2f} seconds")
    print(f"Total Sublimation Time: {ice_sublimation.total_sublimation_time()/60:.2f} minutes")

    # Time array (in seconds)
    total_time_minutes = ice_sublimation.total_sublimation_time() / 60
    time_minutes = np.linspace(0, total_time_minutes, 1000)  # Simulate until full sublimation, in minutes
    time_seconds = time_minutes * 60

    # Calculate surface area and power input over time
    surface_area = [ice_sublimation.surface_area_at_time(t) for t in time_seconds]
    power_input = [ice_sublimation.power_input_at_time(t) for t in time_seconds]

    # Plot results
    plt.figure(figsize=(12, 6))

    # Plot surface area
    plt.subplot(1, 2, 1)
    plt.plot(time_minutes, surface_area, color="blue")
    plt.xlabel("Time (minutes)")
    plt.ylabel("Surface area (m²)")
    plt.title("Surface area of remaining propellant over time")
    plt.grid(True)


    # Plot power input
    plt.subplot(1, 2, 2)
    plt.plot(time_minutes, power_input, color="red")
    plt.xlabel("Time (minutes)")
    plt.ylabel("Power input (W)")
    plt.title("Required power input over time")
    plt.grid(True)


    plt.tight_layout()
    plt.show()
```

D
Drawings

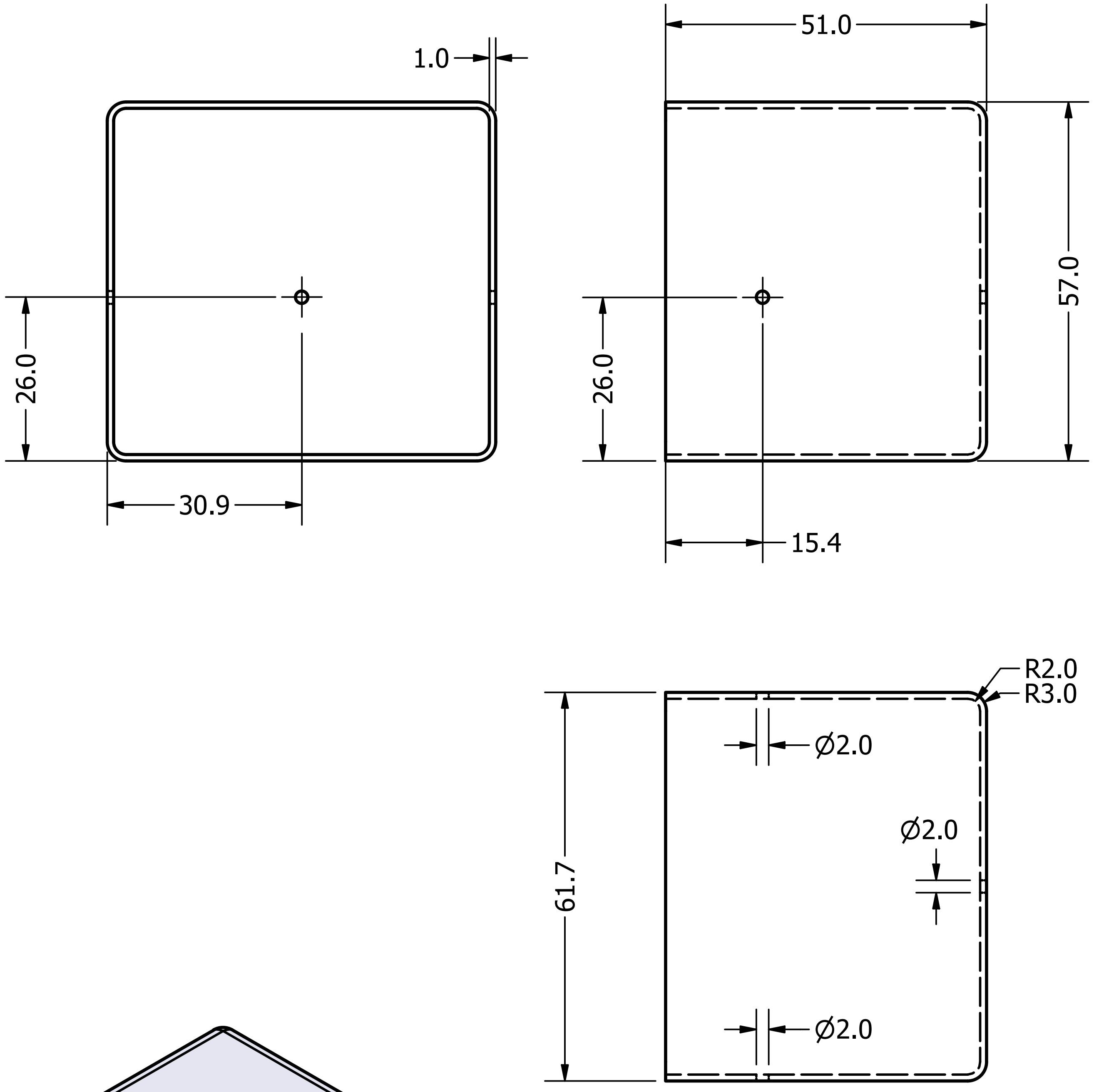

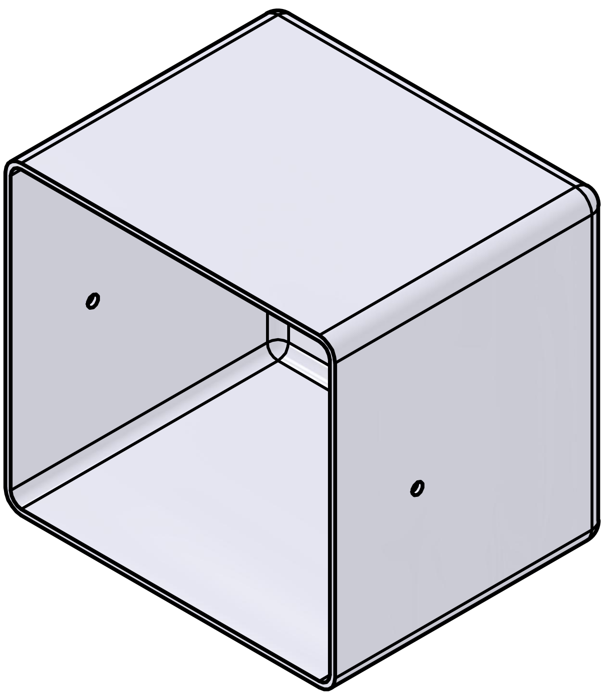

TITLE				
Storage tank part 1				
MATERIAL				
Aluminum 6061				
MANUFACTURING PROCESS				
Deep drawing, Drilling				
SIZE A4	UNIT mm	ITEM# 1	SCALE 1:1	SHEET 1 OF 13
DRAWN BY: Christian Stefan				

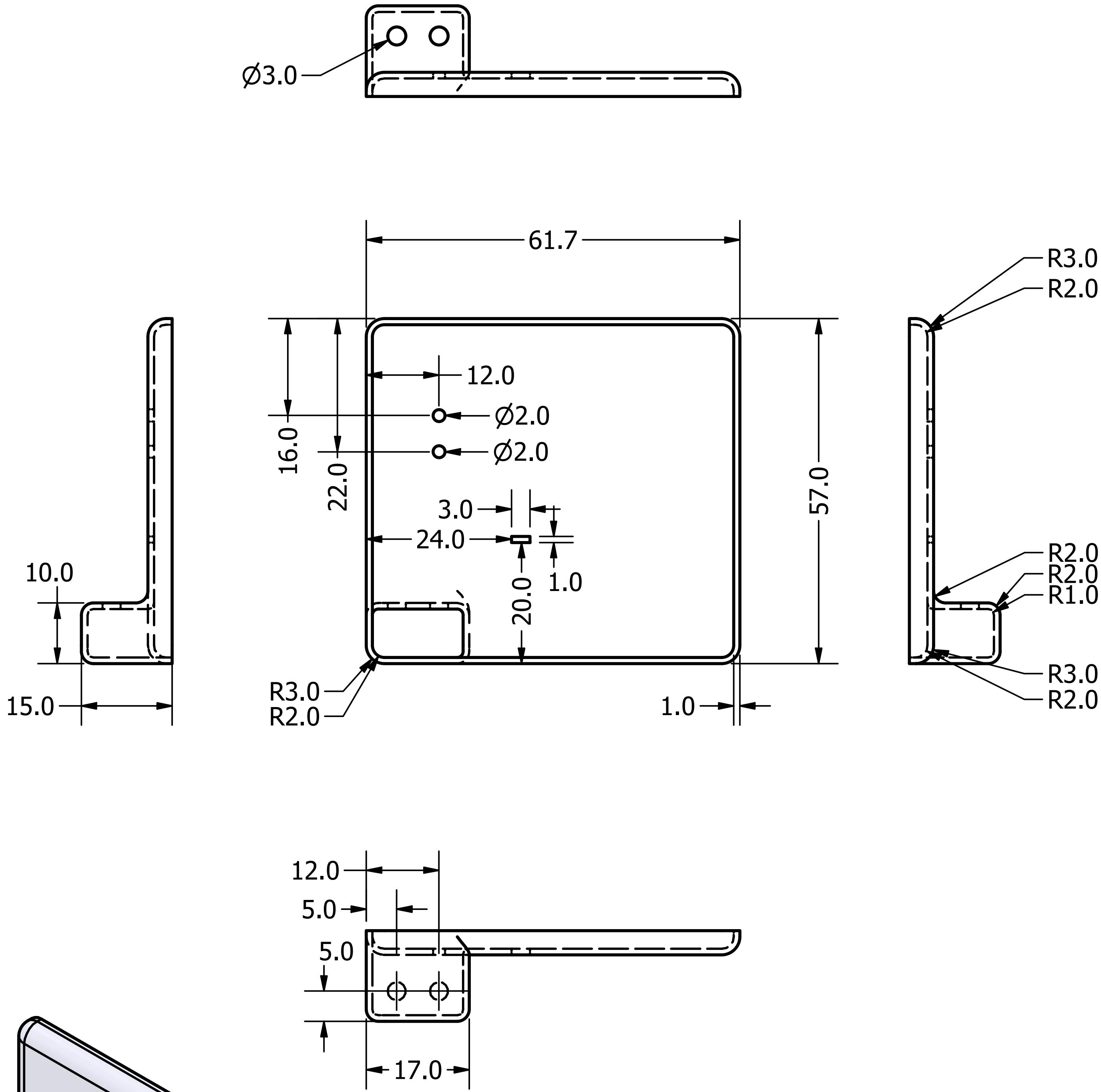

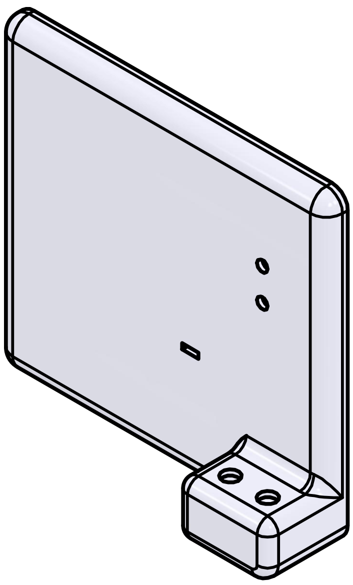

TITLE				
Storage tank part 2				
MATERIAL				
Aluminum 6061				
MANUFACTURING PROCESS				
Deep drawing, Drilling, Milling				
SIZE	UNIT	ITEM#	SCALE	SHEET
A4	mm	2	1:1	2 OF 13
DRAWN BY: Christian Stefan				

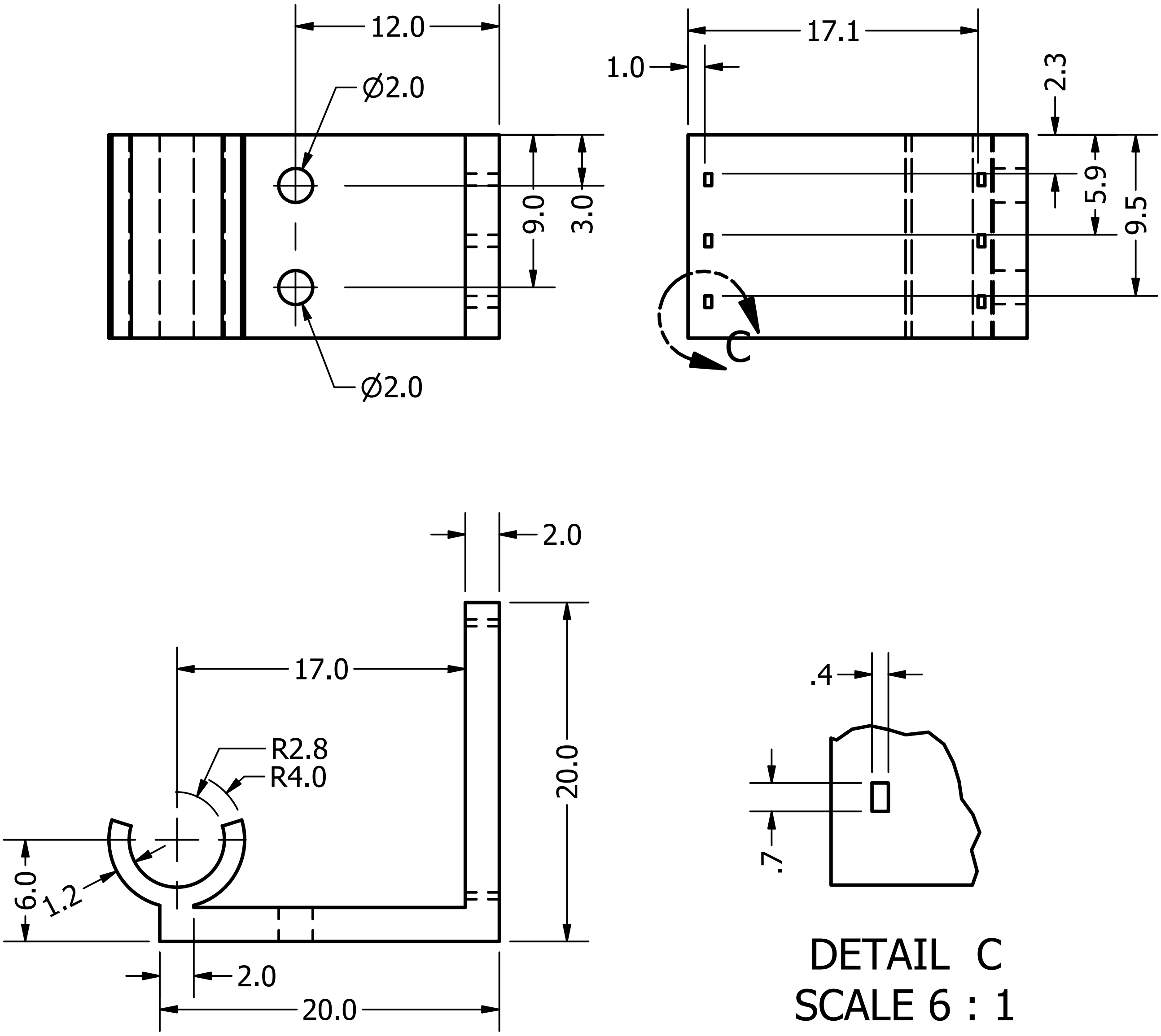

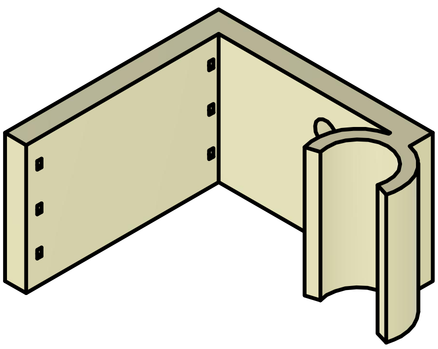

TITLE Tank attachment				
MATERIAL Polypropylene				
MANUFACTURING PROCESS 3D Printing				
SIZE A4	UNIT mm	ITEM# 3	SCALE 2:1	SHEET 3 OF 13
DRAWN BY: Christian Stefan				

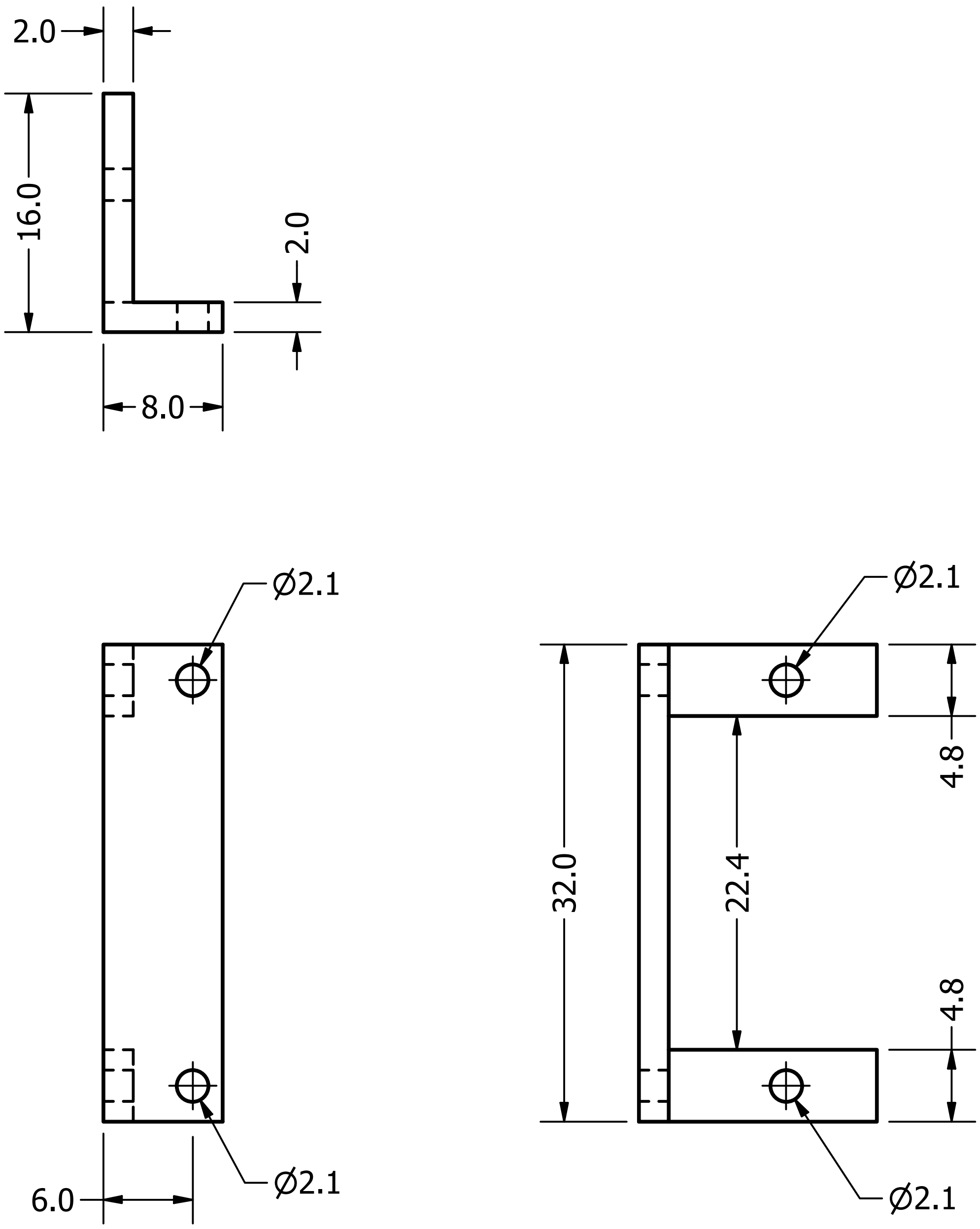

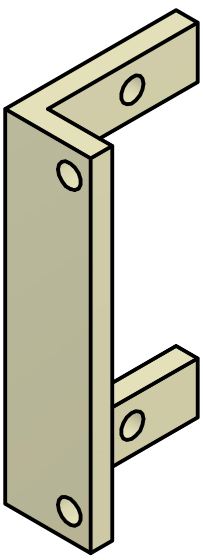

TITLE Servo connector				
MATERIAL Polypropylene				
MANUFACTURING PROCESS 3D Printing				
SIZE A4	UNIT mm	ITEM# 4	SCALE 2:1	SHEET 4 OF 13
DRAWN BY: Christian Stefan				

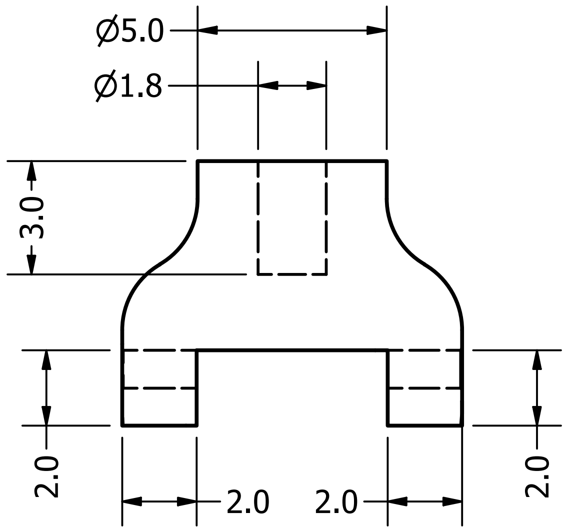

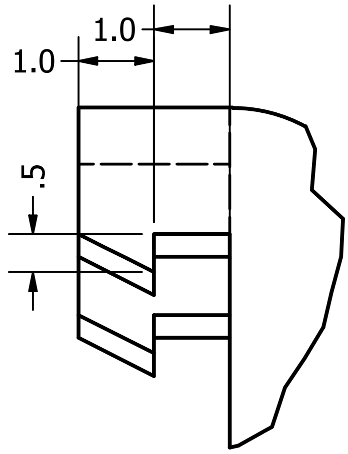

DETAIL A
SCALE 10 : 1

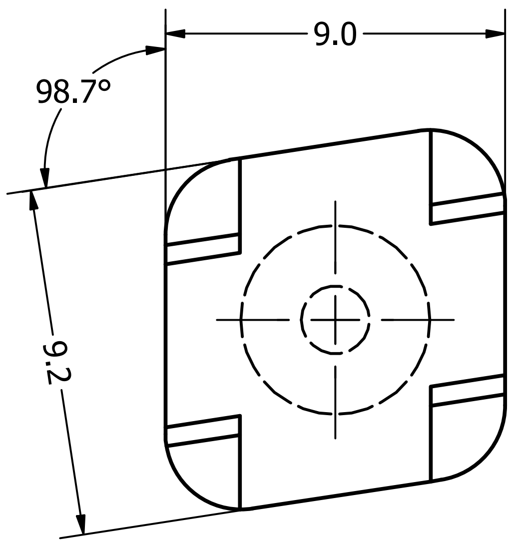

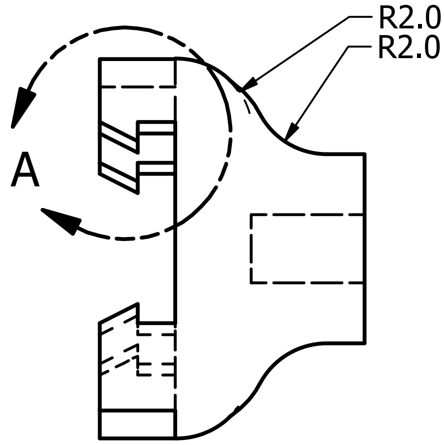

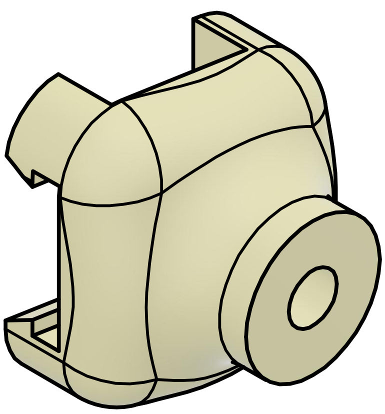

TITLE Tank connection 1				
MATERIAL Polypropylene				
MANUFACTURING PROCESS 3D Printing				
SIZE A4	UNIT mm	ITEM# 5	SCALE 5 : 1	SHEET 5 OF 13
DRAWN BY: Christian Stefan				

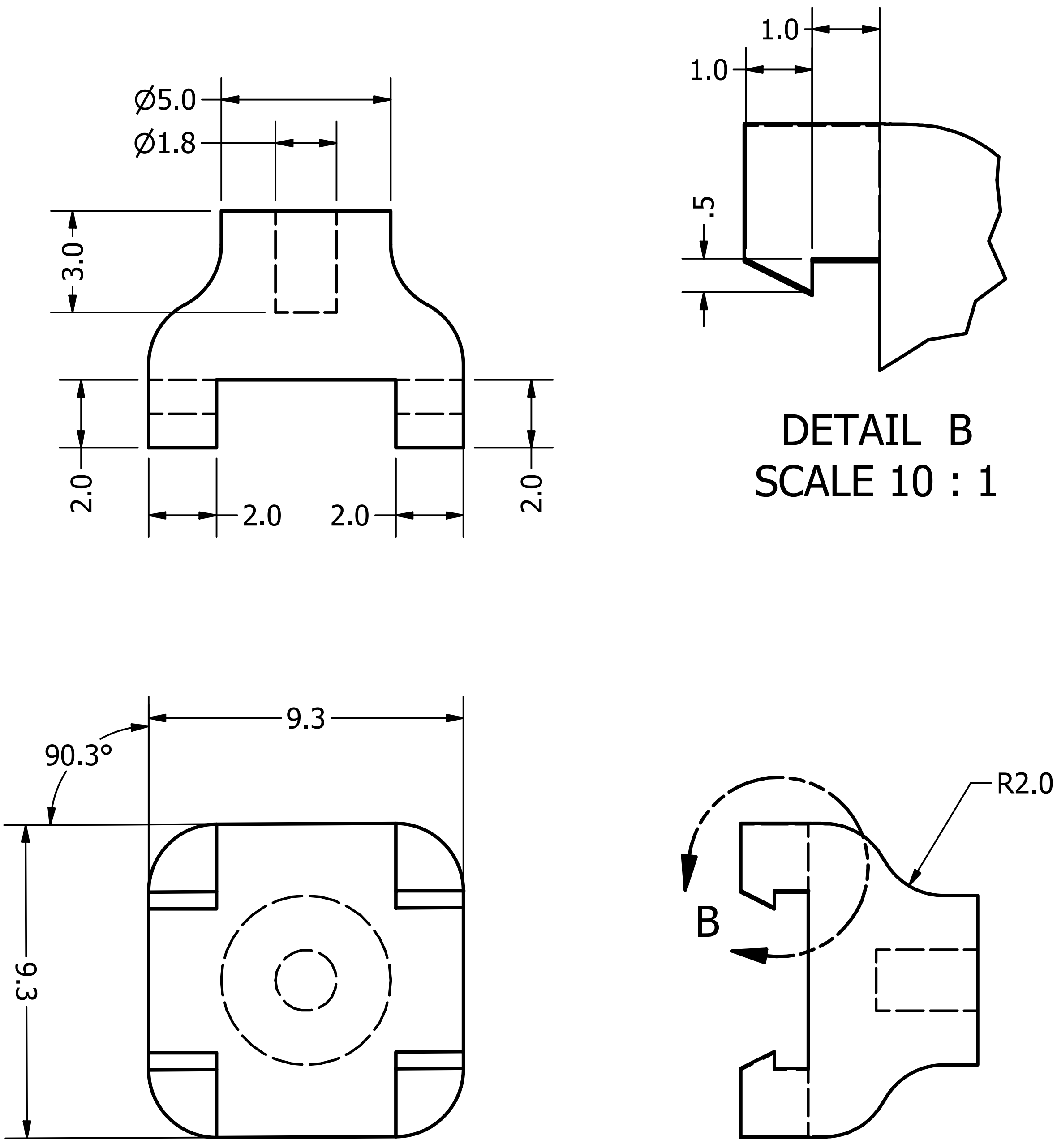

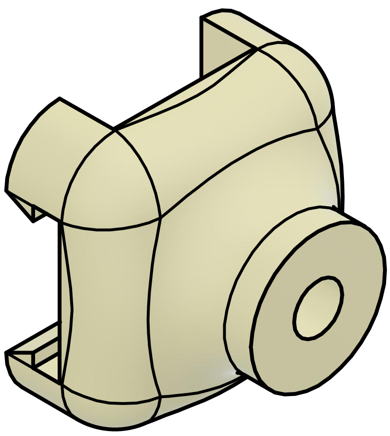

TITLE				
Tank connection 2				
MATERIAL				
Polypropylene				
MANUFACTURING PROCESS				
3D Printing				
SIZE	UNIT	ITEM#	SCALE	SHEET
A4	mm	6	5 : 1	6 OF 13
DRAWN BY: Christian Stefan				

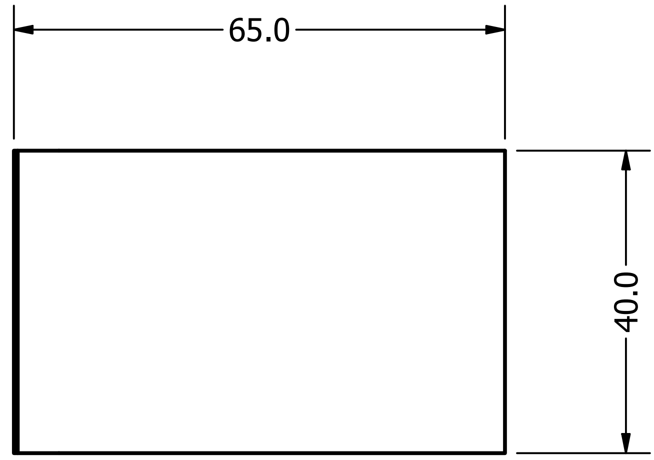

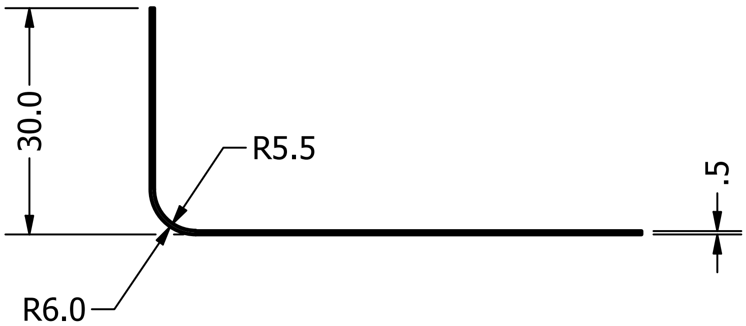

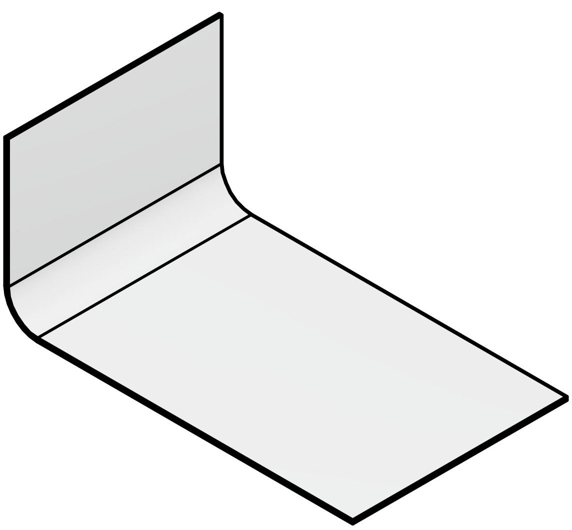

TITLE				
Heat sink connection				
MATERIAL				
Aluminum 6061				
MANUFACTURING PROCESS				
Laser cutting, bending				
SIZE	UNIT	ITEM#	SCALE	SHEET
A4	mm	7	1 : 1	7 OF 13
DRAWN BY: Christian Stefan				

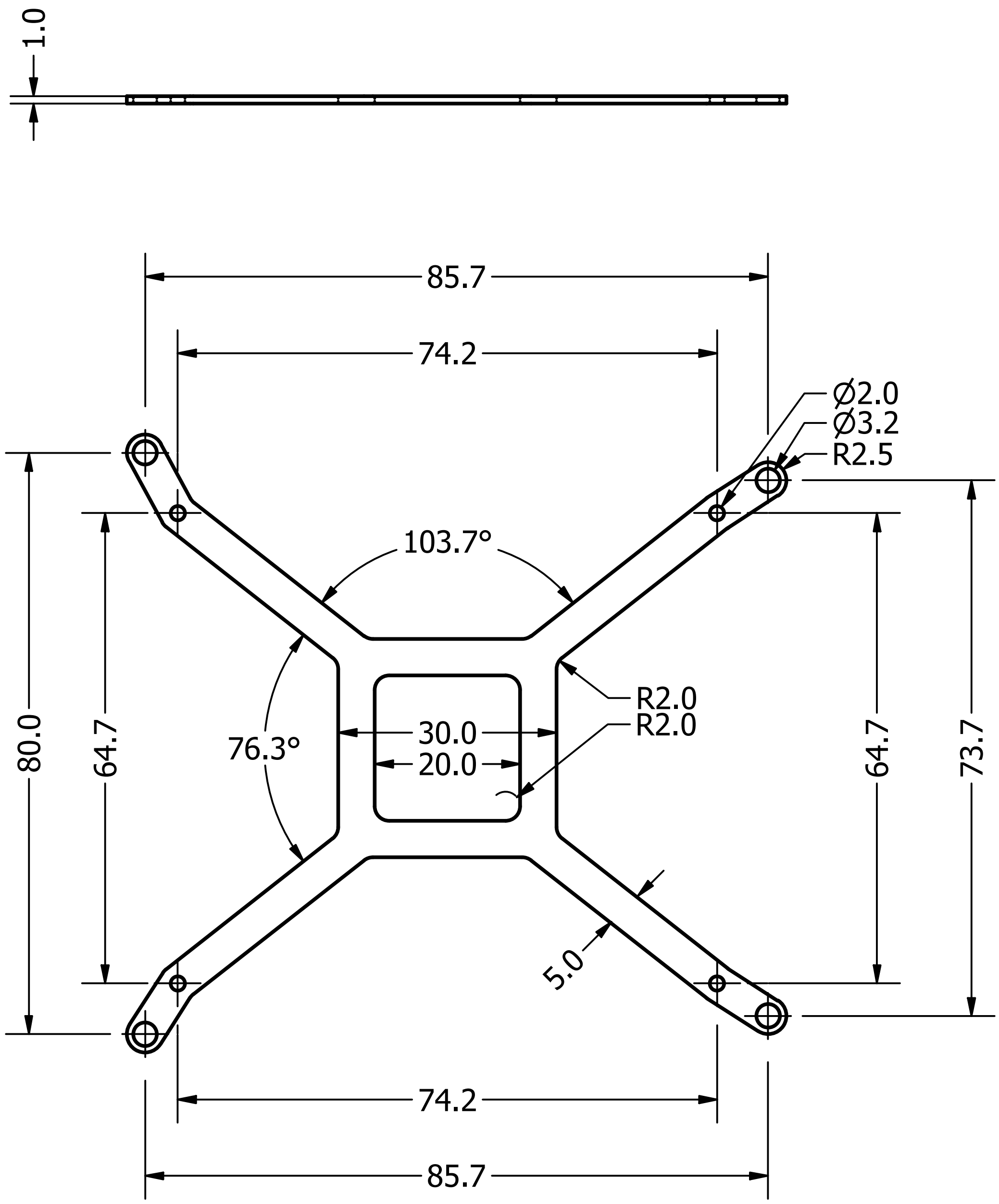

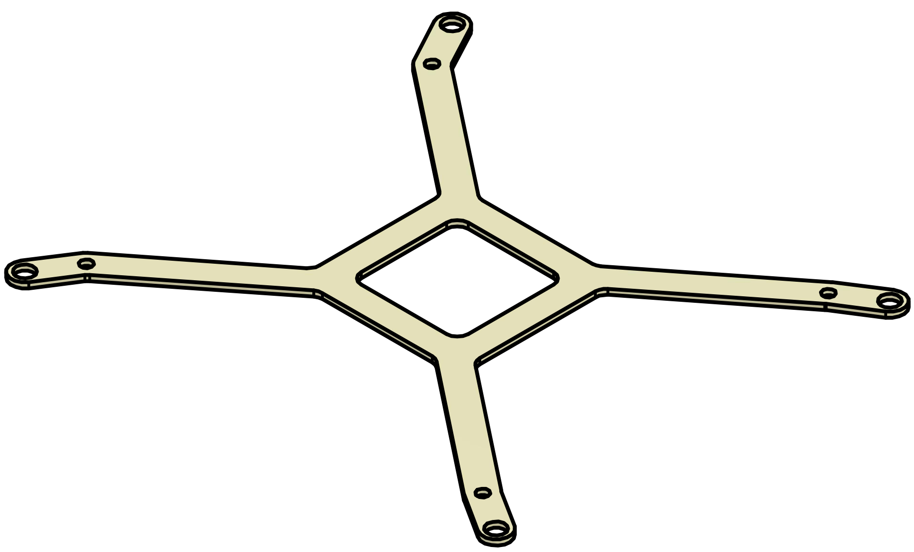

TITLE				
Outside container top				
MATERIAL				
Polypropylene				
MANUFACTURING PROCESS				
3D Printing				
SIZE	UNIT	ITEM#	SCALE	SHEET
A4	mm	8	1 : 1	8 OF 13
DRAWN BY: Christian Stefan				

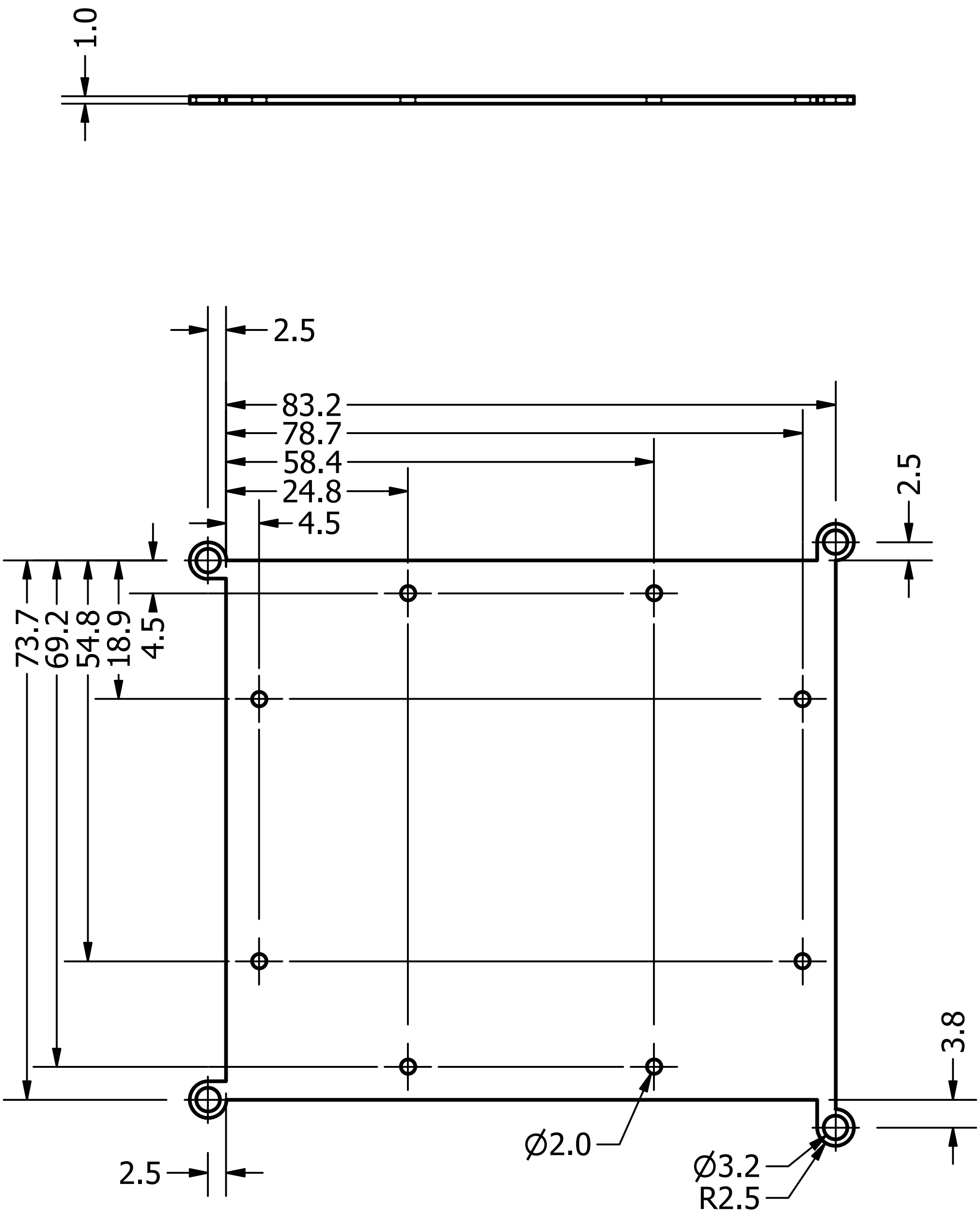

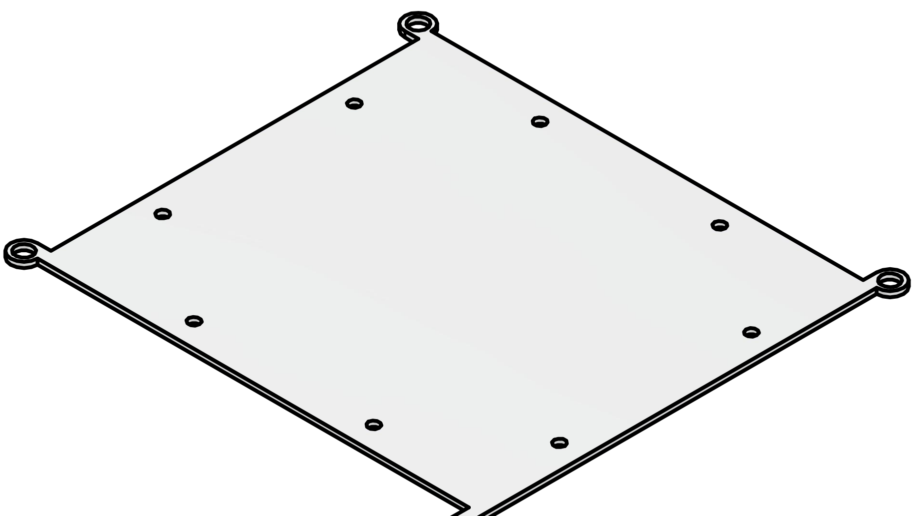

TITLE Outside container bottom				
MATERIAL Aluminum 6061				
MANUFACTURING PROCESS Laser cutting				
SIZE A4	UNIT mm	ITEM# 9	SCALE 1:1	SHEET 9 OF 13
DRAWN BY: Christian Stefan				

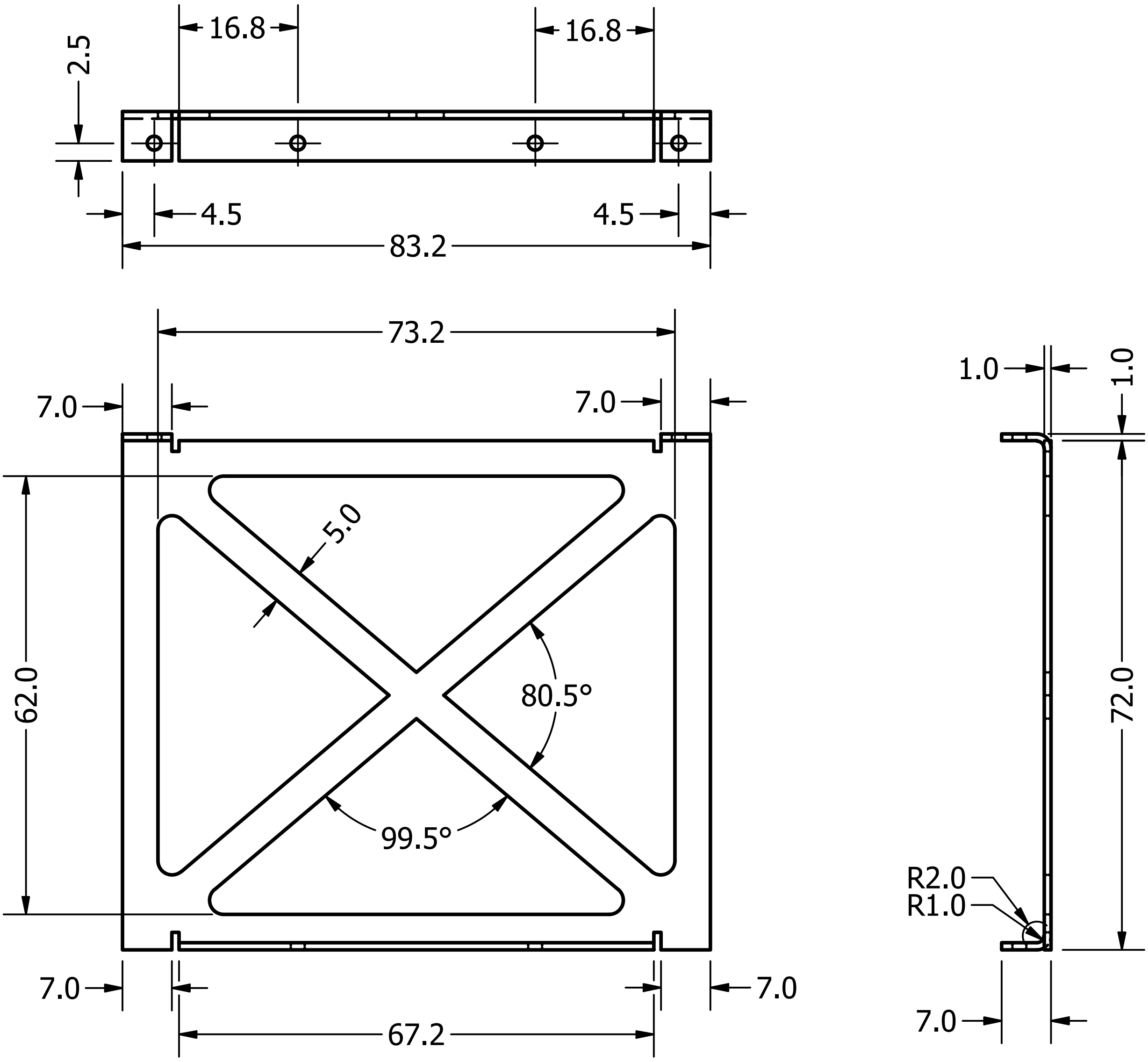

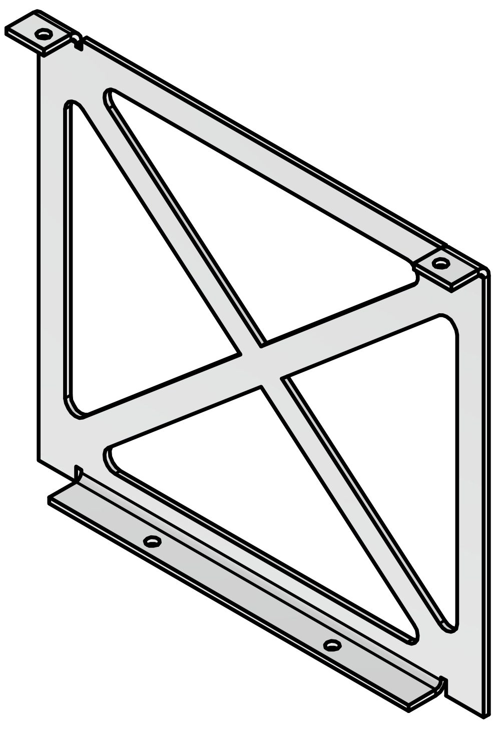

TITLE Outside container wall 1				
MATERIAL Aluminium 6061				
MANUFACTURING PROCESS Laser cutting, bending				
SIZE A4	UNIT mm	ITEM# 10	SCALE 1:1	SHEET 10 OF 13
DRAWN BY: Christian Stefan				

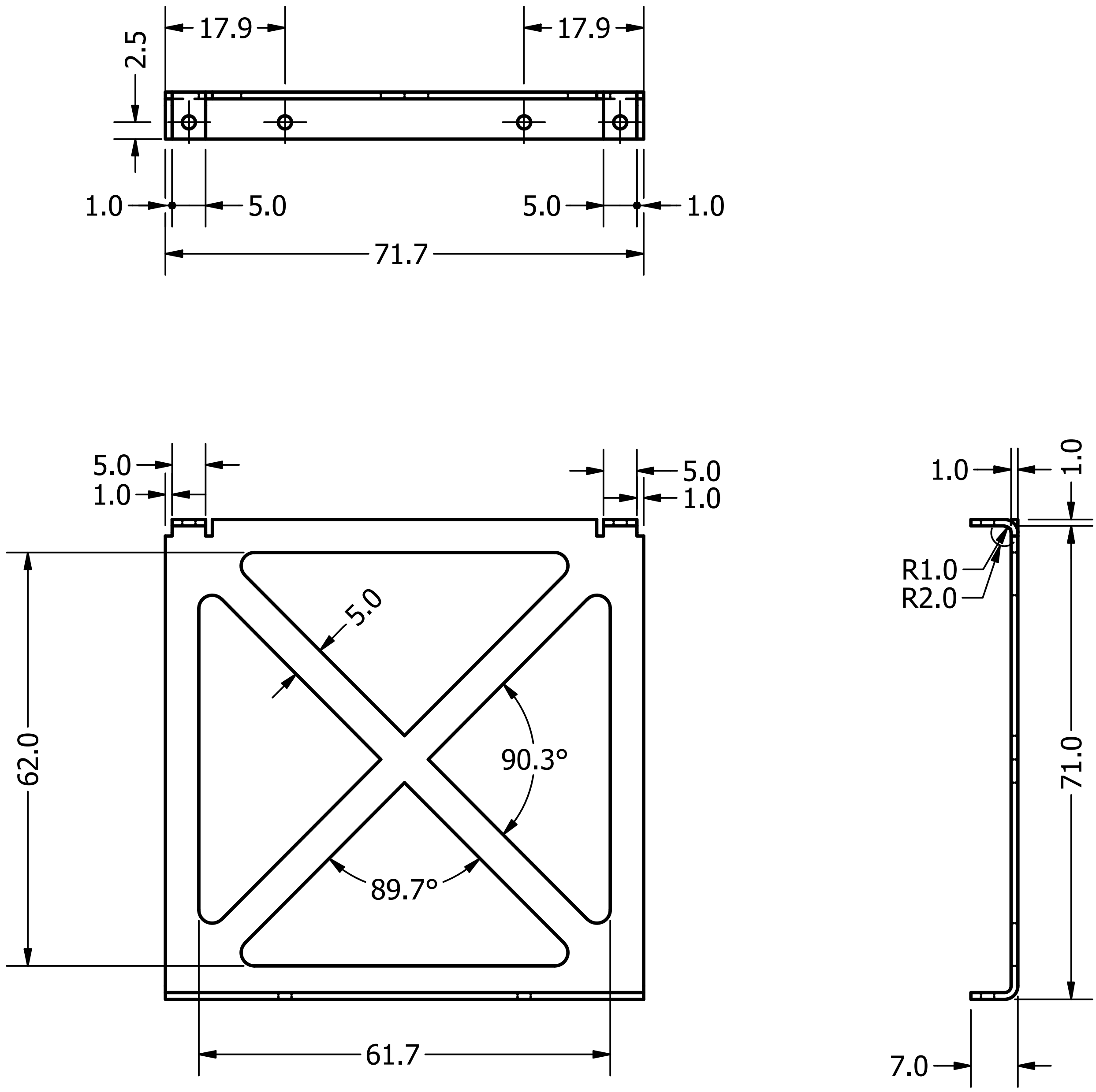

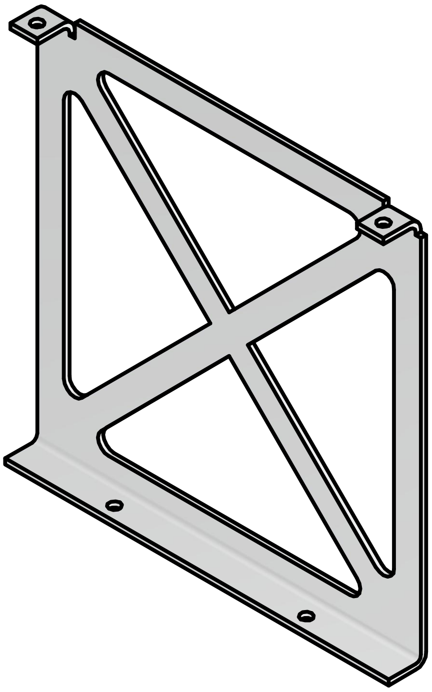

TITLE				
Outside container wall 2				
MATERIAL				
Aluminum 6061				
MANUFACTURING PROCESS				
Laser cutting, bending				
SIZE	UNIT	ITEM#	SCALE	SHEET
A4	mm	11	1:1	11 OF 13
DRAWN BY: Christian Stefan				

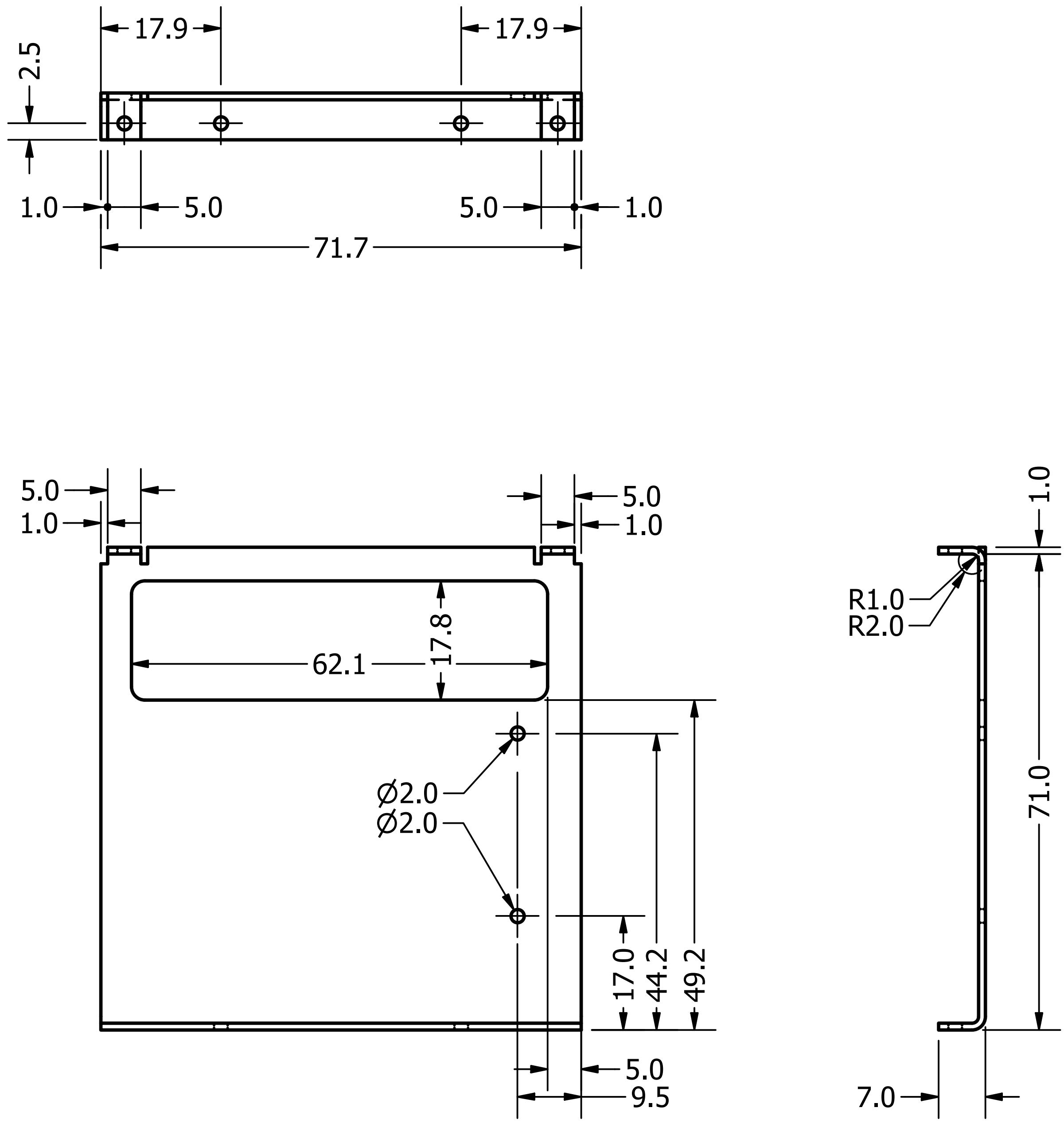

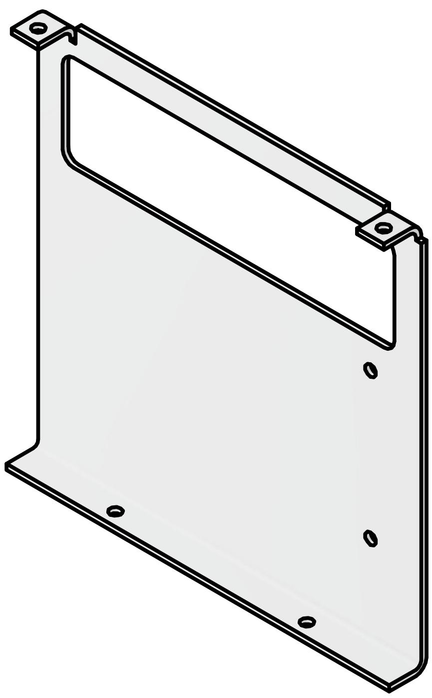

TITLE
Outside container wall 3

MATERIAL
Aluminum 6061

MANUFACTURING PROCESS
Laser cutting, bending

SIZE	UNIT	ITEM#	SCALE	SHEET
A4	mm	12	1:1	12 OF 13

DRAWN BY: Christian Stefan

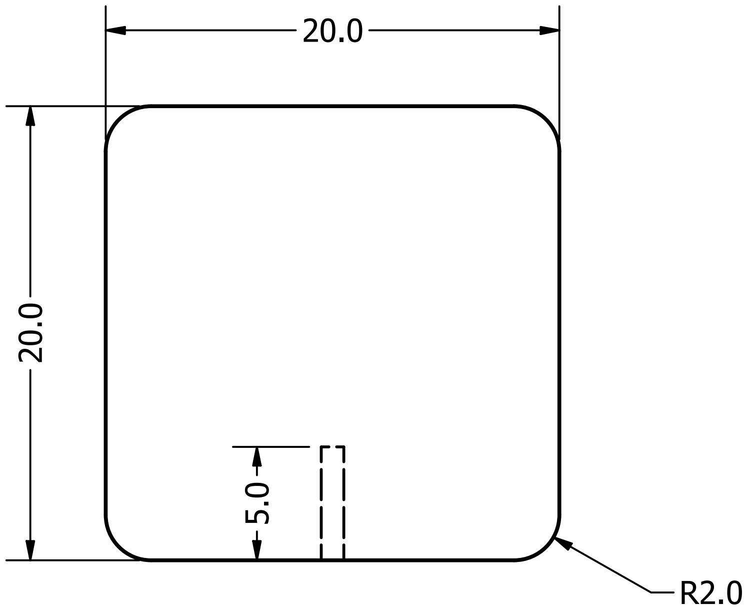

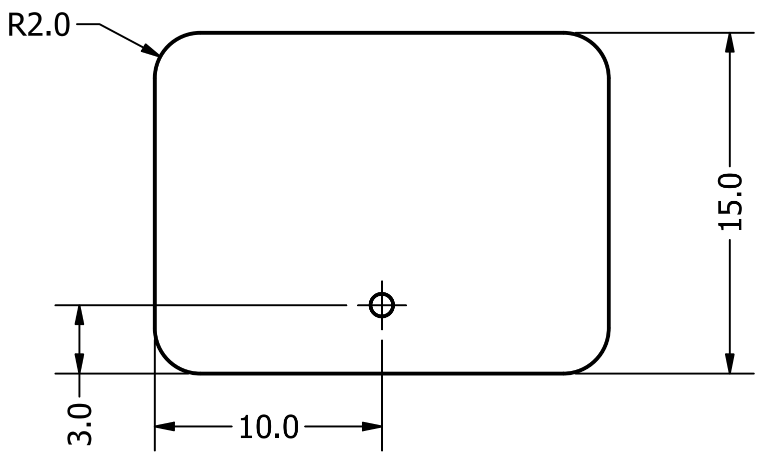

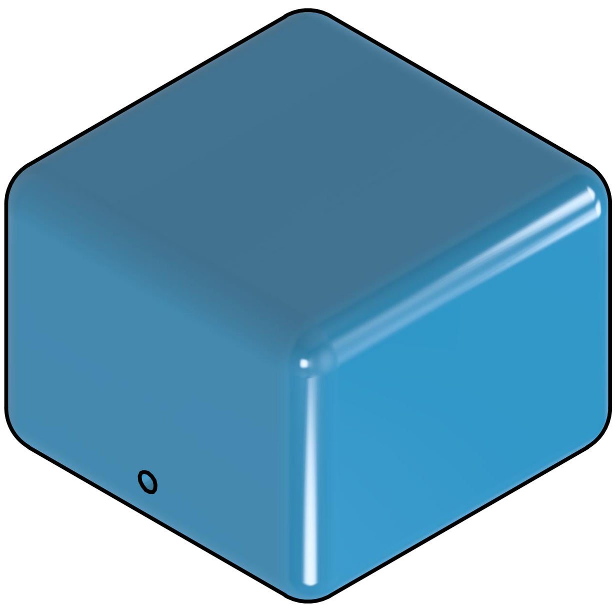

TITLE				
Thruster representation				
MATERIAL				
ABS Plastic				
MANUFACTURING PROCESS				
3D Printing				
SIZE	UNIT	ITEM#	SCALE	SHEET
A4	mm	23	3 : 1	13 OF 13
DRAWN BY: Christian Stefan				